MACRO-/NANO- MATERIALS BASED ULTRASENSITIVE LATERAL FLOW NUCLEIC ACID BIOSENSORS

A Dissertation
Submitted to the Graduate Faculty
of the
North Dakota State University
of Agriculture and Applied Science

By

Sunitha Takalkar

In Partial Fulfillment of the Requirements
for the Degree of
DOCTOR OF PHILOSOPHY

Major Department:
Chemistry and Biochemistry

July 2017

Fargo, North Dakota

North Dakota State University
Graduate School

Title

ULTRASENSITIVE LATERAL FLOW NUCLEIC ACID BIOSENSORS BASED ON NOVEL MACRO-/NANO- MATERIALS

By

Sunitha Takalkar

The Supervisory Committee certifies that this ***disquisition*** complies with North Dakota State University's regulations and meets the accepted standards for the degree of

DOCTOR OF PHILOSOPHY

SUPERVISORY COMMITTEE:

Dr. Guodong Liu
Chair

Dr. D. K. Srivastava

Dr. Pinjing Zhao

Dr. Xiwen Cai

Approved:

07-05-2017
Date

Dr. Gregory Cook
Department Chair

ABSTRACT

Ultrasensitive detection of nucleic acids plays a very important role in the field of molecular diagnosis for the detection of various diseases. Lateral flow biosensors (LFB) are convenient, easy-to-use, patient friendly forms of detection methods offering rapid and convenient clinical testing in close proximity to the patients thus drawing a lot of attention in different areas of research over the years. In comparison with the traditional immunoassays, the nucleic acid based lateral flow biosensors (NABLFB) has several advantages in terms of stability and interference capabilities. NABLFB utilizes nucleic acid probes as the bio-recognition element. The target analyte typically is the oligonucleotide like the DNA, mRNA, miRNA which are among the nucleic acid secretions by the tumor cells when it comes to detection of cancer. Traditionally gold nanoparticles (GNPs) have been used as labels for conjugating with the detection probes for the qualitative and semi quantitative analysis, the application of GNP-based LFB is limited by its low sensitivity. This dissertation describes the use of different nanomaterials and advanced detection technologies to enhance the sensitivities of the LFB based methods.

Silica Nanorods decorated with GNP were synthesized and employed as labels for ultrasensitive detection of miRNA on the LFB. Owing to the biocompatibility and convenience in surface modification of SiNRs, they acted as good carriers to load numerous GNPs. The sensitivity of the GNP-SiNR-based LFSB was enhanced six times compared to the previous GNP-based LFSB.

A fluorescent carbon nanoparticle (FCN) was first used as a tag to develop a lateral flow nucleic acid biosensor for ultrasensitive and quantitative detection of nucleic acid samples. Under optimal conditions, the FCN-based LFNAB was capable of detecting minimum 0.4 fM target DNA without complex operations and additional signal amplification.

The carbon nanotube was used as a label and carrier of numerous enzyme and DNA molecules simultaneously thus resulting in the enormous amplification of the colorimetric signal. This CNT-enzyme label thus aided in ultra-sensitive detection of pancreatic cancer (PC) biomarker miRNA 210 and PC biomarker panel (miRNA 16, miRNA 21 and miRNA 196a). All these LFBs were also applied in the field of real sample detection.

ACKNOWLEDGEMENTS

This dissertation denotes a very challenging journey, involving the support of many people professionally and personally. Firstly, I would like to thank my advisor Dr. Guodong Liu for letting me start my journey of the doctoral degree under his mentorship. His continuous guidance all along the projects, feedback, suggestions and criticism has helped me reach this stage of the dissertation. His patience and support in guiding us was remarkable inspiring all of us in the lab to work towards our goal of establishing ourselves as independent researchers. Thank you Dr. Liu.

I would like to thank my committee members Dr. D. K. Srivastava, Dr. Pinjing Zhao and Dr. Xiwen Cai for their valuable suggestions and positive criticism in the meetings. They were always very accommodating in taking out time from their busy schedules for my committee meetings. Additionally, I would also like to thank all my course instructors for their valuable teaching, which also helped me get ideas for the development of various research projects.

I would like to appreciate my current lab members Kwaku Baryeh and Michelle Lund for making lab a fun place to work. A special thanks to Kwaku for all the trouble shooting we did with the experiments and for being a very helpful friend from my first day at NDSU. I would also like to thank my past lab members Hui Xu, Meenu Baloda and Anant Gurung for their guidance in my initial days of joining the lab and for the fun times we had.

No work and projects in the lab would have been possible without our funding agencies NIH, DOE-ND EPSCOR and NIH-COBRE (1P20GM09024-01A1). I would like to acknowledge them for the financial support provided. The department of chemistry and biochemistry at NDSU for giving me the opportunity to pursue my doctoral studies, the administrative staff at NDSU (Amy, Wendy, Dionna, Linda) for helping us with everything, Cole for helping us with the stock room and Dr. Angel Ugrinov for his guidance with the instruments available in the department.

A special note of thanks to my friends in Fargo, for making the entire period of my stay a very memorable one. Fargo was like a home away from home and I owe a lot to my friends for the awesome get togethers, which served as a stress buster during the stressful graduate school days.

Last but not the least, a very big thanks to my family. My parents for their trust in me and for their continuous support in pursuing my dreams, my sisters for their continuous encouragement and for the long conversations especially in the times when I needed them badly, my beautiful and lovely niece for being my stressbuster, my father-in-law for his constant support and encouragement , my husband, for his patience in the final days of my Ph.D. and for being there for me whenever I needed him to vent my frustration and kudos to his countless trips to Fargo.

DEDICATION

This dissertation is dedicated to my parents Ganpath Takalkar and Anjali Takalkar in appreciation to their support in every stage of my life. They are the most encouraging, caring, loving and best parents anyone could ask for which motivated me to fulfil my dream of pursuing a doctoral degree.

TABLE OF CONTENTS

LIST OF TABLES

LIST OF FIGURES

LIST OF ABBREVIATIONS

ALP…….. ..... Alkaline phosphatase

ATP……. ..... Adenosine triphosphate

AuNP..... Gold nanoparticle

AuNP-SiNR ..... Gold nanoparticle-silica nanorod

BCIP/NBT..... 5-Bromo-4-chloro-3-indolyl phosphate/nitro blue tetrazolium

BSA..... Bovine serum albumin

CNP..... Carbon nanoparticle

CNTs..... Carbon nanotubes

CTAB..... Cetyl trimethylammonium bromide

Cu^{+2} ..... Copper

dATP..... Deoxyadenosine triphosphate

DNA..... Deoxyribonucleic acid

dNTP..... Deoxy ribonucleotide triphosphate

DTT..... Dithiothreitol

E.coli ..... Escherichia coli

EDC..... *N*-(3-dimethylaminopropyl)-N′-ethylcarbodiimide hydrochloride

EDTA..... Ethylene diamine tetra acetic acid

ELISA ..... Enzyme linked immunosorbent assay

EtBr..... Ethidium bromide

FCN..... Fluorescent carbon nanoparticle

fM..... Femtomolar

FTIR..... Fourier transform infrared spectroscopy

GNP..... Gold nanoparticle

H_2SO_4 ..... Sulfuric acid

$HAuCl_4$ ..... Gold (III) chloride trihydrate

HNO_3 ..... Nitric acid

HPV ..... Human papilloma virus

HRP ..... Horseradish peroxidase

ISDPR ..... Isothermal strand displacement polymerase reaction

K_2CO_3 ..... Potassium carbonate

KBr ..... Potassium bromide

LF strip ..... Lateral flow strip

LFA ..... Lateral flow assays

LFI ..... Lateral flow immunoassays

LFIA ..... Lateral flow immunoassays

LFNAB ..... Lateral flow nucleic acid biosensor

LFSBs ..... Lateral flow strip biosensors

MES ..... 2-(*N*-morpholino) ethanesulfonicacid

miRNA ..... Micro RNA

mM ..... Milli molar

mRNA ..... Messenger RNA

MS ..... Mass spectrometry

$Na_3PO_4.12H_2O$ ..... Sodium phosphate tribasic dodecahydrate

$NaBH_4$ ..... Sodium borohydride

NABLFB ..... Nucleic acid based lateral flow biosensors

NaCl ..... Sodium Chloride

NH_4OH ..... Ammonium hydroxide

NHS ..... *N*-Hydroxysulfosuccinimide sodium salt

nM ..... Nano molar

NMR ..... Nuclear magnetic resonance

P_2O_5 ..... Phosphorus pentoxide

Pb^{+2} ..... Lead

PBS ..... Phosphate buffered saline

PBST ..... PBS with 0.05% Tween 20

PC ..... Pancreatic cancer

PCR ..... Polymerase chain reaction

pM ..... Pico molar

POC ..... Point of care

PVP ..... Polyvinyl pyrrolidone

QD ..... Quantum dot

RNA ..... Ribose nucleic acid

RSD ..... Relative standard deviation

RT ..... Room temperature

RT ..... Reverse transcriptase

RT-qPCR ..... Reverse transcription quantitative real-time PCR

S/N ratio ..... Signal to noise ratio

SDS ..... Sodium dodecyl sulfate

SELEX ..... Systematic evolution of ligands by exponential enrichment

SiNR ..... Silica nanorod

SiO_2 ..... Silicon dioxide

SNP ..... Single-nucleotide polymorphism

SSC ..... Saline-sodium citrate

TAE ..... Tris base, Acetic acid, EDTA

TBS ..... Tris-buffered saline

TEM ..... Transmission electron microscope

TEOS..... Tetraethyl orthosilicate

UPT ..... Up converting phosphor technology

1. INTRODUCTION

The rationale behind the research described in this dissertation is to develop ultrasensitive lateral flow assays for nucleic acid detection. These lateral flow assays take advantage of the biomarkers which have gained increased attention in the past few decades. A biomarker can be defined as a biological molecule found in blood, other body fluids, or tissues that is a sign of a normal or abnormal process, or of a condition or disease.[1] Especially in diseases like cancer, the tumor cells release their nucleic acid secretions into the blood stream.[2] The high levels of DNA, mRNA and miRNA in the blood of the patients is the result of active tumor cell secretions along with apoptotic and necrotic cell deaths.[3] Therefore, quantification of these nucleic acid biomarkers using the assays that can progressively monitor the progression of the disease in the blood samples of the cancer patients could serve as an efficient remedy for the early detection of cancer. Early detection of cancer is crucial in improving the survival rate of cancer patients irrespective of the organ affected (breast, pancreas, lungs, skin, colon). Any clinical treatment is effective and successful when the disease is detected at curable stages.[4] Thus the detection of these nucleic acids in low levels at early stages could largely influence in the reduction of mortality rates and sufferings of cancer patients.

Numerous techniques have been exploited for the sensitive detection of various targets. Mass spectrometry (MS),[5-7] blotting techniques (western, southern, northern),[8-9] gel electrophoresis,[10-11] ELISA,[12] microarray,[13-15] nuclear magnetic resonance (NMR),[16-17] *in situ* hybridization,[18] polymerase chain reaction[19] are some examples of those techniques which play a pivotal role in the detection. However these have some disadvantages like multiple washing steps, complex detection procedures and use of expensive reagents, labels and instruments which limit

them to well-financed central testing laboratories. Therefore there always exists a need to develop rapid, simple, low-cost, disposable and easy-to-use platforms for the detection of various targets.

1.1. Point of Care Devices

Point of Care (POC) devices have over the years drawn a lot of attention in different areas of research. POC devices offer rapid and convenient clinical testing in close proximity to the patients. The advantages of POC tests to list a few include

- Speed of diagnosis and treatment: POC tests offer an advantage of providing rapid test results thus expediting the entire process of medical decision making. Also, assistance of a medical supervisor is not required to interpret the test results thus reducing the anxiety among patients waiting for the results.
- Portable devices: POC tests are portable thus eliminating the need of a laboratory space, fume-hoods and other laboratory equipment's. Since these are portable, the tests can be conducted near the patient site thus increasing the flexibility to meet the diversity of medical needs.
- Ease of handling: unprocessed samples such as whole blood can also be applied directly to the POC test strip for testing without the need for any additional processing or centrifugation. The problems such as sample deterioration and insufficient sample volumes can be eradicated since the tests can be done bedside using few microliters of the patient sample.
- Cost per test: The overall cost of patient care will be definitely reduced when POC tests are employed as it allows the patient to be treated or processed more quickly through the health care system compared to the conventional testing.[20]

The idea can be conveniently applied in other areas such as agriculture, food safety and environmental monitoring. Lateral flow strip biosensors (LFSB's) have been developed by various researchers that are very much suited for these applications.[21-22] The lateral flow assay (LFA), introduced in 1988 by Unipath, is a well-known and classic example of a POC diagnostic format available in the commercial market.[23](figure 1.1)

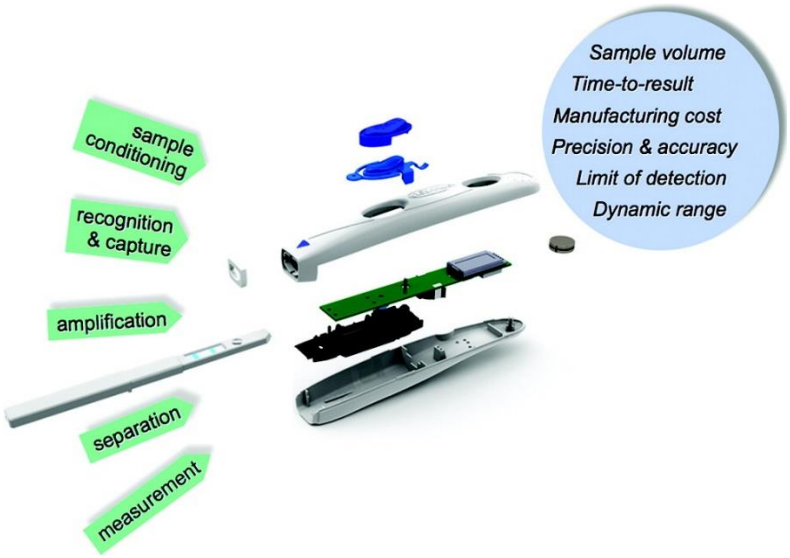

Figure 1.1. The pregnancy test-strip which gives the optical and digital read-out in a single-stick format (left in the picture) works with the interaction of the overall unit operations and specifications. Image by Unipath, Ltd.[23]

1.2. Working Principle of the Lateral Flow Assays

A traditional LFSB is composed of porous membranes, recognition elements and a signal-generating system (commonly called as labels). The typical configuration of LFSB (figure 1.1) is composed of four components: sample pad (sample application zone), conjugate pad, nitrocellulose membrane (detection zone) and absorption pad. (Figure 1.2.) To facilitate the migration of the liquid along the strip, each part overlaps onto the other ensuring the movement of the sample all along the strip. In the presence of liquid sample or suspension, the analyte moves along the membrane by capillary action and interacts with the bio-recognition element (DNA

aptamer or antibody) coupled to a colorimetric, electrochemical, fluorescent, enzyme or any other label which is capable of giving a visual or instrumental detectable signal that can be read using a portable reader.

Typically the LFSB has a sample pad made of cellulose to which the analyte is applied, a conjugate pad made of glass fiber where the detection nucleic acid probe or detection antibody coupled to a signal transducing element is loaded, a nitrocellulose membrane on which the capture probe or capture antibody is immobilized for generating a detectable signal, while the control line is to validate the performance of the strip. The absorption pad at the other end of the strip is to maintain the flow of the liquid since the capillary force of the strip material is the driving force for the movement of the liquid.

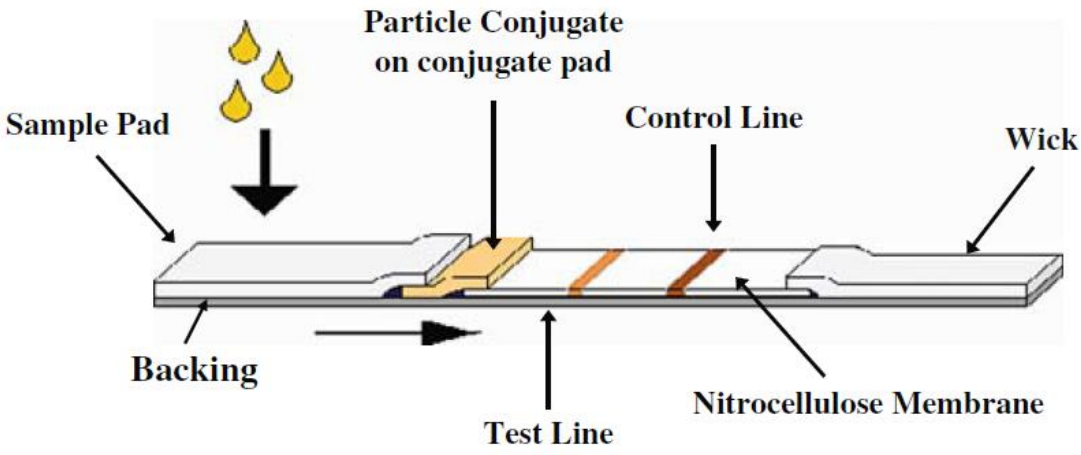

Figure 1.2. Typical configuration of lateral flow strip biosensor.[24]

1.3. Classification of Lateral Flow Assays

Bio recognition elements are a set of biological entity, those that are capable of carrying out specific group reactions or can bind with particular group of compounds, to yield a detectable signal that is read and transformed by the transducer. Examples of the bio recognition elements

include antibodies, enzymes, microbes, organelles, cells, receptors and nucleic acids.[25] (Figure 1.3.)

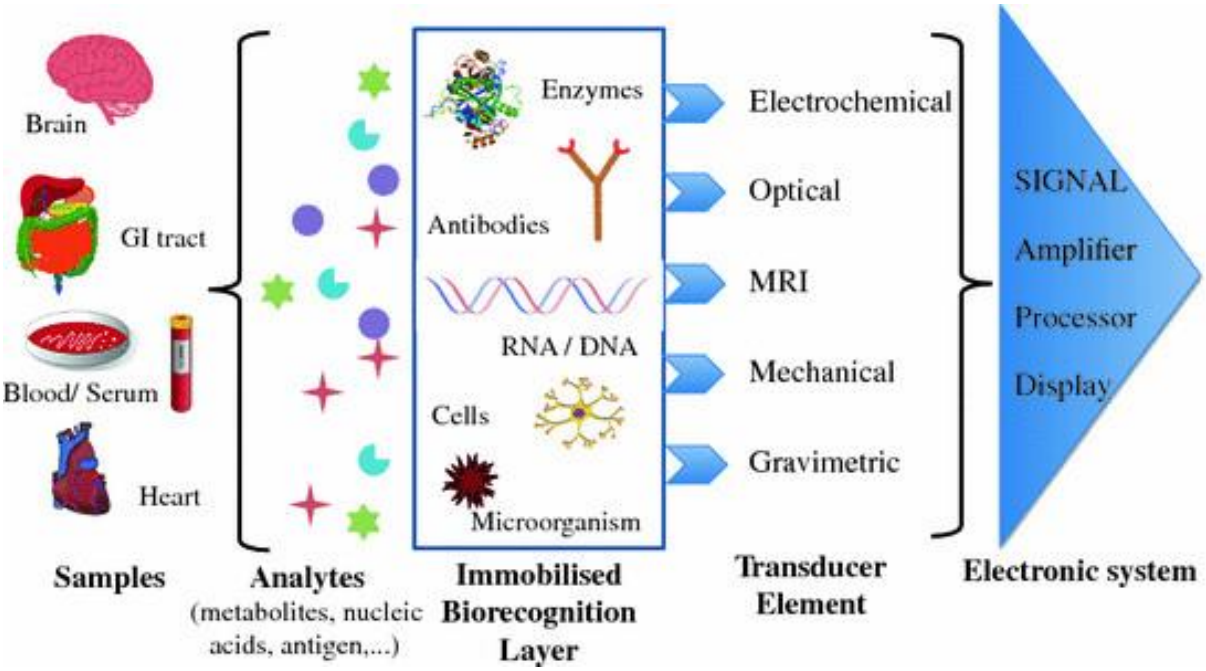

Figure 1.3. Scheme showing the components of a biosensor.

Based on the recognition elements used for the assays, the lateral flow assays can be classified as lateral flow immunoassays (LFIA) in which the recognition element is an antibody and nucleic acid based lateral flow biosensors (NABLFB) in which the bio recognition element is an oligonucleotide.

1.3.1. Lateral Flow ImmunoAssays (LFIA)

LFIA's are based on antigen-antibody immunoreaction and a pair of antibodies serving as detection and capture antibodies are generally used in this format for recognizing and capturing the analyte respectively. LFIA's are carried out in two major detection formats namely competitive and sandwich formats. In the competitive format, there is an immobilization of capture and control antibodies on the nitrocellulose membrane, labeled analyte is applied on the conjugate pad which competes with the sample analyte to bind to the antibodies on the nitrocellulose membrane. Thus,

this format is well suited for low molecular weight compounds which cannot bind two antibodies simultaneously. In the competitive format, the intensity of the test-line is inversely proportional to the analyte concentration. (Figure 1.4.)

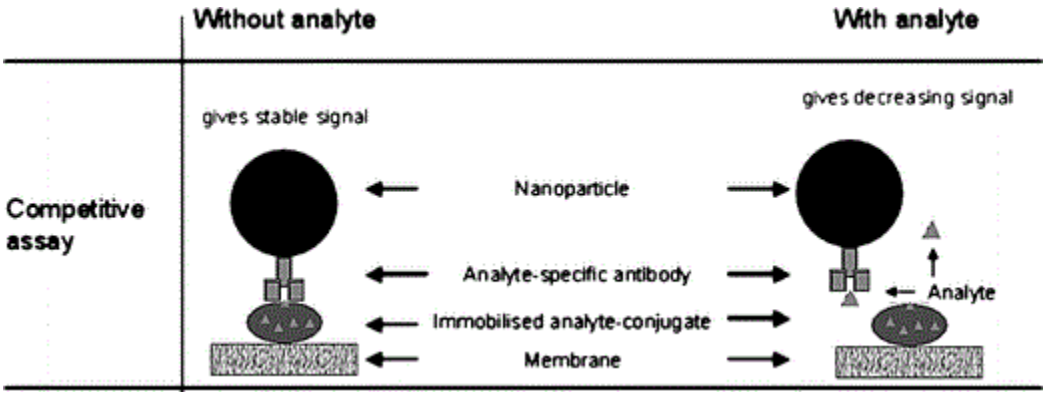

Figure 1.4. Typical format of competitive lateral flow immunoassay.[26]

Conversely, the sandwich format is generally used for the target analytes with multiple epitopes such as proteins. Analyte in this kind of sandwich assays should have multiple binding sites which could be recognized by the two different antibodies. A label conjugated with a reporter antibody is applied on the conjugate pad and capture and control antibodies are dispensed on the nitrocellulose membrane. The assay is initiated by the application of sample on the sample pad followed by the complex formation between the analyte and the reporter antibody on the label. As this complex continues to migrate along the strip, the capture antibody captures the complex by a second immunoreaction resulting in a detectable signal. Excess of the conjugates continues to move along the strip to be captured by the secondary antibody on the control line. In the sandwich assays, the target concentration is directly proportional to the signal intensity. (Figure 1.5.)

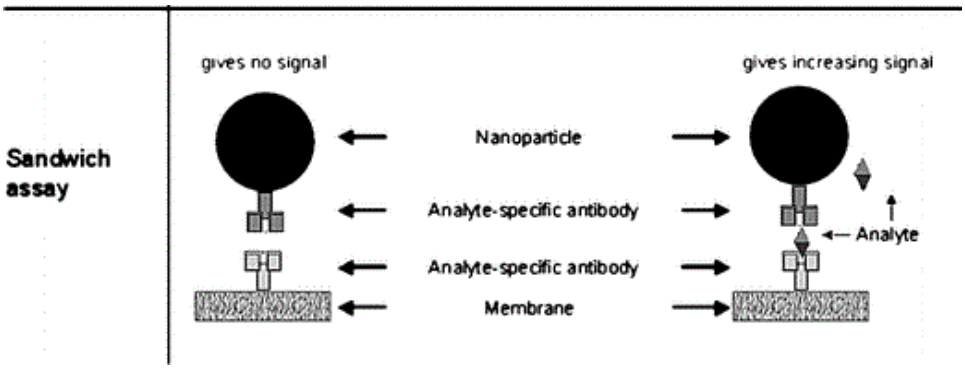

Figure 1.5. Typical format of sandwich lateral flow immunoassay.[26]

1.3.2. Nucleic Acid based Lateral Flow Biosensors (NABLFB)

NABLFB utilizes nucleic acid probes as the bio-recognition element. The target analyte typically is the oligonucleotide like the DNA, mRNA, miRNA which are among the nucleic acid secretions by the tumor cells when it comes to detection of cancer. The colored labels are conjugated to the detection oligonucleotide probe which is partially complimentary to the target analyte. Another half of the target analyte is complimentary to the biotinylated capture probe incubated with streptavidin thus facilitating its immobilization on the nitrocellulose membrane. When the target analyte is applied onto the sample pad, it moves along forming a complex with the label and eventually ending up in the sandwich formed on the test line. The working of the assay is similar to that of the sandwich assay of the LFA where the intensity of the test-line is directly proportional to the concentration of the target analyte.[27] (Figure 1.6.)

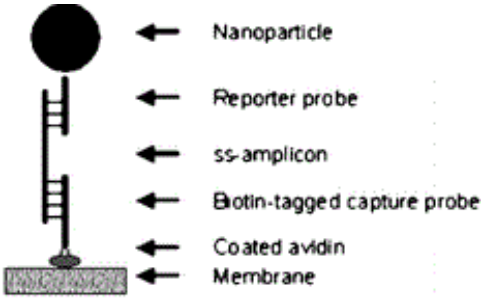

Figure 1.6. Typical format of the sandwich NABLFB.[26]

NABLFB has its own advantages over the LFI. In the LFI since antibodies are used, the inherent instability of the antibodies require the strips to be refrigerated. There is also the issue of cross reactivity, high production cost and loss of affinity when chemically modified.[28]NABLFB on the contrary because of the stability of nucleic acids can be kept under less rigorous conditions for longer periods and this comes in handy when testing is to done in remote areas. These utilize nucleic-acid probes as the bio-recognition element which are referred to as aptamers. Aptamers are obtained from a random pool of oligonucleotides in a process referred to as systematic evolution of ligands by exponential enrichment (SELEX). Various aptamers have been developed that bind biologically important proteins,[29-32] whole cells,[33,34] bacteria,[35,36] metal ions,[37,38] and other small molecules.[39,40] Aptamers have very high affinity for their targets and can have dissociation constants in low nano molar ranges.

1.4. Applications of NABLFB in Sensing

The versatility of the NABLFB (Figure 1.7.) has been shown over the years as various applications have been reported for the detection of biologically important proteins, nucleic acids, cells and pathogens.

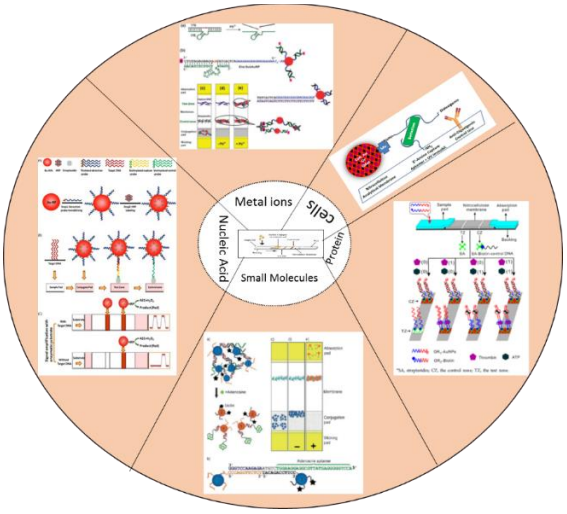

Figure 1.7. Versatility of NABLFB in the detection of various targets.

In the area of environmental monitoring, it has been used in the detection of heavy metals that pose a major health problem.

1.4.1. NABLFB in Nucleic Acid Detection

Nucleic acid detection is important for diagnosis of genetic disorders, detecting the presence of pathogens and even the detection of genetically modified species. Molecular detection of DNA sequences provide a more accurate and generally faster method of detecting pathogen presence than the conventional culture based methods.[41,42] Among all the POC devices, NABLFB offer a POC device that is less expensive and a more user friendly format while maintaining sensitivity and selectivity. Previous lateral flow biosensors utilized antibodies immobilized on the test line to detect hapten labeled target nucleic acids or a sandwich assay that utilized an up-converting phosphor as a reporter to detect single-stranded DNA on a NABLFB was also reported.[43-44](Figure 1.8.)

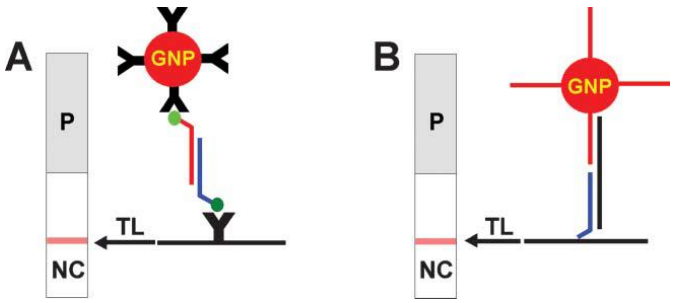

Figure 1.8. (A) Section through test line (TL) of a NABLFB based on antibodies and haptens (green circles). (B) Section through test line of antibody-free lateral flow device.[45]

In spite of the good sensitivity achieved by NABLFB, they still require some form of target nucleic acid amplification prior to the testing on NABLFB. Various clinically important pathogens have been detected on NABLFB using PCR amplified sequences[46] and also other polymerase mediated amplification techniques like reverse transcription loop-mediated isothermal

amplification.[47-48] The major advantage of isothermal amplification is that it is carried out at a single temperature and thus doesn't require costly equipment as PCR.

PCR products analyzed by gel electrophoresis can only indicate amplicon length. DNA hybridization analysis on the contrary gives information on sequence homology thus finding its use in the detection of single nucleotide polymorphism (SNP). SNP hybridization reactions are based on probes that selectively capture target nucleic acid strands in a sandwich assay. NABLFBs that are able to detect single nucleotide mutations have been reported.[49-50]

1.4.2. NABLFB in Protein Detection

The first report of protein detection on a NABLFB was for the detection of thrombin; where in the thrombin in blood plasma was captured in a sandwich assay between a capture aptamer immobilized on the test line and a primary aptamer conjugated to AuNP. The setback with this method is that this assay requires multiple binding sites on the target protein enabling the binding to both capture aptamer and conjugated primary aptamer.[51]

A new improved computational NABLFB was reported based on aptamer assembly in the presence of target. The target protein induced the assembly of split aptamers where in one half was conjugated on to AuNP and the other half was immobilized on the test zone. It was able to give positive results in the presence of either thrombin or ATP.[52]

1.4.3. NABLFB in Metal Detection

Metal detection is very important as metals play a variety of roles in our day to day lives. Various metals have been detected using NABLFB's. A dipstick method was developed for the detection of Pb^{+2} in paints using non-crosslinked gold nanoparticle-DNAzyme conjugates.[53] The same principle of DNAzyme cleavage was also used for the detection of Cu^{2+}. A NABLFB was

used for detecting Cu^{2+} with Cu^{2+}-specific DNAzyme and Au-NPs.[54] NABLFB was also used for the detection of mercury using Gold nanoparticles and thymine rich DNA probes.[55]

1.4.4. NABLFB for the Detection of Whole Cells

Since the introduction of Selex (Systematic Evolution of Ligands by Exponential Enrichment) numerous aptamers have been developed for various cancer cells and pathogenic bacteria. These have offered a much more stable alternative to antibody based systems which have been the gold standard in clinical detection of whole cells. Not much work has been done on the detection of whole cells on NABLFB. The only work reported so far in this area was for the detection of Ramos cells where a pair of aptamers that were able to specifically bind to the cells. Ramos cells were captured in a sandwich assay with the AuNP-aptamer conjugate acting as the optical indicator of Ramos cell presence. This method was subsequently used for the detection of Ramos cells in spiked blood samples.[56]

Direct detection of bacteria using NABLFB has been recently reported. In this work, a dual labeled E.coli aptamer with biotin at 5' end and digoxigenin at 3' end conjugated to streptavidin coated AuNP and an amino modified aptamer immobilized on nitrocellulose membrane captured the cells in a sandwich assay. This approach was further used for the detection of *Listeria monocytogenes* and *Salmonella enteric*.[22]

1.4.5. NABLFB for the Detection of Small Molecules

Adenosine was detected on the NABLFB using aptamer-DNA-AuNP aggregates. Adenosine aptamer-DNA-AuNP conjugates were dispensed on the conjugate pad. In the presence of adenosine, the aptamer undergoes conformational change to bind to adenosine. This causes the AuNP cluster to disassemble leading to its capture by the biotinylated AuNP on the test zone togive

a red line whose intensity indicates the adenosine concentration. Same approach was also used for the detection of cocaine.[57]

1.5. Nanolabels Used

Different types of nanoparticle labels have been used for the detection of a variety of targets using lateral flow biosensors. Various factors including the required sensitivity of the assay, the cost associated, the type of detection method desired can influence the choice of nanolabels used for the detection. Labels can be colored or fluorescent with different sizes ranging anywhere between 15nm-800nm (Figure 1.9.). The size is chosen based on both assay type and the target to be detected. The nanolabels that have been used for the detection are often made of gold, carbon, selenium, latex and phospholipids.

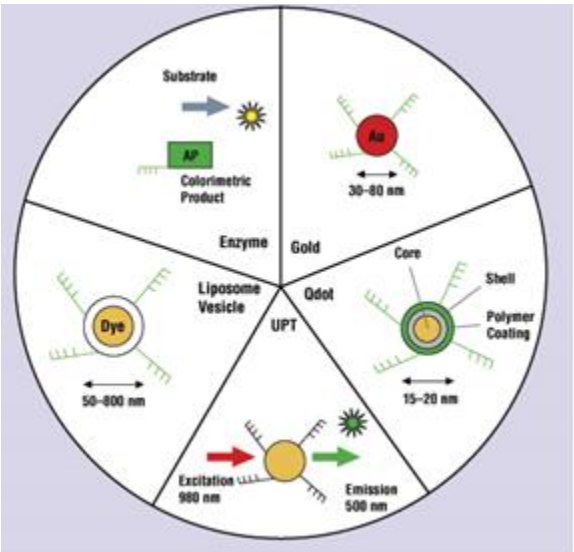

Figure 1.9. Different nano labels used on NABLFB.

1.5.1. Gold Nanoparticles (AuNPs)

Gold nanoparticles have been widely used for the detection of various targets on NABLFB's. They have been used for the detection of thrombin, where AuNPs have been conjugated to the aptamers. This assay demonstrates successful detection of thrombin proving that

the aptamers can replace antibodies maintaining the sensitivity.[51] It was also applied for the detection of DNA binding protein in which the target protein binds to the DNA aptamer that is coated on the AuNP to form the AuNP-DNA protein complexes which are then captured on the test line facilitating the visual detection of target protein.[58]Using the same principle, miRNA[59] and specific sequences in bacterial 16S ribosomal RNA[60] were also detected.

1.5.1.1. Signal Amplification in AuNP based NABLFB

Traditional NABLFBs which used gold nanoparticles as labels suffered from detection limits ranging from lower nM to mM. To be able to successfully use NABLFBs for real diagnostic applications and for other purposes like environmental monitoring, it is imperative to lower the detection limits to lower nM to sub fM ranges. Over the years, various improvements have been made to the traditional AuNP based NABLFB increasing the detection limits.

AuNPs have been used for the detection of nucleic acids in conjunction with isothermal strand displacement reaction which gave them improved sensitivity and very low detection limits compared to traditional colorimetric assay.[50] Gold enhancement after capture of target has been used in detection of target genetic DNA sequence specific to *Enterohemorragic E.coli*.[61] This method was also utilized in RNA detection.[62]

Silver enhancement similar to gold deposition has also been applied on NABLFB's.[63] Rohrman and co-workers compared gold enhancement and silver enhancement and realized the former increased the signal to noise ratio by about 10% more than the latter.[62] Dual AuNPs have also been used for signal amplification in lateral flow biosensors.[64-65] The test zone intensity is increased by two AuNP-DNA conjugates leading to increased accumulation of AuNP. Detection limit was improved by 30 times as compared to detection with single AuNP. This allows one-step detection of analyte and thus reduces solvent handling as seen in silver and gold enhancement.[62,65]

Taking advantage of the functional groups on the surface of AuNPs, they have been widely used in the conjugation with other labels like HRP. Mao and co-workers introduced a NABLFB based on enzyme-DNA AuNP dual label for ultra-sensitive detection of DNA. In this experiment AuNP were dually labeled with HRP and probe DNA sequences. Target DNA sequences were captured in a sandwich assay with the dual labeled AuNP serving as colorimetric indicators. HRP substrate was then introduced which served to amplify the signal enabling lower detection limits of 0.1pM [66] which was about 500 times less than the previous work.[67] This method was further enhanced and fine-tuned by the introduction of sodium dodecyl sulfate in the preparation of thiolated DNA and HRP immobilized AuNP conjugates.[21] Detection limit of 0.01pM was achieved without instrumentation which was the lowest among all the previously reported AuNP- based NAFLFBs. HRP labeled DNA was also used for the detection of nucleic acids. In this work, streptavidin was labeled with biotinylated DNA capture probe. The streptavidin was subsequently coupled to biotinylated HRP. Upon capture of the HRP labeled DNA probe, substrate was introduced which was oxidized by the enzyme. This technique allowed detection limits of 0.5fmol/ul (.5nM) to be achieved.[68]

1.5.2. Fluorescent Nanoparticles

Fluorescent nanoparticles have gained importance lately due to sensitivity enhancement detection assays. Dye-doped silica nanoparticles were used as a fluorescent label for the detection of nucleic acids. The experimental results showed that the developed lateral flow assay was more sensitive compared with the traditional colloidal gold test strips. The limit of detection for the fluorescent lateral flow assay developed is approximately 0.066 fmols as compared to approximately 15 fmols for the colloidal gold.[69] Juntunen and coworkers successfully demonstrated that the fluorescent nanoparticles yielded 7- and 300-fold better sensitivity compared

with colloidal gold after comparing to the performance of fluorescent europium (III) [Eu(III)] chelate dyed polystyrene nanoparticles and colloidal gold particles in lateral flow assays.[70]

Use of Quantum dots in the area of fluorescent detection is also an emerging field. Quantum dots have been used for the detection of food-borne pathogen for highly sensitive aptamer-Qdot LF strip assays. The best *E. coli* aptamer-LF system yielded a visible limit of detection (LOD) of ~3,000 *E. coli* 8739 and ~6,000 *E. coli* O157:H7 in buffer. These LODs were reduced to ~300–600 bacterial cells per test respectively by switching to a Qdot 655 aptamer-LF system.[22]

1.5.3. Other Nanoparticle Labels

Phospholipids which can form closed nano vesicles called liposomes offer a unique advantage of being able to encapsulate various signal markers ranging from enzymes, substrates, electrochemical markers to dyes. Using liposomes, a quantitative universal biosensor on the basis of oligonucleotide sandwich hybridization for the rapid (30 min total assay time) and highly sensitive (1nM) detection of specific nucleic acid sequences. They used a universal dye-entrapping liposome nano vesicle as their nanolabel for the detection of synthetic DNA sequences from *B. anthracis, C. Parvum* and *E. coli* with very low detection limits.[71] Liposomes encapsulating the dye, sulfo rhodamine B have also been used for the detection of viable *Mycobacterium avium* subsp. *Paratuberculosis* (MAP) cells in fecal samples.[72]

Up-converting Phosphor Technology (UPT) particles were used as reporters in lateral-flow (LF) assays to detect single-stranded nucleic acids. Corstjens *et al*. reported that the UPT reporter particles provide improved sensitivity, simplicity of detection, quantification and multiplexing enabling the detection of 0.1fmol of a specific single-stranded nucleic acid target in a background of 10µg fish sperm DNA.[44] The same method was also used to detect PCR-amplified HPV16 sequences with convenient and reproducible detection of 10 pg (30 attamol) of target.[73]

1.6. Aims and Objectives of this Study

The main aim of this dissertation is to explore a rapid, inexpensive, simple and an easy-to-use platform for the detection of DNA and miRNA biomarkers eventually leading to early detection of a disease condition. In the field of biomedicine, detection of nucleic acid biomarkers is of utmost importance. In diseases like cancer, the tumor cells release their nucleic acid secretions into the blood. Quantification of these nucleic acid biomarkers (DNA, mRNA, miRNA) using bioassays that can progressively monitor the progression of the disease in the blood samples of the cancer patients could serve as an efficient remedy for the early detection of cancer.

In light of this, effort has been put towards developing affordable lateral flow biosensors using various labels to find the best suitable condition leading to ultrasensitive detection of nucleic acids. Colorimetric lateral flow biosensors using gold nanoparticle as a label is the most common and well known format available in the market in the form of pregnancy strip. Though there are quite a number of gold based nucleic acid detection assays reported due to the perks in terms of ease of preparation and low cost, the detection limit acquired remains questionable when it comes to trace analysis. So, in the field of molecular diagnostics, there still exists a need for the development of sensitive, selective, efficient and affordable method for the detection of nucleic acid biomarkers.

Various other labels which can be integrated to different detection modes like colorimetric, fluorescent and chemiluminiscence have been exploited in this dissertation to improve the overall analytical performance of the lateral flow biosensor. To improve the applicability of these sensors in the molecular diagnostics, this research also focused on multiplex detection of miRNA biomarkers directly from the pancreatic cancer patient samples.

- A rapid and highly sensitive approach for visual detection of microRNA (miRNA) using a gold nanoparticle coated silica nanorod label (AuNP-SiNR) on a lateral flow biosensor was developed. The visual detection limit of miRNA on the lateral flow nucleic acid biosensors was enhanced dramatically and the detection limit was six times lower with the AuNP-SiNR than that of the AuNP-based lateral flow nucleic acid biosensors.
- A fluorescent lateral flow assay using carbon nanoparticles for the rapid detection of DNA sequence was developed. The FCN-based NABLFB in this research is by far the most sensitive method reported for the rapid detection of DNA sequence on a lateral flow device without additional signal amplification and the use of conventional fluorophores and QDs. We demonstrated that the biosensor was able to detect a minimum concentration of 0.4 fM DNA. The resulting fluorescent lateral flow assay presents a rapid, low-cost and a very sensitive DNA detection method without the need for target amplification or any expensive instrumentation.
- A colorimetric enzyme based lateral flow assay for the detection of miRNA-210 was developed. Improved detection sensitivity was obtained by using Carbon nanotubes as carriers to load a large amount of enzymes. The more enzymes on the test zone resulted in color enhancement because of the colored insoluble precipitate formed after the enzyme-substrate reaction. The resulting colorimetric assay presents a rapid, low cost and an ultra-sensitive method for the detection of miRNA-210, a pancreatic cancer biomarker.
- A multiplex assay was developed for the detection of miRNA 16, miRNA 21, miRNA 196a as this is the reported miRNA panel for the detection of pancreatic cancer. Carbon nanotubes coated with the enzymes was used as the label for the simultaneous detection of the biomarker panel thus presenting a more specific miRNA detection method for PC.

2. GOLD NANOPARTICLE COATED SILICA NANORODS FOR SENSITIVE VISUAL DETECTION OF microRNA ON A LATERAL FLOW STRIP BIOSENSOR

2.1. Introduction

MicroRNAs (miRNAs) play important roles in numerous developmental, metabolic and disease processes for plants and animals.[74] By degrading miRNA transcripts or inhibiting protein translation, the gene expression is negatively regulated for a variety of fundamental biological processes, such as apoptosis, development, differentiation, and proliferation.[75] miRNA has been regarded as a useful biomarker for cellular events or early disease diagnosis. Several biological processes, such as developmental timing, proliferation, differentiation, metabolism, cell maintenance and tissue identity, are regulated by miRNA. Animals that fail to produce certain mature miRNAs are unable to survive or reproduce.[76-77] It has been estimated that the human genome contains hundreds of miRNAs which are thought to regulate thousands of protein-coding genes. miRNAs are highly specific for gene regulation in a sequence-specific manner.[78] Thus, the altered expression patterns for these molecules indicate the dysregulation of important biological processes, which is often the cause of disease. Current methods for detecting miRNA include northern blot analysis with radiolabeled probes; microarray-based methods; quantitative real-time polymerase-chain reaction-based approaches; *in situ* hybridization and high-throughput sequencing.[79] The disadvantages, such as utilizing harsh conditions for the sample pre-treatment and having a high experimental cost, hinder the use of these methods for all practical applications.[80-81] Preferably, an ideal detection method should be able to detect the target quantitatively with high sensitivity using small amounts of starting material; the method should be specific enough for reproducible detection of the target miRNA; and importantly, the detection should be easy to perform without the need for expensive reagents or equipment. The novel

miRNA detection strategies provide a powerful tool to not only depict the functions of these miRNA molecules in a variety of biological systems, but also to improve human health with early disease diagnostics.[82]

For point-of-care analysis of miRNAs, there are still great demands for innovative detection methods.[82] Lateral-flow biosensors are of considerable interest due to their wide application in the field of detections and their capability to obtain sequence-specific information in a faster, simpler and cheaper manner compared to traditional hybridization assays.[83] Recently, DNA-functionalized gold nanoparticles (GNPs) have been used to construct lateral flow strip biosensor (LFSB) for visual detection of nucleic acid segments including DNA and miRNA.[66,84] However, the applications of those GNP-based lateral flow nucleic acid biosensors are limited by the low sensitivities. More recently, a highly sensitive immuno chromatography strip biosensor using a GNP coated silica-nanorod (SiNR) label was reported by our group.[85] The detection limit of the strip biosensor was 50 times lower than that of a GNP-based strip biosensor. Herein, we report a lateral flow nucleic acid biosensor based on GNP coated SiNR label for visually detecting low concentrations of miRNA. SiNR is used as a carrier to load numerous GNPs for signal amplification on the lateral flow nucleic acid biosensors. The visual detection of miRNA on the NABLFB is enhanced dramatically due to the increased number of GNPs per DNA-RNA hybridization event. The detection limit for the GNP-SiNR-based NABLFB is six times lower than that of GNP-based lateral flow nucleic acid biosensors. The promising properties of the GNP-SiNR-based lateral flow nucleic acid biosensors are reported in following sections.

2.2. Experimental Section

2.2.1. Apparatus and Reagents

The Airjet AJQ 3000 dispenser, Biojet BJQ 3000 dispenser, Clamshell Laminator and the Guillotine cutting module CM 4000 were from Biodot Ltd. (Irvine, CA). Streptavidin, $HAuCl_4$, sucrose, tween 20, triton X-100, trisodium citrate, deoxyadenosine triphosphate (dATP), polyvinylpyrrolidone (PVP), hydroxylamine hydrochloride,1-pentanol, TEOS, sodium chloride-sodium citrate (SSC) buffer 20x concentrate (pH 7.0), and PBS (pH 7.4) were purchased from Sigma-Aldrich (St. Louis, MO). All the other reagents were purchased from Sigma and used without further purification. Glass fibers (GFCP000800), cellulose fiber sample pads (CFSP001700), laminated cards (HF000MC100) and nitrocellulose membranes (HFB 18004 and HFB 24004) were purchased from Millipore (Billerica, MA). The target miRNAs and oligonucleotide probes used in this study were obtained from Integrated DNA Technologies, Inc. (Coralville, IA). The oligonucleotide sequences used for the miRNA detection were as follows:

Target miRNA-215 (*has-miR-215*): 5'-rArUrG rArCrC rUrArU rGrArA rUrUrG rArCrA rGrArC-3'[16]

Capture probe: 5'-ATA GGT CAT/3Bio/-3'

Control probe: 5'- /5Biosg/TGG ACA GAC- 3'

Detection probe: 5'-/5ThioMC6-D/GTC TGT CAA-3'

All the chemicals used in this assay were of analytical reagent grade. All other solutions were prepared using ultrapure water from a millipore milli-Q water purification system (Billerica, MA).

2.2.2. Preparation of Gold-Nanoparticle Coated Silica Nanorod (GNP-SiNR)

2.2.2.1. Synthesis of Silica Nanorod (SiNR)

First, the SiO_2 core was synthesized through a reverse-emulsion method. Two grams of PVP were dissolved in 30.00 mL of pentanol in a conical flask by sonication for about 30 min. To the above mixture, 3.00 mL of 95% ethanol was added along with 840 µL of ultrapure water and 0.2 mL of 0.17 M sodium citrate. In the next step, 0.3 mL of TEOS and 0.5 mL of NH_4OH were added to stabilize the core, and the solution was left for 18 hr under stirring. The surplus solution was removed by centrifuging the solution at 11,000 rpm for 30 min followed by two ethanol washes. This synthesis results in the formation of SiNR which was finally suspended in water (10 mg mL^{-1} SiNR in water).

2.2.2.2. Preparation of Gold-Nanoparticle Seeds (GNP)

Typically, 4.00 mL of 1% $HAuCl_4$ solution were added to 100.00 mL of H_2O in an ice bath, followed by the addition of 0.50 mL of 0.20 M K_2CO_3 to reduce Au(III) to Au(I). The solution is then stirred for 10 min until its color changes from yellow to light yellow or colorless. Then, 1.00 mL of freshly prepared $NaBH_4$ (0.50 mg/mL) was slowly added. The formation of a reddish solution indicated the successful synthesis of gold seeds.

2.2.2.3. Synthesis of GNP-SiNRs

The GNP-SiNRs were prepared according to the slight modifications.[86] An aliquot with 1.00 mL of 10.00 mg/mL SiNR solution was added to a 40.00 mL gold-seed solution, and the mixture was stirred vigorously for 20 min. Surplus gold seeds were removed by centrifugation at a speed of 6,500 rpm for 15 min. The obtained, reddish precipitate was gold-seed-decorated SiNRs and was re-dispersed in 10.00 mL water. In the gold-shell growth process, 4.00 mL of 1% $HAuCl_4$ solution and 0.025 g of K_2CO_3 were added to 90.00 mL water. The mixture was stirred until it

turned to light yellow or colorless. Then, 10.00 mL of a gold-seed-decorated SiNR solution, 1.00 mL of 0.5 M hydroxylamine hydrochloride, and 1.00 g of PVP were sequentially added to the growth solution. After overnight incubation, the solution was centrifuged at 6,500 rpm for 15 min followed by three water washes.

2.2.3. Preparation of DNA-GNP-SiNR Conjugate

Ten microliters of dATP was added to 1 mL of threefold-concentrated GNP-SiNR solution (The final concentration of dATP is 7.05 μM.), and the mixture was incubated at room temperature for 20 min. Then, fifteen microliters of 1% SDS were slowly added to the mixture, and it was incubated on a shaker for another 10 min. Fifty microliters of 2.0 M NaCl was added at a rate of 2.0 μL every 2-3 min. Then, one OD thiolated DNA (detection probe) was added and incubated for 3 hr in a water bath at 60 ℃. After the incubation, the mixture was centrifuged at 8,000 rpm for 5 min, and the supernatant was discarded. Then, the DNA-GNP-SiNR conjugates were washed with 1 mL of PBS 3 times; the resulting pellet was re-suspended in 1 mL eluent buffer (20 nM $Na_3PO_4 \cdot 12H_2O$, 5% BSA, 0.25% Tween 20 and 10% sucrose).

2.2.4. Preparation of Streptavidin-Biotinylated DNA Probe Conjugate

Two hundred microliters of 2.5 mg mL^{-1} streptavidin were mixed with 50 nmoles biotinylated DNA probe (capture probe or control DNA probe). The mixture was incubated at room temperature for 1 hr. After adding 500 μL PBS to the mixture, the solution was centrifuged for 20 min at 6,000 rpm at 4 ℃. This step was repeated 3 times. The remaining solution, in a filter, was diluted to 600 μL with PBS.

2.2.5. Preparation of Lateral-Flow Strip Biosensor

The lateral flow strip biosensor consisted of four components: sample application pad, conjugate pad, nitrocellulose membrane, and absorbent pad.[21] All components were mounted on a

common backing layer (typically an inert plastic, e.g., polyester) using the clamshell laminator (Biodot; Irvin, CA). The sample application pad (17 mm × 30 cm) was made from glass fiber (CFSP001700, Millipore) and treated with a Tris-HCl solution (pH 8.0) containing 0.23% Triton X-100, 0.05 M Tris-HCl, and 0.15 M NaCl. After drying the pad at 37 °C for 2 hrs, they were stored in desiccators at room temperature (RT). The streptavidin-biotinylated DNA probes were used to prepare the test zone and the control zone on the nitrocellulose membrane, and the DNA-GNP-SiNR conjugates were dispensed on the conjugate pad. The distance between the test and control zones was 3 mm. The membrane was then dried at 37 °C for 1 hr and stored at 4 °C in a dry state. A clamshell laminator was used to assemble all the components (the sample pad, conjugate pad, nitrocellulose membrane, and absorption pad) on a plastic adhesive backing (60 mm × 30 cm) which is the final step in the preparation of LFSB. Each part overlapped 2 mm to ensure that the solution could migrate through the strip during the assay. Strips with a 3-mm width were cut using the guillotin CM 4000 cutting module.

2.2.6. Analytical Procedure

Sample solutions containing various concentrations of target miRNA were prepared in an eightfold, diluted SSC buffer containing 4% BSA. In a typical test, one hundred microliters of the sample solution were added to the sample pad region of the LFSB. The solution migrated toward the absorption pad to hydrolyze DNA-GNP-SiNR and formed miRNA-DNA-GNP-SiNR complexes. The complexes moved along the strip toward the test zone and were captured by the capture DNA probe on the test zone. The accumulation of GNP-SiNRs resulted in the color change (to purple) at the test zone. After waiting for 10 min, 30 µL running buffer (1/8 SSC + 4% BSA) were added to the sample pad to wash the LFSB. For quantitative measurements, a digital camera

was used to take the photo images of the LFSB, and the optical intensity of the test bands was read using the Image J Viewer software.

2.3. Results and Discussion

2.3.1. Principle of Detection Using the GNP-SiNR-based Lateral Flow Strip Biosensor

In this study, gold-nanoparticles coated silica nanorod (GNP-SiNR) was used as a new nanolabel for sensitive visual detection of miRNA on the lateral-flow strip biosensor (LFSB). SiNRs with a length of 3.4 to 7.0 μm were prepared with a typical reverse-emulsion method (**Fig. 2.1.(A)**). A two-step procedure, with GNP seeding and growth, was employed to load the GNP layer on the SiNR surface. The GNPs with a diameter of 9.7±1.6 nm were first adsorbed by the PVP polymer on the SiNR surface (GNP seeding); the growth of GNPs was performed in a growth solution containing $HAuCl_4$ and hydroxylamine hydrochloride. **Figure 2.1.(B)** presents the typical SEM images of GNP-SiNRs. One can see a layer of GNPs with a diameter of 16.7 ± 2.4 nm (see insert of **Fig 2.1.(B)**) covered on the SiNR surface. It was found that the GNP-SiNRs would be well-dispersed in the PBS buffer.

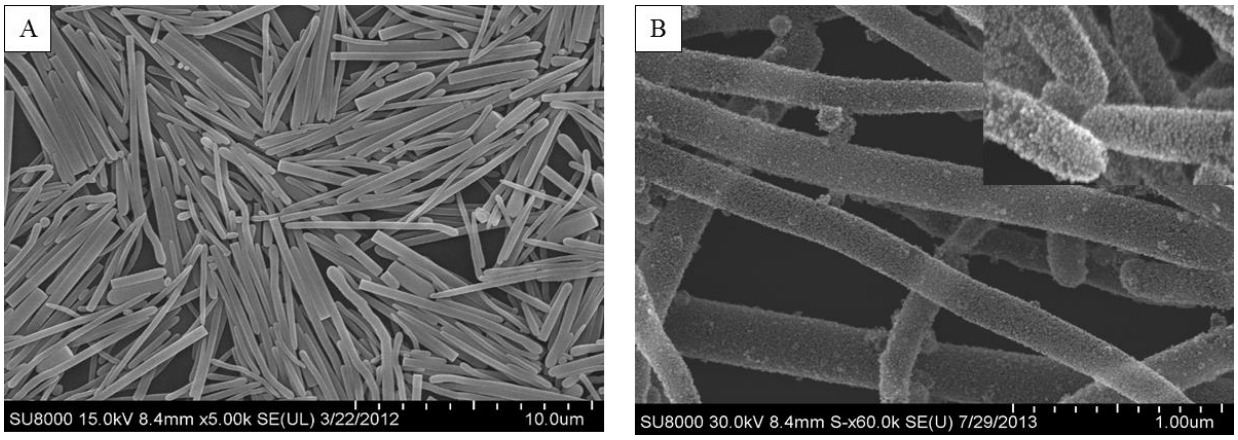

Figure 2.1. (A) SEM images of silica nanorods (B) Gold-nanoparticle-coated silica nanorods.

The principle of miRNA detection using the GNP-SiNR nanolabels is based on on-strip DNA-RNA hybridization reactions to form sandwich-type DNA-miRNA-DNA-GNP-SiNR

complexes, which are captured on the test zone of the lateral flow strip biosensor; the change in the color on the test zone due to the accumulation of GNPs enables the visual detection of miRNA (**Fig 2.2**). One can expect that the use of GNP-SiNR nanolabels would increase the number of the captured GNPs per DNA-RNA hybridization event, thus an enhanced visual effect. The self-assembly reaction via the Au-S bond results in the immobilization of the thiolated detection DNA probe on the GNP surface of the GNP-SiNR (**Fig 2.2.(A)**). The DNA-GNP-SiNR conjugates were dispensed on the conjugate pad of the lateral flow strip biosensor. Streptavidin-biotinylated capture DNA probe (complementary with a part of miRNA target) and control DNA probe(complementary with detection DNA probe on the GNP surface) were pre-dispensed on the nitrocellulose membrane to form test zone and control zone, respectively (**Fig 2.2.(B)**). The sample solution containing the target miRNA was applied on the sample pad (**Fig 2.2.(C).a**). The sample solution migrates by capillary action and comes in contact with the DNA-GNP-SiNR conjugates on the conjugate pad. The miRNA binds with the detection DNA probe on the GNP surface to form the miRNA-DNA-GNP-SiNR complex through a RNA-DNA hybridization reaction (**Fig 2.2.(C).b**). As the formed complexes continue to move along the strip by capillary action, they are captured by the capture DNA probes on the test zone. Thus without any instrumentation, the accumulation of GNP-SiNRs leads to the color change of the test zone, enabling visual detection of miRNA. The excess of DNA-GNP-SiNR conjugates continue to migrate and pass the control zone, where the control DNA probe (complementary with the detection DNA probe) was immobilized.

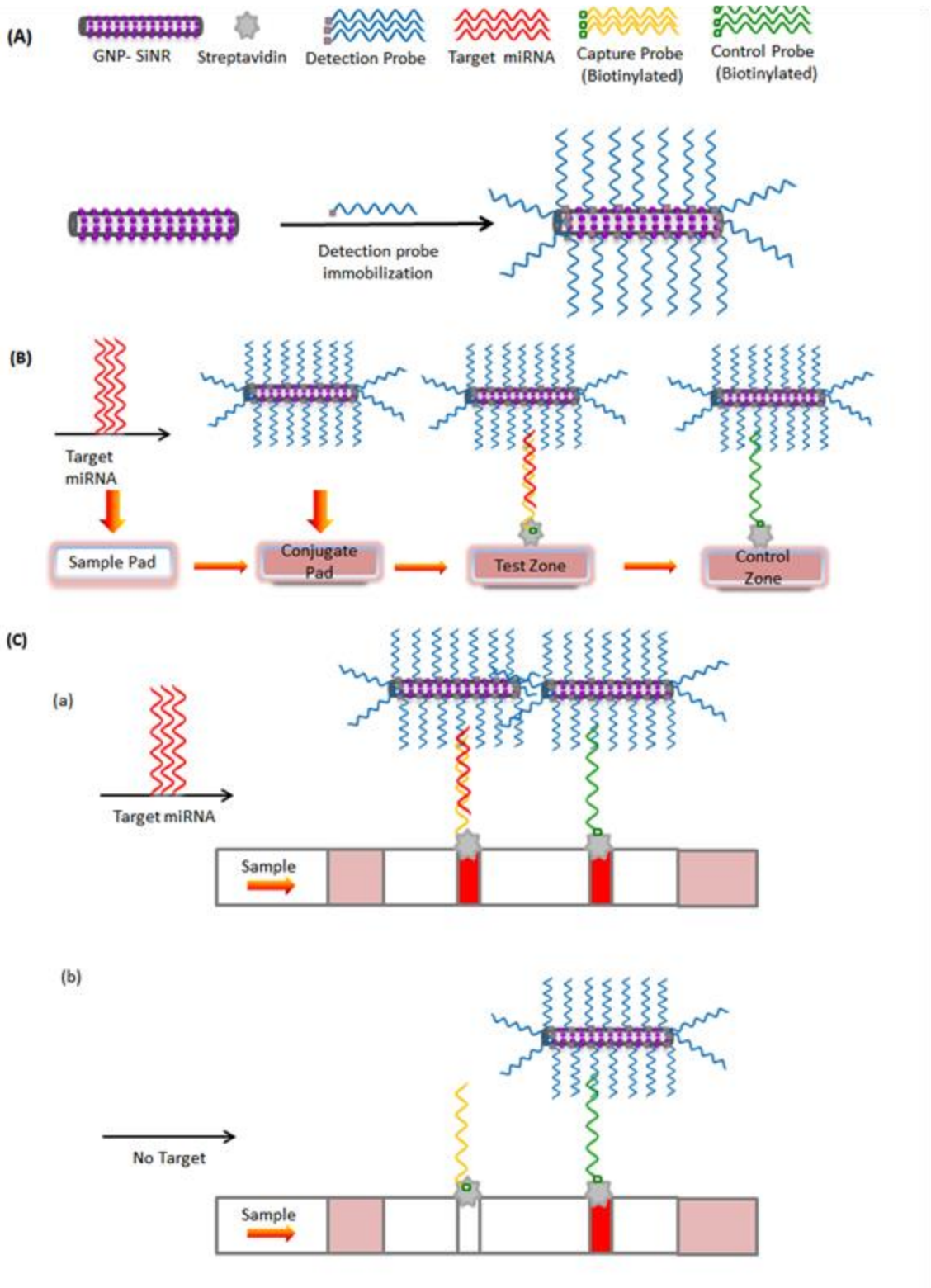

Figure 2.2. Schematic illustration of the configuration of lateral flow biosensor and the principle of the test.

Then, a second colored band forms as the excess DNA-GNP-SiNR conjugates are captured by the hybridization events between the detection DNA probe and the control DNA probe (**Fig. 2.2.(C).a**). No band was observed on the test zone indicating the absence of miRNA. A band observed on the control zone is an indication that the lateral flow strip biosensor is working properly (**Fig. 2.2.(C).**b).

As a proof of concept experiment, we tested the responses of 0-nM miRNA (control), 5-nM miRNA, 50-nM non-complementary miRNA and the mixture of 5-nM miRNA and 50-nM non-complementary miRNA on the GNP-SiNR-based lateral flow strip biosensors. **Figure 2.3.(A)** presents the photo images of the lateral flow strip biosensors after the completed assays. There was no test band observed with the 0-nM miRNA and the 50-nM non-complementary miRNA while a distinct, purple band appeared in the presence of 5.0-nM miRNA. The results indicated that the proposed GNP-SiNR-based lateral flow strip biosensor would detect miRNA selectively. The selectivity was further demonstrated by detecting the response of 5-nM miRNA in the presence of 50-nM noncomplementary miRNA. It was found that the presence of excess non complementary miRNA does not affect the signal of target miRNA.

To demonstrate the signal amplification of GNP-SiNR nanolabels, we compared the optical responses of 0.1-nM miRNA on the GNP and GNP-SiNR-based lateral flow strip biosensors. (**Fig 2.3.(B)**). The signal-to-noise (S/N) ratio of the GNP-SiNR-based lateral flow strip biosensor was almost six times higher than that of the GNP-based lateral flow strip biosensor. Such a significant enhancement in S/N ratio was ascribed to the higher number of captured GNPs per hybridization event on the lateral flow strip biosensor test zone. The inset of Fig. 3B presents the typical images of GNP- and GNPs-SiNR-based lateral flow strip biosensors in the presence of 0.1-nM miRNA. A distinct, purple band was seen on the test zone of the GNP-SiNR-based lateral

flow strip biosensor while a weak, red band was observed on the test zone of the GNP-based lateral flow strip biosensor. The purple color was ascribed to the large size of the GNPs on the GNP-SiNR conjugates.

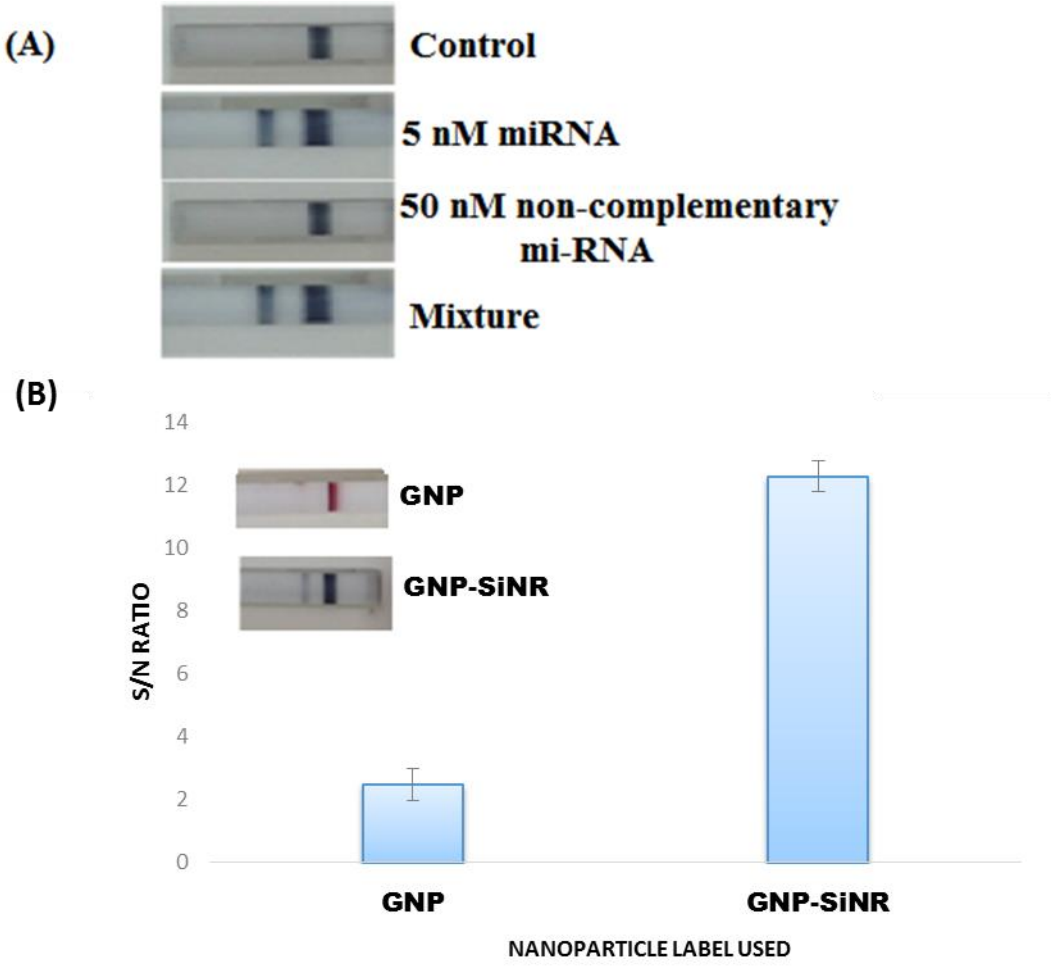

Figure 2.3. (A) Typical photo images of lateral flow strip biosensors in the presence of 0-nM miRNA (control), 5.0-nM miRNA, 50-nM non-complementary miRNA and the mixture of 5.0-nM miRNA +50-nM noncomplementary miRNA. Assay time: 30 min. (B) Histogram for the response of 0.1-nM miRNA using GNP and GNP-SiNR nanolabels. Inset: Corresponding photo images of the GNP-based (above) and GNP-SiNR-based lateral flow strip biosensor (below).

2.3.2. Optimization of Assay Parameters

Analytical parameters, including the volume of the DNA-GNP-SiNR on the conjugate pad, the quantities of capture DNA probes on the test zone and the components of the running buffers,

would affect the lateral flow strip biosensor's response. First, we studied the effect of the DNA-GNP-SiNR conjugate volume on the S/N ratio of the lateral flow strip biosensor, which was the ratio of the test-line intensities in the presence of a particular concentration of miRNA versus the absence of miRNA. To obtain the best S/N ratio, the DNA-GNP-SiNR on the conjugate pad was optimized by loading different volumes of DNA-GNP-SiNR on the conjugate pad. **Figure 2.4.(A)** presents the effect of conjugate volume on the S/N ratio of the lateral flow strip biosensor. It can be seen that the S/N ratio increased with the increase of conjugate volume up to 5.0 µL; a further increase resulted in a decrease of the S/N ratio. The decrease of S/N ratio at a larger conjugate volume may be attributed to a saturation of signal intensity and increased nonspecific adsorption due to the presence of excess conjugates. Therefore, 5.0 µL of DNA-GNP-SiNR conjugate was used as the optimal conjugate volume throughout the entire study.

The amount of capture DNA probes at the test zone of the lateral flow strip biosensor also affects the response of miRNA. In the current study, the quantities of capture DNA were optimized by dispensing different amounts of streptavidin-biotinylated DNA complexes. The effect of the capture DNA amount (dispensing cycles) on the lateral flow strip biosensor's S/N ratio is shown in **Fig 2.4.(B).** The highest S/N ratio was obtained with four dispensing cycles, which was then used in the following assays. The decreased S/N with more dispensing cycles may be caused by the increased background signal.

The nitrocellulose membrane is one of the most important materials to prepare LFSB. There are two types of nitrocellulose membranes: 3-min and 4-min membranes. The time indicates the movement time of the sample solution from the sample pad to the absorption pad. We compared the S/N ratios of the LFSBs **(Fig 2.4.(C))** and found that the 3-min membrane showed a higher S/N ratio and was a suitable membrane for the movement of GNP-SiNR.

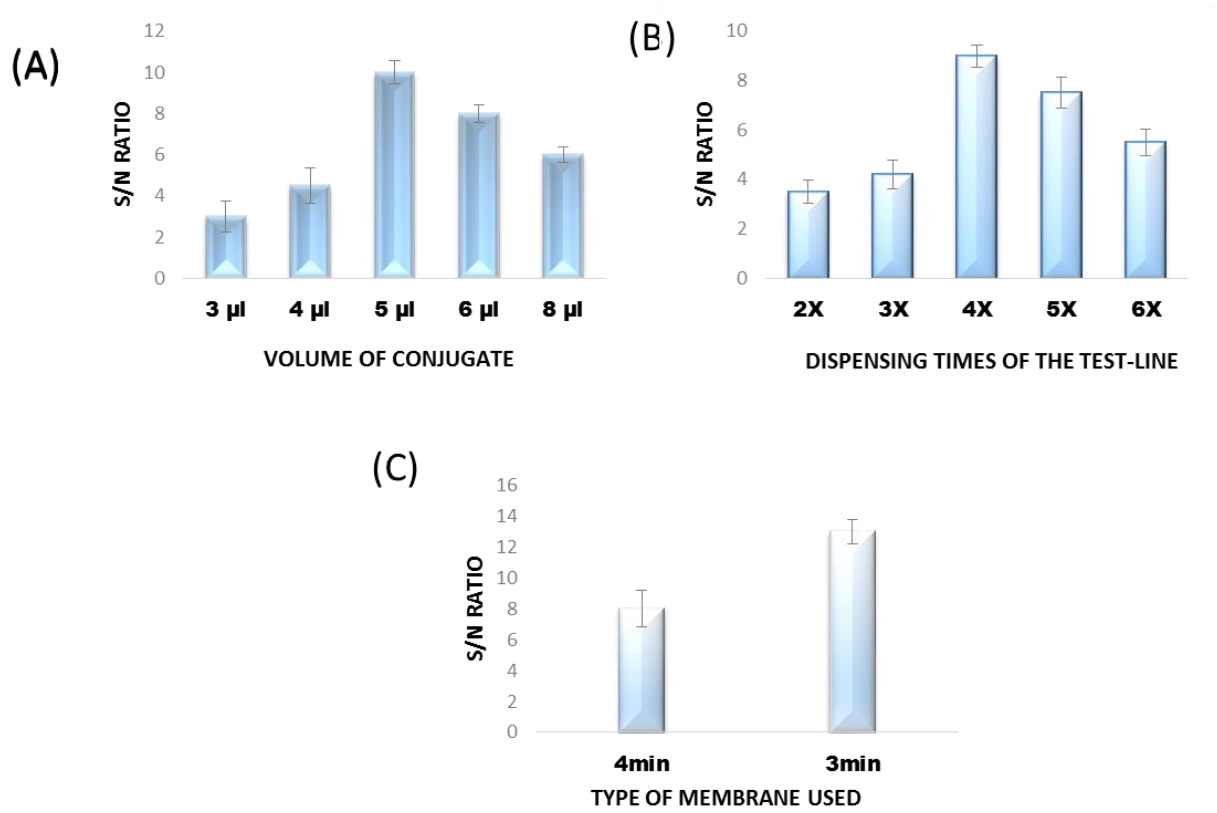

Figure 2.4. (A) Effect of conjugate volume on the response of LFNAB (B) Effect of dispensing times on the response of LFNAB (C) Optimization for the type of nitrocellulose membrane used. miRNA-215 concentration: 0.1nM.

The composition of the running buffer plays a very important role to minimize the nonspecific adsorption of nanolabels and increases the hybridization efficiency. PBS (1% BSA), PBST (1% BSA), Tris-HCl (1% BSA) and SSC (1% BSA) were used as running buffer and the S/N ratios were compared (**Figure 2.5.(A)**). It was found the highest S/N ratio was obtained with SSC+1% BSA buffer. We also optimized the concentrations of SSC and BSA to further improve the S/N ratio of LFSB (**Figs. 2.5.(B) and 2.5.(C)).** The SSC buffers were prepared by diluting the stock SSC buffer solution (3 M, Sigma-Aldrich) with different dilution times that ranged from 4 to 32 times. BSA concentrations in the running buffer varied from 1% to 4%. The highest S/N ratio was obtained with the 1/8 SSC buffer containing 4% BSA.

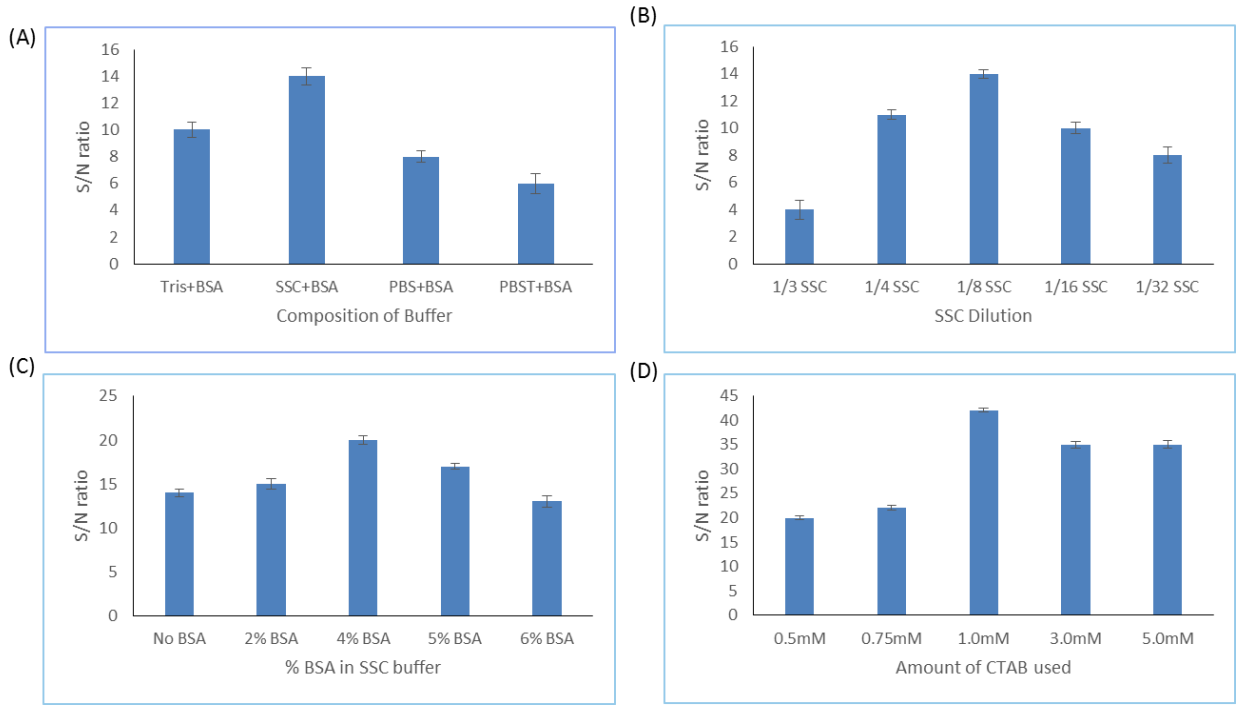

Figure 2.5. Effect of buffer on the performance of LFSB (A) different buffers used (B) SSC concentrations in the buffer (C) BSA concentration in the buffer (D) CTAB concentration in the buffer. miRNA concentration: 0.1nM.

During the optimization, it was noticed that some of the conjugates remained on the conjugate pad and that the assay time was longer than the GNP- based LFSB. This can be attributed to the large size of the SiNRs. To facilitate better movement of the DNA-GNP-SiNR conjugates across the LFSB, CTAB (a surfactant) was added to the running buffer. The addition of CTAB greatly improved the conjugate movement on the strips thus impacting the overall performance of LFSB. The CTAB concentration in the running buffer was, thus optimized (**Fig. 2.5.(D)**). The highest S/N ratio for the LFSB was obtained with 1mM CTAB.

2.3.3. Analytical Performance

After the optimizations of the DNA-GNP-SiNR conjugate amount (5 µL), the amount of capture probe (4 dispensing cycles) and the components of running buffer (1/8 SSC + 4% BSA+ 1 mM CTAB), the GNP-SiNR-based LFSB was assessed by detecting different concentrations of

target miRNA-215, ranging from 0 to 100 nM. The photo images of the LFSBs were taken by a digital camera and the intensities of the bands were obtained by using the Image J viewer software. Figure **2.6.(A)** shows the typical photo images of LFSBs after applying the sample solutions containing miRNA concentrations. No test band was observed in the control test (0 nM miRNA), indicating the nonspecific adsorption was negligible under the optimized experimental conditions. The intensities of the test bands increased with the increase of miRNA-215 and the threshold of visual detection of was 0.01-nM (10 pM). The calibration curve was plotted using the peak areas versus the microRNA-215 concentration. (**Fig 2.6.(B))**

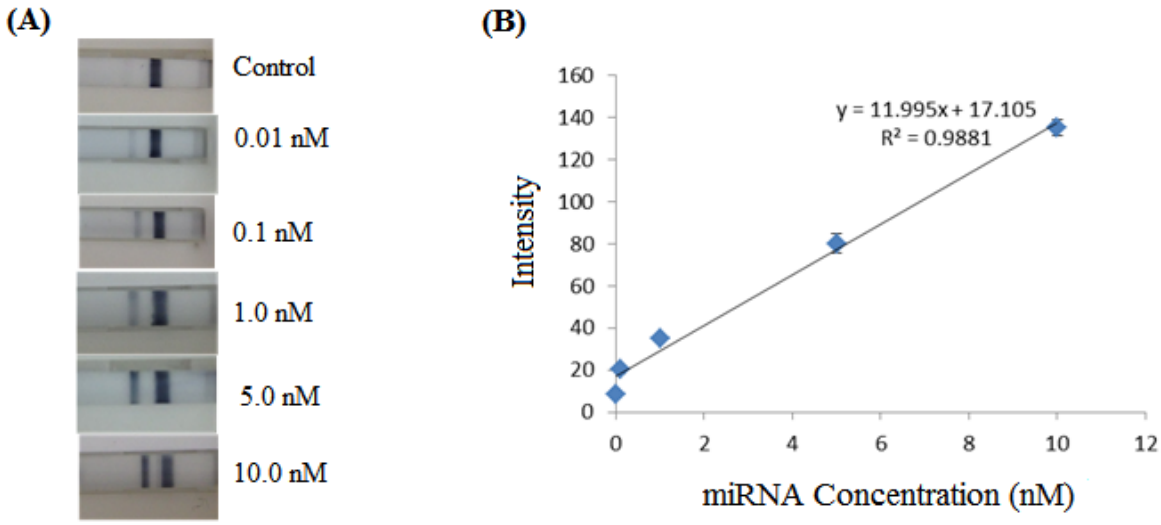

Figure 2.6. Photo images: (left) The LFNABs with different concentrations of the target under optimal experimental conditions and (right) Optical responses of the test bands on the LFSBs test zones.

A good linearity relationship was obtained over the 0.01 nM to 10 nM range, and the detection limit was estimated to be 0.01 nM (S/N=3). This detection limit is a six-fold improvement compared to the GNP-based LFSB.[14] In addition to high sensitivity, the GNP-SiNR-

based LFSB also exhibited high reproducibility. The reproducibility of the LFSB was studied by testing the LFSBs in the absence and presence of 5.0-nM target miRNA-215. Each sample was tested 6 times with 6 different LFSBs, and one could see that similar responses were obtained at the same concentration level. The relative standard deviations (RSD) of the signal for control and 5-nM were 2.8%, and 3.0% respectively, which indicates a good reproducibility of the measurements.

2.4. Conclusion

The present study reported a new nanolabel, gold-nanoparticle-coated silica nanorod (GNP-SiNR), for visually detecting miRNA on a lateral-flow strip biosensor with high specificity and sensitivity. The sensitivity of the GNP-SiNR-based LFSB was enhanced six times compared to the previous GNP-based LFSB. After systematic optimization, the GNP-SiNR was capable of detecting 10 pM miRNA without instrumentation. The concept should be extended to visually detect protein biomarkers using the GNP-SiNR nanolabels. Further work will aim to detect miRNA in cell-lysate and biological fluids. The GNP-SiNR-based LFSB, thus, provides a rapid and low-cost platform for sensitive detection of biological molecules, and shows great promise for point-of-care diagnosis of genetic and infectious diseases.

3. FLUORESCENT CARBON NANOPARTICLE-BASED LATERAL FLOW BIOSENSOR FOR ULTRASENSITIVE DETECTION OF DNA

3.1. Introduction

In the field of molecular diagnostics, there exists an urgent need for the development of ultrasensitive tools for the detection of nucleic acids and proteins with high sensitivity and low cost.[87] Lateral flow strip biosensor, also called immunochromatography strip test, that combines the optical properties of colloidal gold with conventional immunoassay has attracted significant attention in biological analysis and clinical diagnosis. [88-90] Recently the lateral flow device has been used to develop nucleic acid biosensors for qualitative (visual) or quantitative detection of nucleic acids, [21,66] protein biomarkers, [51] cancer cells [56] and heavy metal ions. [55] at low cost. Gold nano particles (GNP) were used as a colored tag and the produced red bands on the test zone of the device were detected by naked-eye for visual detection, or a portable strip reader for quantitative analysis. [21,51,55,56,66] One of the drawbacks of the GNP-based lateral flow nucleic acid biosensors (LFNAB) is low sensitivity, which limits the applications in detecting very low concentrations of targets. Great effort has been applied to enhance the sensitivity of the LFNABs. Carbon nanotubes, [91] GNP-coated silica nano rods [85] and horseradish peroxidase (HRP) – coated GNP[21] have been used as colored tags to improve the sensitivities of the NABLFB. The NABLFB integrated with conventional nucleic acid amplification techniques including PCR (Polymerase Chain Reaction), [92-93] isothermal amplification, [94-96] and other signal amplification techniques [97-98] have shown a great enhancement of the sensitivities , however complex operations and the use of many reagents offset the part of the advantages of the lateral flow biosensors.

Fluorescent nanoparticles are a great alternative to counterfeit the problems of sensitivity associated with colorimetric detections,[99-100] Quantum dots,[101] fluorophore-labeled sequences,[102]

dye-doped silica nanoparticles,[103] and up-converting phosphor reporters[104] have been used as fluorescent tags to prepare the fluorescent lateral flow biosensors for ultrasensitive detection of nucleic acid sequences. The sensitivities of the fluorescent lateral flow nucleic acid biosensors without additional signal amplification were 1-3 orders higher than that of GNP-based colorimetric lateral flow biosensors. Despite the high sensitivities of fluorescent lateral flow nucleic acid biosensors, there are some drawbacks such as toxicity, complexity in synthesis of quantum dots and dye-doped silica nanoparticles, photo bleaching of the dye labelled sequences, defects in doping of the dye into nanoparticles. In light of all these problems, we have developed a fluorescent carbon nanoparticle (FCN)-based lateral flow biosensor for ultrasensitive detection of DNA sequences using a relatively simple, easy, and green synthetic procedure. FCNs as a new kind of fluorescent nanoparticles have recently attracted considerable research interests in a wide range of applications due to their low-cost and good biocompatibility.[105] FCNs have been used in bio imaging,[106-107] photo catalysis,[108-109] light emitting devices,[110] biosensors [111,112] and fluorescent detection of metal ions.[113-114] As per our knowledge, this is the first report to use FCN as a tag on the lateral flow biosensors for DNA detection. The FCN-based NABLFB in this research is by far the most sensitive method reported for the rapid detection of DNA sequence on a lateral flow device without additional signal amplification and the use of conventional fluorophores and QDs. We demonstrated that the biosensor was able to detect a minimum concentration of 0.4 fM DNA. The resulting fluorescent lateral flow assay presents a rapid, low-cost and a very sensitive DNA detection method without the need for target amplification or any expensive instrumentation. The promising properties of the FCN-based NABLFB are reported in the following sections.

3.2. Materials and Methods

3.2.1. Apparatus

The Biojet BJQ 3000 dispenser, Airjet AJQ 3000 dispenser, clamshell laminator and the guillotine cutting module CM 4000 were purchased from Biodot LTD (Irvine, CA) and used to prepare the lateral flow nucleic acid biosensors. A portable ESE-Quant Lateral Flow Reader (ESE GmbH, Germany) was used to measure the fluorescent intensities of the test zone and control zone of the lateral flow nucleic acid biosensors. A Hitachi HT7700 field transmission electron microscope (TEM; Tokyo, Japan) was used to take images of carbon nanoparticles. Fluorescent spectra of the fluorescent carbon nanoparticle solution was recorded on a F-4500 fluorescence spectrophotometer (Hitachi, Tokyo, Japan). The ultraviolet-visible (UV-vis) absorption spectra was recorded on a Varian Cary 50 spectrophotometer. Infrared spectra was collected on a Thermo Scientific Nicolet 8700 FTIR Spectrophotometer. PowerPac^{TM} basic power supply and mini-sub cell GT cell were purchased from Bio-Rad (Hercules, CA).

3.2.2. Reagents and Materials

Glacial acetic acid, diphosphorus pentoxide, streptavidin, methane diamine, 1,3 di-amino-propane, hexa methylene diamine, bovine serum albumin (BSA), EDC (N-(3-dimethylaminopropyl)-N′-ethylcarbodiimide hydrochloride), sulfo NHS (*N*-Hydroxysulfosuccinimide sodium salt), MES (2-(*N*-morpholino)ethanesulfonicacid) buffer, caesin, PVP (polyvinylpyrrolidone), tween 20, ethidium bromide, Orange-G dye, PBS (phosphate buffer saline) buffer, TBS (Tris-buffered saline), PBST (phosphate-buffered saline with tween-20) were purchased from Sigma-Aldrich (St. Louis, MO). Glass fibers (GFCP000800), cellulose fiber sample pads (CFSP001700), laminated cards (HF000MC100) and nitrocellulose membranes (HFB18004) were purchased from Millipore (Billerica, MA). TAE (Tris base, acetic acid and

EDTA) buffer and agarose were purchased from Promega (Madison, WI). 50-500 bp DNA ladder were purchased from Norgen (Ontario, Canada).

All the chemicals used in this study were analytical reagent grade. Solutions were prepared with ultrapure (Z18 MΩ) water from Millipore Milli-Q water purification system (Billerica,MA). All the DNA oligonucleotides used in this study were purchased from Integrated DNA Technologies, Inc. (Coralville, IA) and had the following sequence:

Target DNA: 5′-ATGACCTATGAATTGACAGAC-3′.

Amine-modified detection DNA probe: 5′-Amino-GTCTGT CAA-3′.

Biotinylated capture DNA probe: 5′-ATAGGTCAT/Biotin-3′.

Biotinylated control DNA probe: 5′-Biotin/MC6-D/TTGACA GAC-3′.

Non-complementary DNA probe: 5′-CATTCCAGCAGCTGTTT-3′.

One-base mismatched DNA probe: 5’-ATAACCTATGAATTGACAGAC-3’.

Two-base mismatched DNA probe: 5’-ATAATCTATGAATTGACAGAC-3’.

3.2.3. Preparation of Fluorescent Carbon Nanoparticles (FCN) and FCN-DNA Conjugates

FCNs were synthesized as follows using the procedure reported by *Fang et.al*.[105] One milliliter of glacial acetic acid containing 80 μL of water was added to 2.5 g of P_2O_5 in a 25 mL beaker without stirring. The reaction mixture was quickly foaming because of the spontaneous heat and gradually cooled down to room temperature. The dark brown mixture was then dispersed in water and centrifuged at 13000 rpm for 10 min to collect the supernatant. One milliliter of FCN solution was then mixed with 9.6 mg of EDC and 5.43 mg of sulfo-NHS in 1.0 mL MES buffer (0.1 M, pH 4.7). The mixture was incubated at room temperature for 30 min. The pH was then adjusted to 7.0 followed by the addition of 2-mercaptoethanol to inactivate the EDC. The amine-modified detection DNA probe was then added to the activated FCNs with a final concentration

of 0.1 OD mL^{-1} and incubated for 3 h at room temperature. The conjugates were blocked with 1% BSA for 30 min. A centrifugal filter unit (cutoff: 3K) for concentration and purification of biological solution was used to separate the unbound DNA in the conjugate solution. Molecular weight of DNA probe was less than the cutoff value of the filter (3K). Hence any unbound DNA would be removed. The washes were done multiple times and the final eluent was checked with UV- Visible spectrometry to ensure there was no DNA absorption peak. The remaining FCN-DNA conjugate in the filter was also examined with UV-Visible spectrometry.

3.2.4. FTIR Sample Preparation

The FCNs were first extracted from water using ethyl acetate followed by the addition of KBr powder. Then the ethyl acetate was completely vaporized and the solid was kept for drying in a vacuum oven for 12h for the collection of FTIR spectra.

3.2.5. Preparation of Streptavidin-Biotin-DNA Conjugates

One hundred nano moles of biotinylated DNA probe (capture DNA probe) was mixed with 2.5 mg mL^{-1} streptavidin and incubated at room temperature for 1 hour. After adding 500 µL PBS to the mixture, the new solution was centrifuged using a centrifugal filter for 20 minutes at 6000 rpm at 4 ℃ to remove the unbound DNA. The above step was repeated for 3 times. The remaining solution in filter was diluted with PBS and used for dispensing. The same procedure was followed for the preparation of streptavidin-biotin-control DNA probe.

3.2.6. Preparation of Lateral Flow Nucleic Acid Biosensor (LFNAB)

A nucleic acid based lateral flow biosensor (NABLFB) consists of the following components: sample application pad, conjugate pad, nitrocellulose membrane, and absorbent pad. The sample application pad (17 mm x 30 cm) was made from cellulose fiber (CFSP001700) and soaked in a solution containing 0.25% Triton X-100, 0.05M Tris-HCl and 0.15 M NaCl for one

hour, dried and stored at room temperature for further use. The FCN-DNA (detection probe) conjugate solution was dispensed on the glass fiber conjugate pad with Airjet AJQ 3000 dispenser. Streptavidin-biotin-capture DNA probe and streptavidin-biotin-capture control DNA probe solutions were dispensed on the nitrocellulose membrane to form the test and control zones, respectively. After dispensing, the conjugate pad and nitrocellulose membrane were dried at 37^{o}C for 1 hr before assembly. Finally, all the components were assembled onto a plastic adhesive backing (60 mm x 30 cm) using a clamshell laminator. Each part overlapped 2 mm to ensure the solution could migrate through the strip during the assay. Strips with 3 mm width were cut by the Guillotin cutting module CM 4000.

3.2.7. Sample Assay Procedure

Sample solutions with different concentrations of target DNA were prepared in the running buffer (PBS + 0.5% BSA). In a typical assay, 100 μL of sample solution was applied onto the sample pad, then the solution migrated toward absorption pad. During the assay process, the solution migrated up by capillary force. The test zone and control zone were evaluated visually under UV light within 20 min. For quantitative measurements, the fluorescent intensities of the test line and control line were recorded by a portable ESE-Quant lateral flow reader.

3.3. Results and Discussion

3.3.1. Preparation of Fluorescent Carbon Nanoparticles (FCNs) and FCN-DNA Conjugates

Fluorescent carbon nanoparticles (FCNs) have been considered as an alternative for fluorescent chalcogenide semiconductor nanocrystals (QDs) and used in bio imaging, photo catalysis, and light-emitting services.[105]The analytical applications of FCNs mainly concentrated on the fluorescent detection of metal ions.[113-114] There are very few reports on biosensors and bioassays.[111-112] In this study, FCNs were first used as tags to develop a fluorescent lateral flow

nucleic acid biosensor for ultrasensitive detection of DNA sequences. FCNs were prepared according to the reported methods with slight modifications.[105] Transmission electron microscopy (TEM), FT-IR and fluorescent spectra were used to characterize the FCNs.

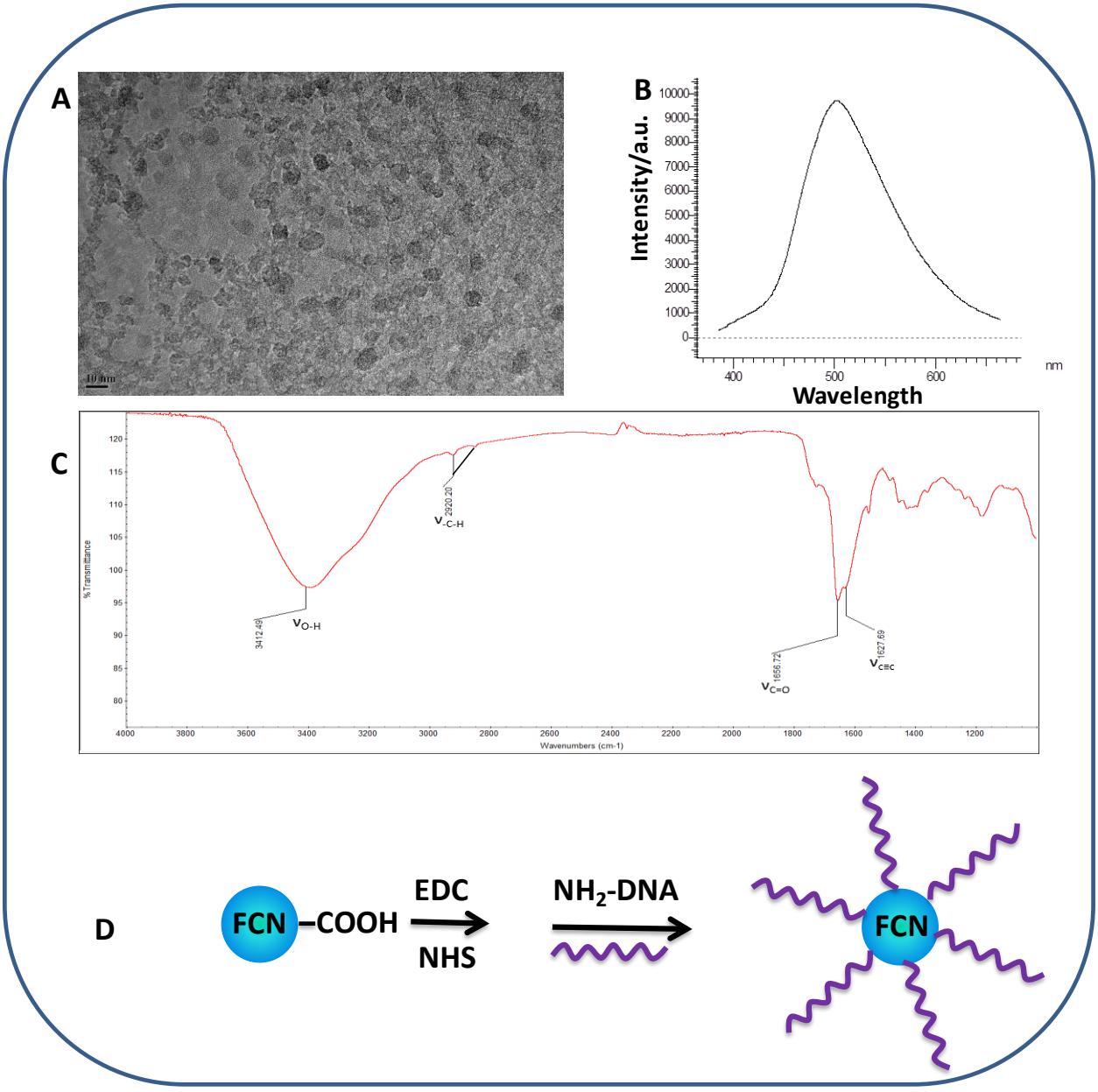

Figure 3.1. (A) Typical TEM image of fluorescent carbon nanoparticles (B) Fluorescent emission spectra of carbon nanoparticle solution, excitation wavelength: 346nm (C) FTIR spectrum of fluorescent carbon nanoparticles (D) Schematic illustration of preparation of the FCN-DNA conjugates.

Figure 3.1.(A) shows the typical TEM image of the as-prepared FCNs. One can see the diameter of FCN is around 15 nm and the size distribution is uniform. **Figure 3.1.(B)** presents the fluorescent emission spectra of a 100-fold diluted FCN solution with an excitation wavelength of 365 nm, a well-defined emission peak with the maxima emission wavelength of 510 nm was obtained. The FTIR spectrum of the FCNs **(Figure 3.1.(C))** has an apparent peak around 3400cm^{-1} indicating the presence of –OH groups and a peak at 1656cm^{-1} indicating the existence of C=O group conjugated with aromatic carbons respectively. A peak at 1627cm^{-1} indicate the presence of conjugated c=c stretching vibration. These data reveal that the synthesized FCNs are rich in carboxylic groups. The amino-modified detection DNA probe was conjugated to the FCN surface by using EDC and NHS coupling reagents (**Figure 3.1.(D)**). The fluorescent intensities of the FCN solution increased with the increase of the concentration of FCN. **(Figure 3.2.)**

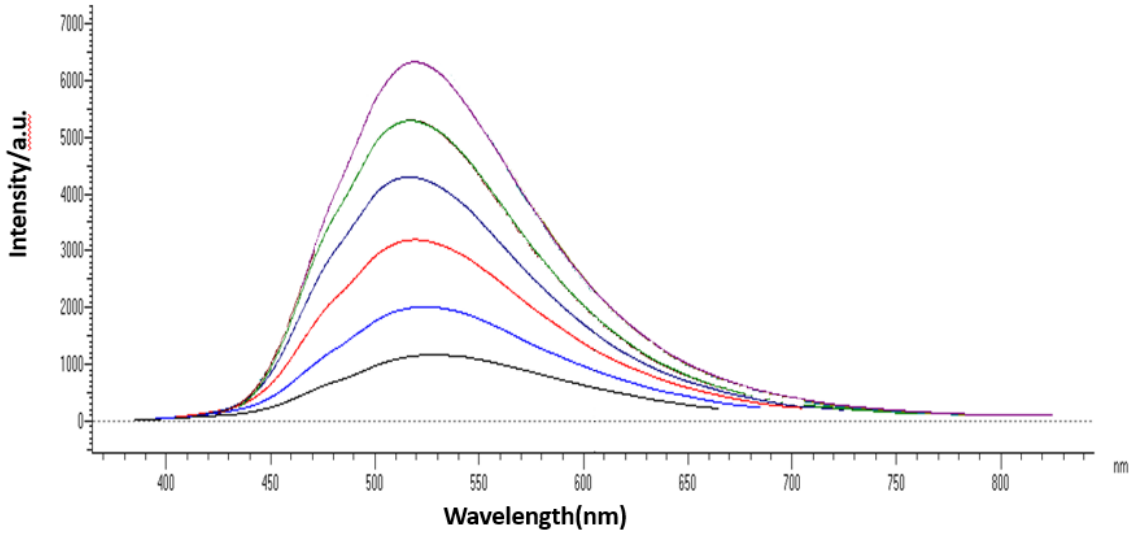

Figure 3.2. Fluorescent emission spectra of carbon nanoparticle solution with different dilutions, excitation wavelength: 346 nm. The prepared FCN solution was diluted 100, 125, 150, 200, 400 and 800 times with distilled water (top to bottom).

There was no change of the fluorescence intensity of the FCN observed prior to and after DNA conjugation **(Figure 3.3).**

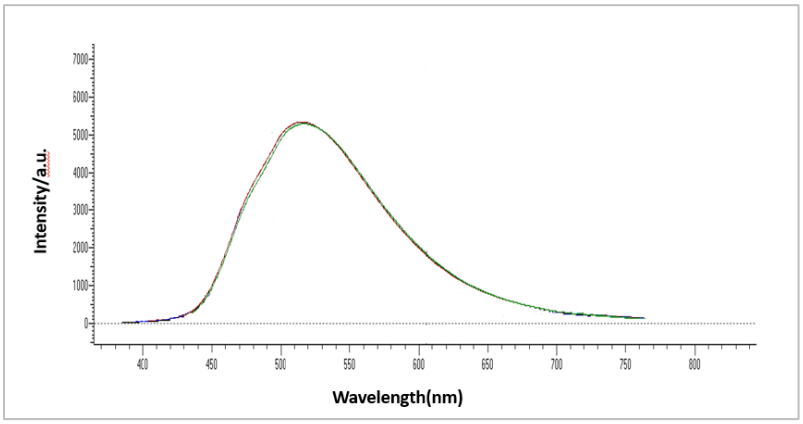

Figure 3.3. Fluorescent emission spectra of FCN (purple) and FCN-DNA (green) solutions, excitation wavelength: 346nm.

UV-Visible spectrum was used to characterize the FCN-DNA conjugates. There are two absorption peaks at 260 nm and 300 nm in the UV-Visible spectrum of FCN **(Figure 3.4)**. The absorption peak at 260 nm is overlapped with the absorption peak of DNA. It was found that the absorption peak intensity at 260nm increased significantly, indicating the successful conjugation of DNA probes to FCN.

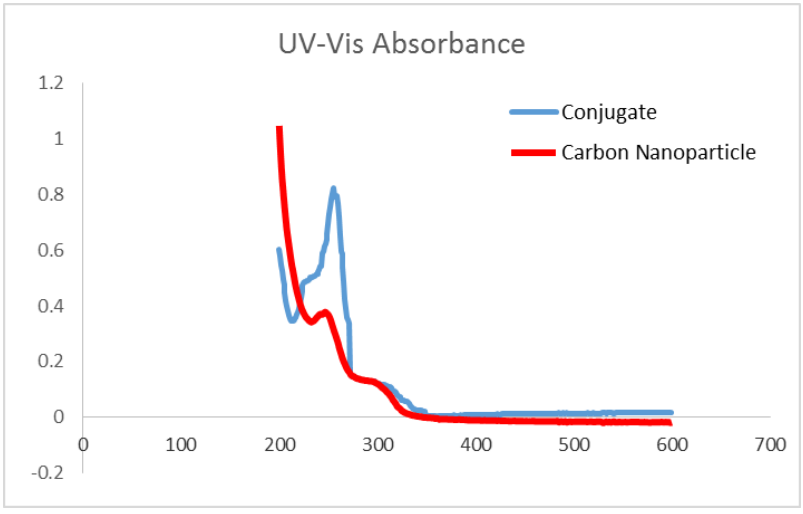

Figure 3.4. UV-Visible spectrum of fluorescent carbon nanoparticles (FCN) and FCN-DNA conjugates.

Agarose gel electrophoresis was used to further confirm the formation of carbon nanoparticle-DNA conjugates **(Figure 3.5)**. This was done by evaluating the mobility of the single stranded detection probe, the conjugate (carbon nanoparticle conjugated with detection probe) and the carbon nanoparticle. All were incubated with complimentary control probe leading to the formation of duplex DNA which facilitated the intercalation of ethidium bromide aiding the visualization of DNA bands. **Figure 3.5. (A)** presents the typical agarose image. The following samples were loaded in the wells: lane 1 contained the DNA ladder, lane 2 was the duplex DNA, lane 3 was the CNP-DNA conjugate and control probe, lane 4 was the carbon nanoparticle only and lane 5 was the carbon nanoparticle with the detection probe and control probe.

The formation of the conjugate was confirmed by comparing the mobility of the samples as listed. The duplex DNA in lane two, with no label had greater mobility than when the detection probe is conjugated onto the CNP as shown in lane three. Upon the detection probe conjugation the mass of the particle became larger, thus making it more difficult to travel the length of the agarose gel. To ensure that the signal from lane three was from the detection probe CNP conjugate, not from the CNP itself, the CNP sample was ran in lane four. As shown, there is no signal in lane four, contributing to the assurance that the detection probe had indeed conjugated onto the CNP surface in lane three. As another confirmation run, the sample in lane five is the CNP and detection probe with no conjugation. As seen in figure 3.5. (A) lane-5, it appeared as the same as lane two indicating the movement of the detection probe is only slowed by its conjugation upon the CNP and formation of duplex. From this data, it is apparent that the method used to make the conjugates was successful. **Fig.3.5.(B)** shows the images of the wells before (top) and after (bottom) the electrophoresis assay). It can observed that the solutions in lanes 1,2,3 moved out of the well upon electrophoresis, however CNPs without conjugation with detection DNA probe wouldn’t move

out the wells (well 4 and 5). Lane-5 showed the same movement as lane-2 leaving the nanoparticles in the well. The above results confirmed that the detection DNA probes were conjugated with CNPs successfully.

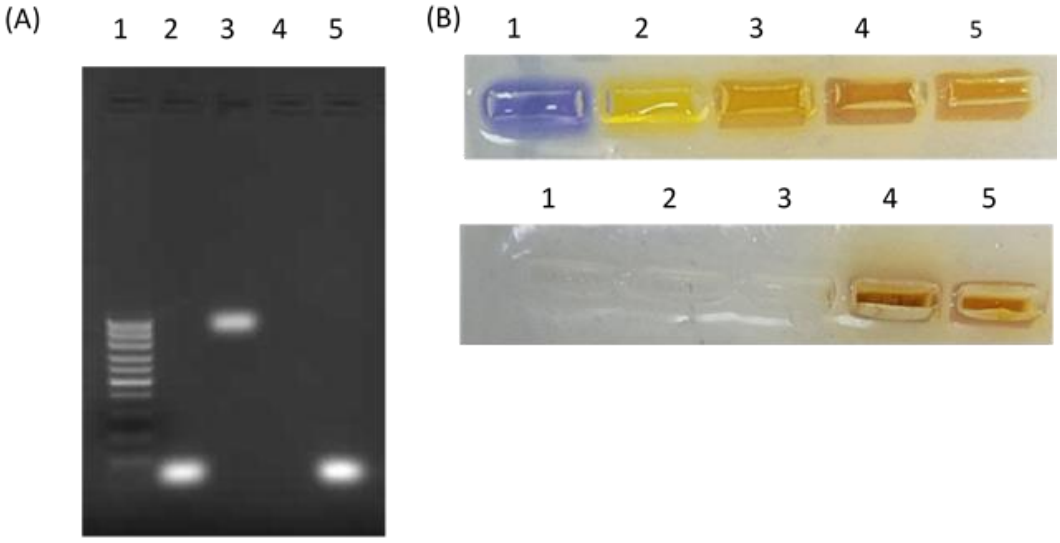

Figure 3.5. (A) Agarose gel electrophoresis image. Lane-1: Ladder (50-500 bp); Lane-2: Detection probe + target DNA; Lane-3: CNP-DNA conjugate + target DNA; Lane-4: CNP; Lane-5: CNP + detection DNA probe + target DNA (Gel contained 1% w/v agarose and 0.5 ug/ml ethidium bromide) (B) Images of the wells before and after the electrophoresis assay respectively.

We compared the performances the FCN-DNA conjugates with and without spacers. Methane diamine, 1,3 di-amino-propane, hexa methylene diamine were used as spacers to prepare the FCN-DNA conjugates. It was found that the fluorescence intensities of the test line with FCN-DNA-spacer was much lower than that FCN-DNA without spacer **(Figure 3.6.).** The decrease of fluorescence intensity may be caused by the small size of FCN. The addition of spacers on the FCN surface decreased the DNA probes immobilized on FCN surface and reduced the DNA hybridization efficiency during the lateral flow assay, resulting less FCNs were captured on the test line and a decrease of fluorescence intensity. Therefore, FCN-DNA conjugates were prepared without adding the spacers in the following experiments. The formed FCN-DNA conjugate was

dispersed in the eluent buffer and used to prepare the lateral flow nucleic acid biosensors (LFNABs).

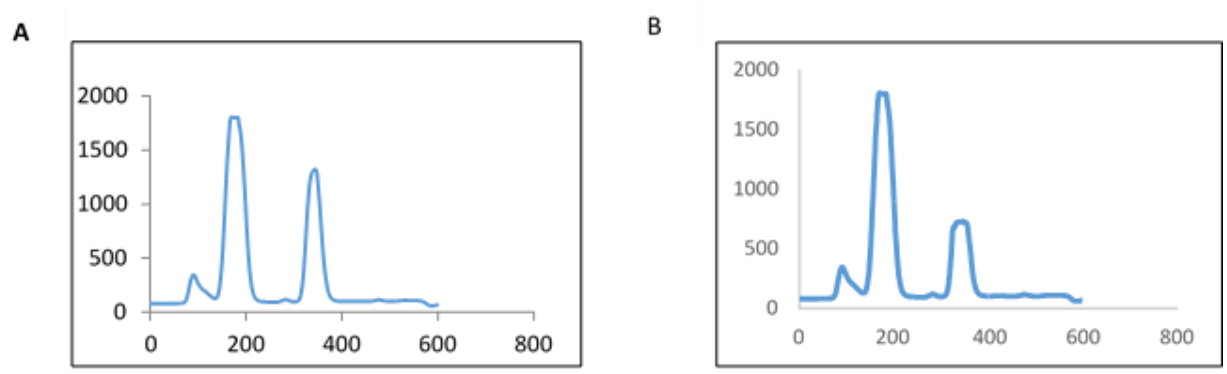

Figure 3.6. (A) The fluorescent responses of the test line and control line of the FCN-based LFNAB in the presence of 1.0pM target DNA, FCN-DNA conjugates were prepared in the absence of spacer (B) The fluorescent responses of the test line and control line of the FCN-based LFNAB in the presence of target 1.0pM DNA, FCN-DNA conjugates were prepared with 1,3 di-amino-propane spacer. Left peak: control line; Right peak: test line.

3.3.2. Principle of DNA Detection with the FCN-based LFNAB

The FCN-based NABLFB configuration is illustrated in **Figure 3.7.** A pair of DNA probes, named detection DNA probe and capture DNA probe, was used to prepare the NABLFB. The capture DNA probe and detection DNA probe are complementary with target DNA at different portions. The detection DNA probe was conjugated with FCN and the FCN-DNA conjugates were dispensed on the conjugate pad of the NABLFB. Biotin-modified capture DNA probe was first reacted with streptavidin and the resulting streptavidin-biotin-capture DNA complexes were dispensed on test zone of the NABLFB to form a test line. The third DNA probe, named control DNA probe, which is fully complementary with the detection DNA probe, was immobilized on the control zone to form a control line. In a typical assay, the sample solution containing desired concentrations of target DNA was applied to the sample pad. The solution migrated along the strip by capillary force and FCN-detection DNA probe-target DNA complexes were formed due to the DNA hybridization reactions between the target DNAs and the detection DNA probes. Upon

reaching the test-zone, it forms a sandwich-type complex because of the second DNA hybridization reaction between the capture DNA and target DNA **(Figure 3.7.(A)**). The excess of the FCN-DNA conjugates continues to move until it reaches the control zone where it was captured by the control DNA probe. The control line is used to confirm if the LFNAB is working properly. In the absence of the target DNA, there is no sandwich-type complex formed on the test zone and only the FCN-detection DNA-control DNA complexes formed on the control zone. The amount of the captured FCNs on the test zone is proportional to the target DNA concentration in the sample solution and can be used to quantify the target DNA concentration qualitatively and quantitatively. Qualitative analysis can be performed by observing the test line and control line under a UV light **(Figure 3.7.(B))**. In the presence of target DNA, a test band and a control band will show on the nitrocellulose will show on the nitrocellulose membrane **(Figure 3.7.(B), middle)** and only the control band will appear in the absence of target DNA **(Figure 3.7.(B), left)**. There is no visible band if the NABLFB is not working properly **(Figure 3.7.(B), right).**

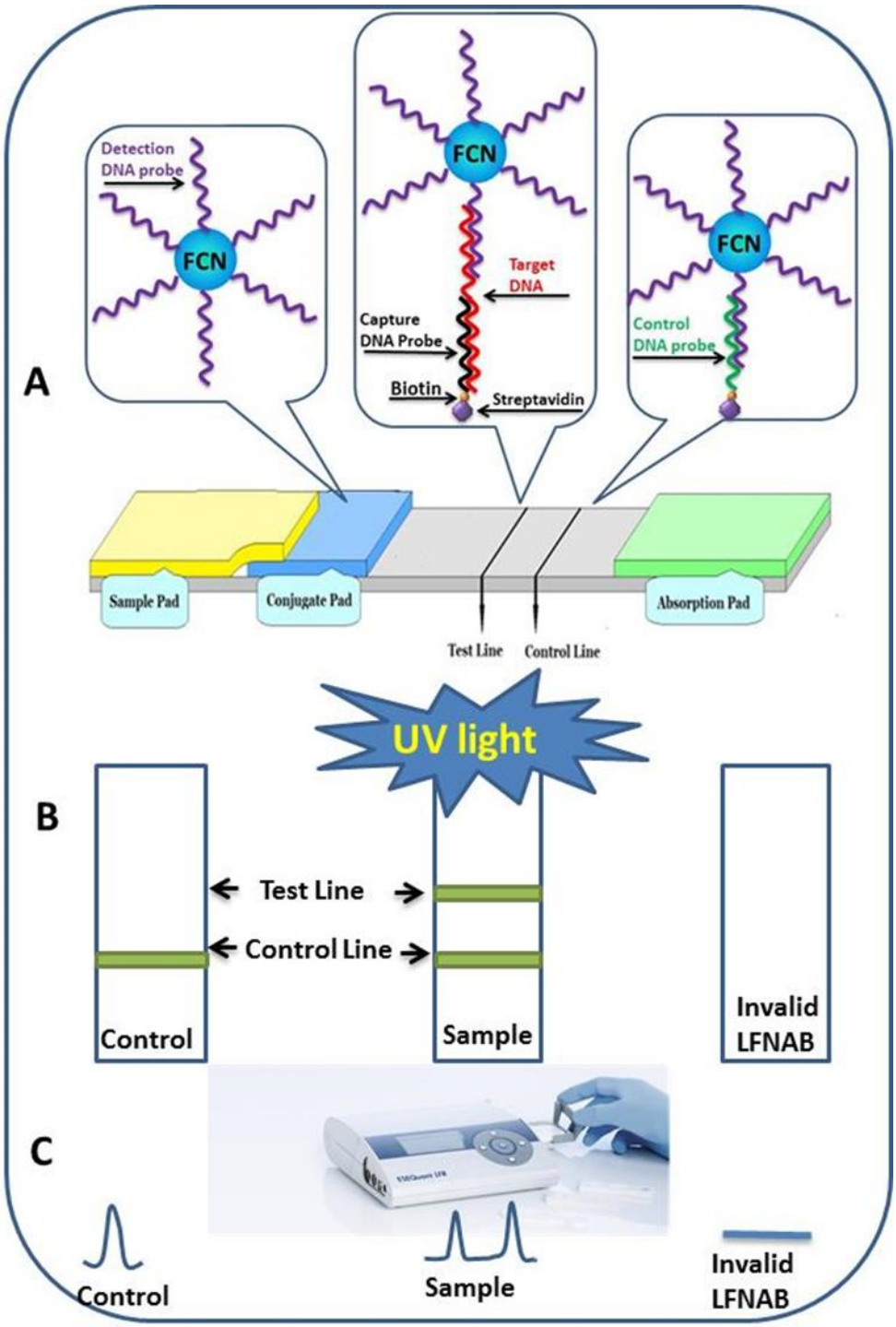

Figure 3.7. (A) Schematic illustration of the configuration and measurement principle of the fluorescent carbon nanoparticle based lateral flow nucleic acid biosensor (B) Principle of qualitative detection of DNA on the fluorescent carbon nanoparticle based lateral flow nucleic acid biosensor (C) Principle of quantitative detection of DNA with a portable ESE-Quant lateral flow reader. Left: Control (in the absence of target DNA); Middle: Sample (in the presence of target DNA); Right: Invalid test.

Quantitative analysis can be done by reading the fluorescent intensities of the test zone using a portable ESE-Quant lateral flow reader (**Figure 3.7.(C)**). In the presence of target DNA, two peaks depicting the responses from the test zone and the control zone will be observed (**Figure 3.7. (C), middle)**. Only one peak from the control zone will be detected in the absence of target DNA (**Figure 3.7.(C), left),** as there was no FCN captured on the test zone. No peak from both the test zone and the control zone indicates the NABLFB is not working properly **(Figure 3.7.(C), right).**

Figure 3.8. (A) presents the typical photo images of the LFNABs in the presence of 0 pM target DNA (control test), 1.0 pM target DNA, 50 nM noncomplementary DNA and the mixture of 50 nM noncomplementary DNA and 1.0 pM target DNA. The images were taken under an UV light with a wavelength of 365 nm. The fluorescent intensities of the bands were recorded with a portable ESE-Quant lateral flow reader and the responses are shown on **Figure 3.8.(B)** (no target DNA) and **Figure 3.8.(C)** (1 pM target DNA). Well-defined peaks were observed, and the peak areas were proportional to the captured FCNs in the control line (left side) and test line (right side). It was also noticed that there was a small peak observed in the test zone of the biosensor in the absence of target DNA (**Figure 3.8.(B)**), which was caused by the nonspecific adsorption of the FCN-detection DNA conjugates on the membrane. In order to reduce such nonspecific adsorption, the nitrocellulose membrane was blocked for an hour prior to the dispensing of the streptavidin-biotin-capture DNA and streptavidin-biotin-control DNA solutions by using a buffer containing 0.01% BSA, 0.02% PVP, 0.005% Casein, 1X TBS and 0.002% Tween-20.

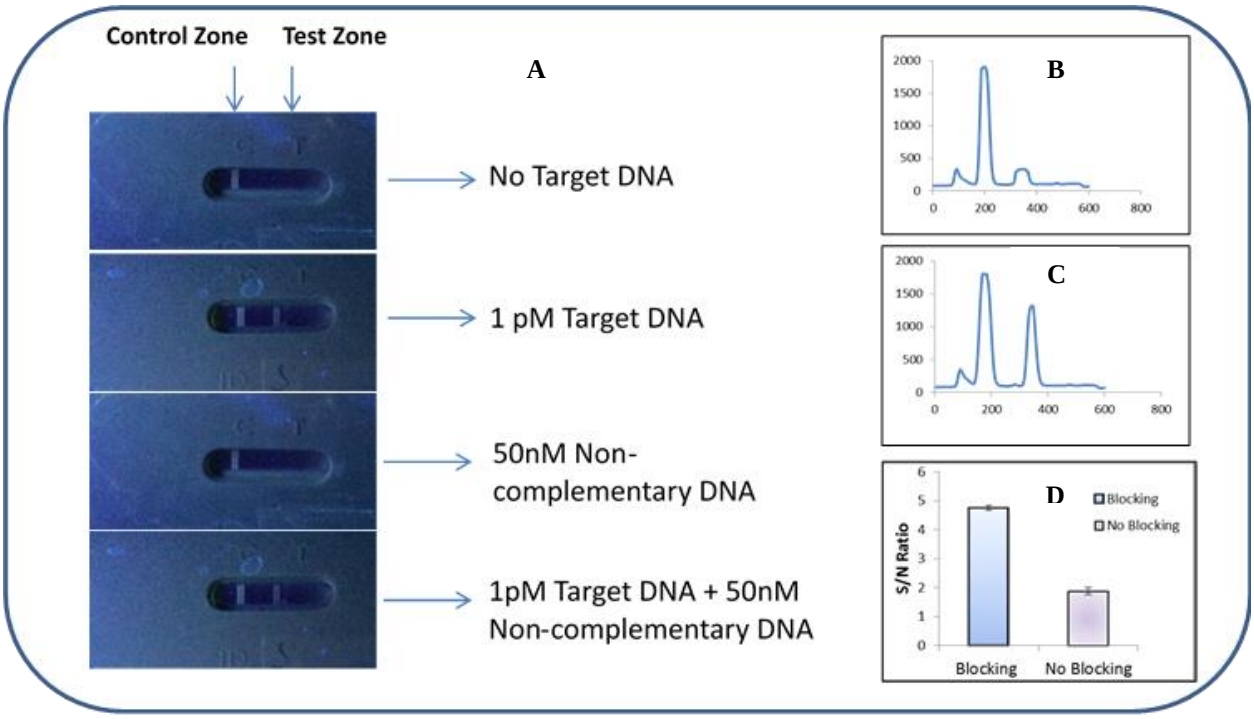

Figure 3.8. (A) Typical photo images of FCN-based LFNABs after applying 0 nM target DNA, 1.0 pM target DNA, 50 nM noncomplementary DNA and the mixture of 1.0 pM target DNA and 50 nM target DNA. The images were recorded under a UV lamp (B) The fluorescent responses of the test line and control line of the FCN-based LFNAB in the absence of target DNA. Peak on the left: fluorescent signal from the control line; peak one the right side: fluorescent signal from the test line; (C) The fluorescent responses of the test line and control line of the FCN-based LFNAB in the presence of target 1.0 pM DNA; (D) The histogram of the S/N ratio of the FCN-LFNAB without and with blocking step. Target DNA concentration: 1.0 pM.

Two bright bands were observed in the presence of 1.0pM target DNA, and only one band (control line) was observed in the absence of target DNA and presence of excess of noncomplementary DNA. The intensities of test bands in the presence of 1.0 pM target DNA and the mixture of 1.0 pM target DNA and 50 nM noncomplementary DNA are almost equal, indicating the presence of excess of noncomplementary DNA does not affect the signal of target DNA. **(Figure 3.9.)**

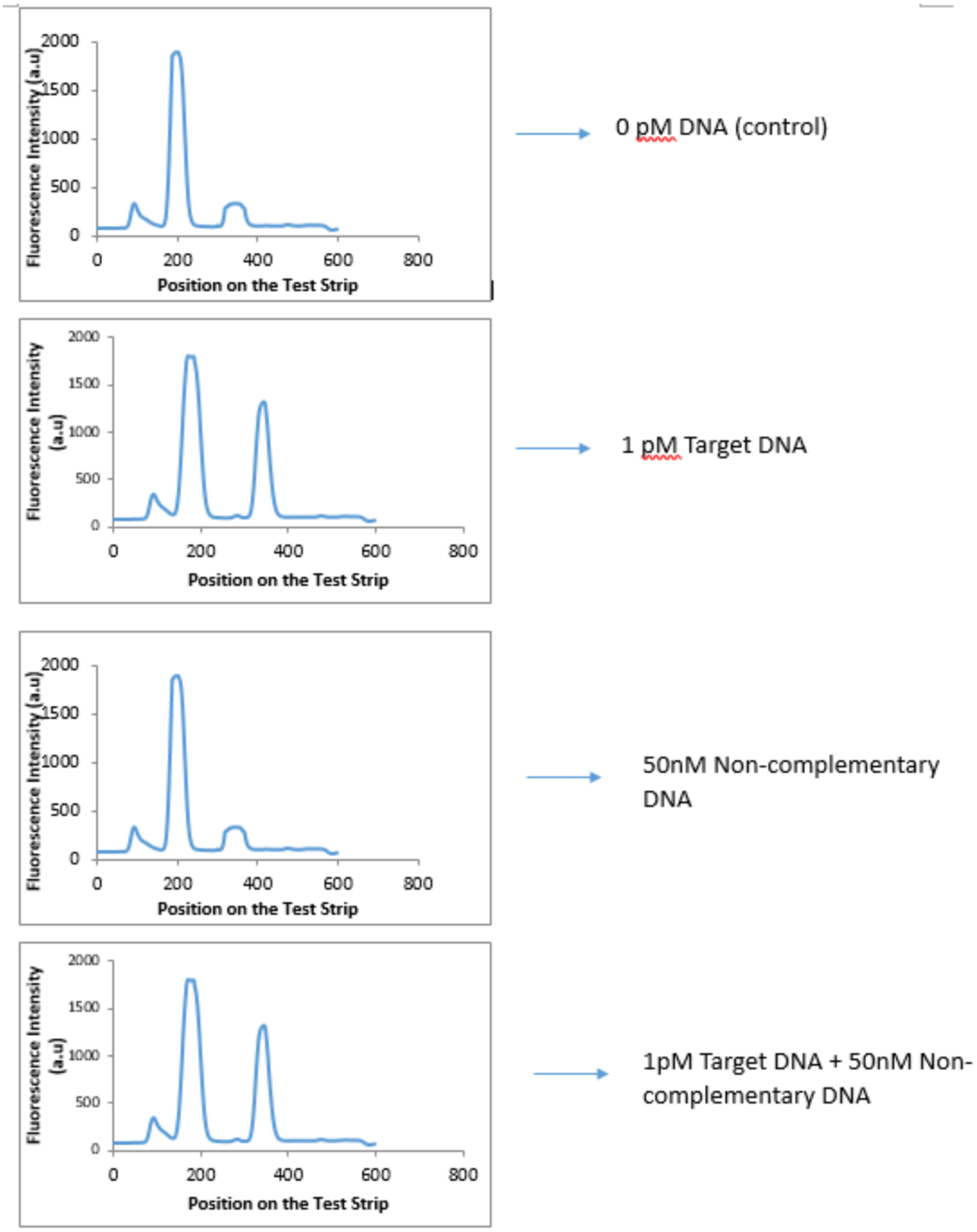

Figure 3.9. The fluorescent responses of the test line and control line of the FCN-based LFNAB in the presence of 0 pM target DNA, 1 pM target DNA, 50 nM non-complementary DNA and the mixture of 1 pM target DNA+50 nM non-complementary DNA. Left peak: control line; Right peak: test line.

3.3.3. Optimization of Experimental Parameters

To acquire the sensitive DNA detection using the FCN-based LFNAB, different experimental parameters including the running buffers, the concentration of amino-modified detection DNA probe used in the preparation of FCN-DNA conjugates, the volume of the conjugate dispensed on the conjugate pad and the dispensing cycles of the capture DNA probes on the test-zone were optimized.

The effect of the running buffers is considered as one of the most important parameters in the optimization of the lateral flow assays. Appropriate buffers would minimize the nonspecific adsorption and increase the sensitivity and reproducibility of the assay. We compared the performances of FCN-based NABLFB tests with different running buffers including PBS+1% Tween, PBS + 1% BSA, PBS + 0.5% BSA, PBS + 0.1% BSA and PBST+0.5% BSA. As shown in the **figure 3.10.(A)**, the highest S/N ratio was obtained by using PBS+0.5% BSA, which was used as the running buffer for all the assays.

In the current study, the FCN-detection DNA probe conjugates were dispensed on the glass fiber. The fluorescent intensities of test zone and control zone depended on the amount of FCN-detection DNA probe conjugate captured on the zones, which in turn correspond to the amount of conjugates dispensed on the conjugate pad. The amount of FCN-detection DNA probe conjugates on the conjugate pad was controlled by the dispensing volume of the conjugate solution. **Figure 3.10.(B)** presents the histogram of the S/N ratio for 1.0 pM target DNA test with the different amount of FCN-detection DNA probe conjugate loaded conjugate pads. The S/N ratio of the assay increased up to 6 µL on the conjugate pad, which was used as the optimal volume of the FCN-detection DNA probe conjugates for most of the experiments. The further increase of the

dispensing volume of FCN-DNA conjugates led to a decrease in the S/N ratio due to an increasingly nonspecific adsorption.

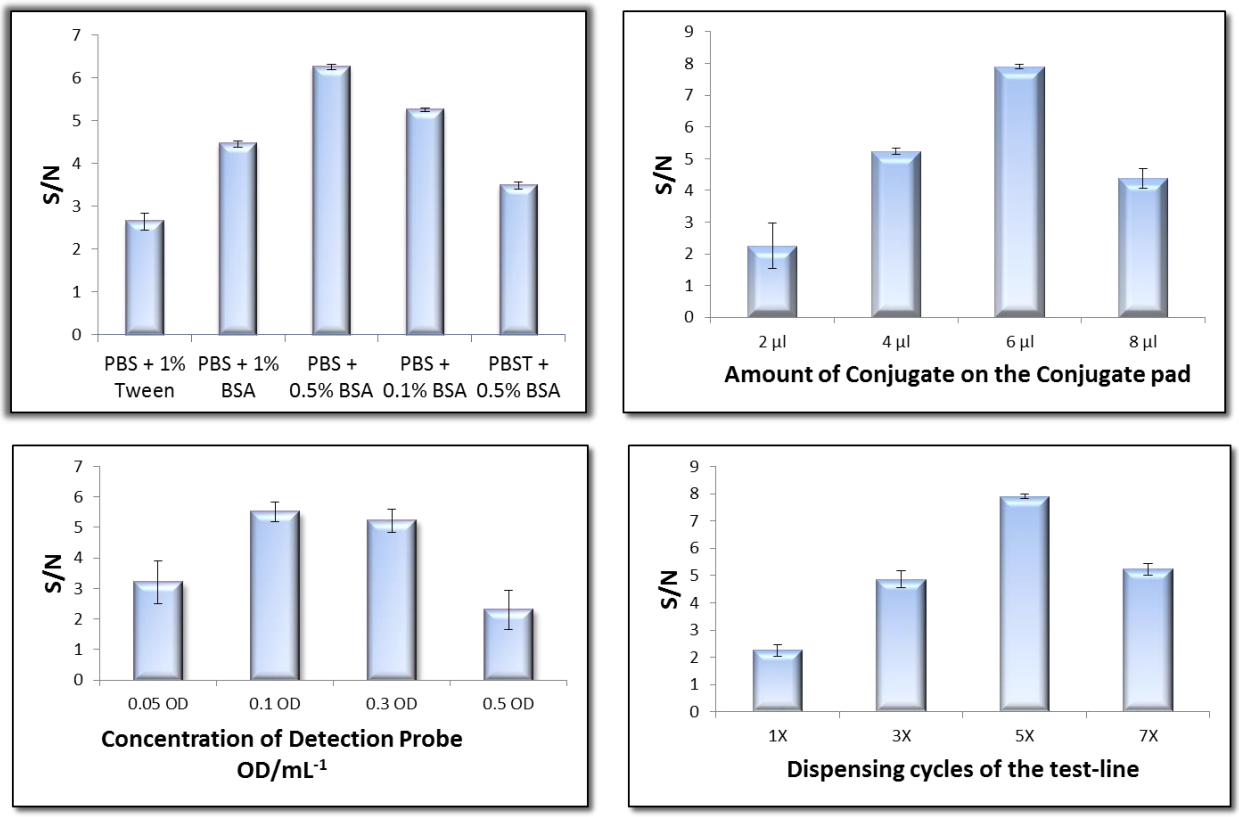

Figure 3.10.(A) Effect of running buffers on the S/N ratio of the FCN-based LFNAB (B) Effect of the volume of FCN-DNA conjugate used on the S/N ratio of FCN-based LFNAB (C) Effect of the concentration of detection DNA probe conjugated to FCN on the S/N ratio of FCN-based LFNAB (D) Effect of the dispensing times of capture DNA on the S/N ratio of FCN-based LFNAB. Target DNA concentration: 1 pM.

In addition, the amount of detection DNA probe on the FCN surface would affect the responses of the LFNABs. We studied the effect of DNA probe concentration during the preparation of FCN-detection DNA probe conjugates on the S/N ratio of the LFNAB **(Figure 3.10.(C))**. One can see that the S/N ratio increases upon raising the DNA concentration in the conjugate solution from 0.05 OD/mL to 0.1OD/mL, and then it starts to level off till 0.3 OD/mL; the further increase of the DNA concentration led to a decrease in the S/N ratio. The decrease of

S/N at high concentration of detection DNA probe would be caused by the number of DNA probes on the FCN surface. More DNA probes were immobilized on the FCN surface and less FCNs would be captured on the test zone. Therefore, a DNA probe concentration of 0.1 OD/mL in the conjugate solution was used to prepare the FCN-detection DNA probe conjugates for the following experiments.

Another factor to affect the sensitivity and reproducibility of the LFNAB test is the amount of capture DNA probes dispensed on the test-zone. To obtain the best S/N ratio, increasing amounts of biotin-streptavidin capture DNA probe were used to prepare the test line of the LFNAB. This was done by increasing the number of dispensing cycles. As shown in **Figure 3.10.(D)**, five times dispensing of the capture DNA probe was giving the highest S/N ratio. This optimized condition was used in further assays.

3.3.4. Analytical Performance

Under optimized experimental conditions, the performance of the FCN-LFNAB was tested in the presence of different target DNA concentrations. The captured FCNs on the test line would be observed visually by using a UV lamp, and quantified by measuring the fluorescent intensity of the test line with the portable fluorescent reader. The test-line was quite visible even in the presence of 0.05 pM target DNA, which could be estimated as a threshold for the qualitative detection of the target DNA. A series of well-defined peaks were observed and the intensity increased with increasing target DNA concentration. The resulting calibration curve of the logarithm of target DNA concentration versus the fluorescent intensity was linear over a range of 1.0 fM to 10 nM **(Figure 3.11)** with a detection limit of 0.4fM. The assay time was around 20 min.

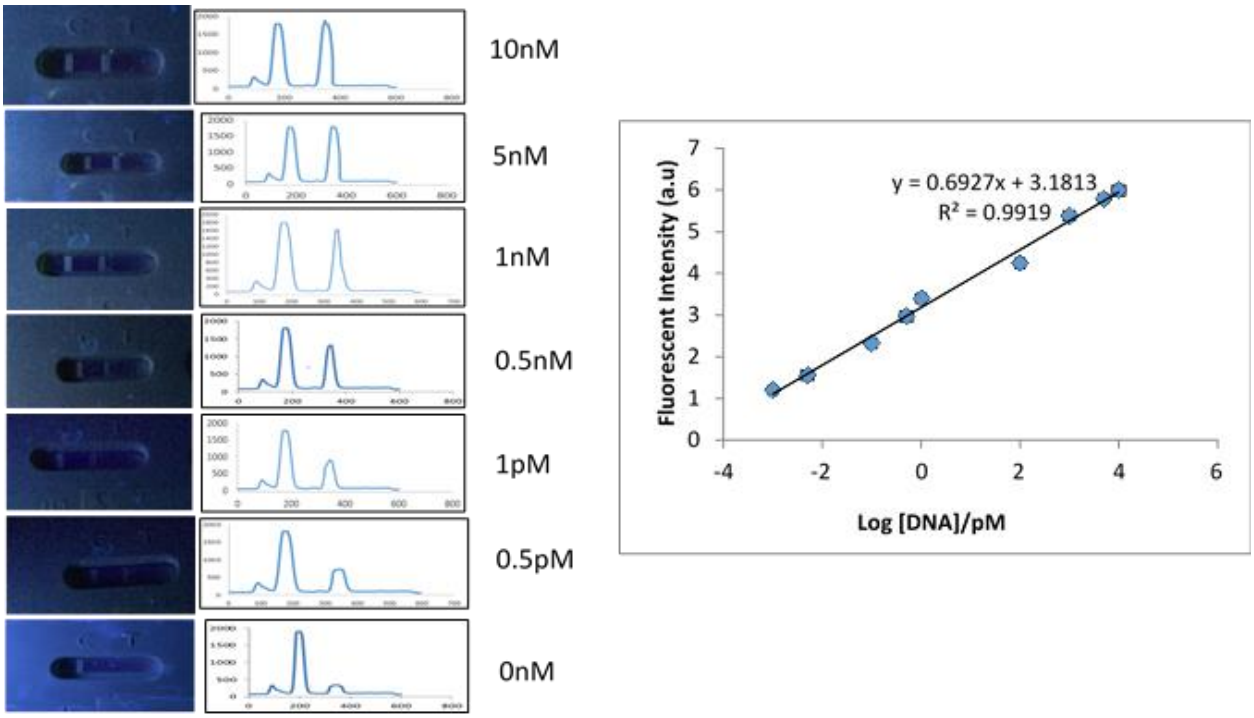

Figure 3.11. Typical photo images and calibration curve of the FCN-based LFNAB with different concentrations of target DNA under the optimal experimental conditions. Error bars represent standard deviation, *n*=6.

Selectivity of FCN-based LFNAB was studied by testing the responses of one-base mismatched DNA, two-base mismatched DNA and complementary target DNA at the same concentration level. It was found that similar responses were obtained from the one-base mismatched DNA and complementary DNA, and the response of two-mismatched DNA was much lower than that of complementary DNA **(Figure 3.12.)**. The results indicated the FCN-based LFNAB was able to differentiate two-base mismatched DNA from the target DNA. Reproducibility of FCN-based LFNAB was tested in the absence and presence of 0.5 pM and 1.0 nM concentrations of target DNA. Samples were tested for 6 times with the same concentrations and the fluorescence intensities of the LFNAB test line were measured. The relative standard deviation for 0 nM, 0.5 pM and 1.0 nM was 3.9%, 7.2% and 4.7%, respectively, indicating a very good reproducibility.

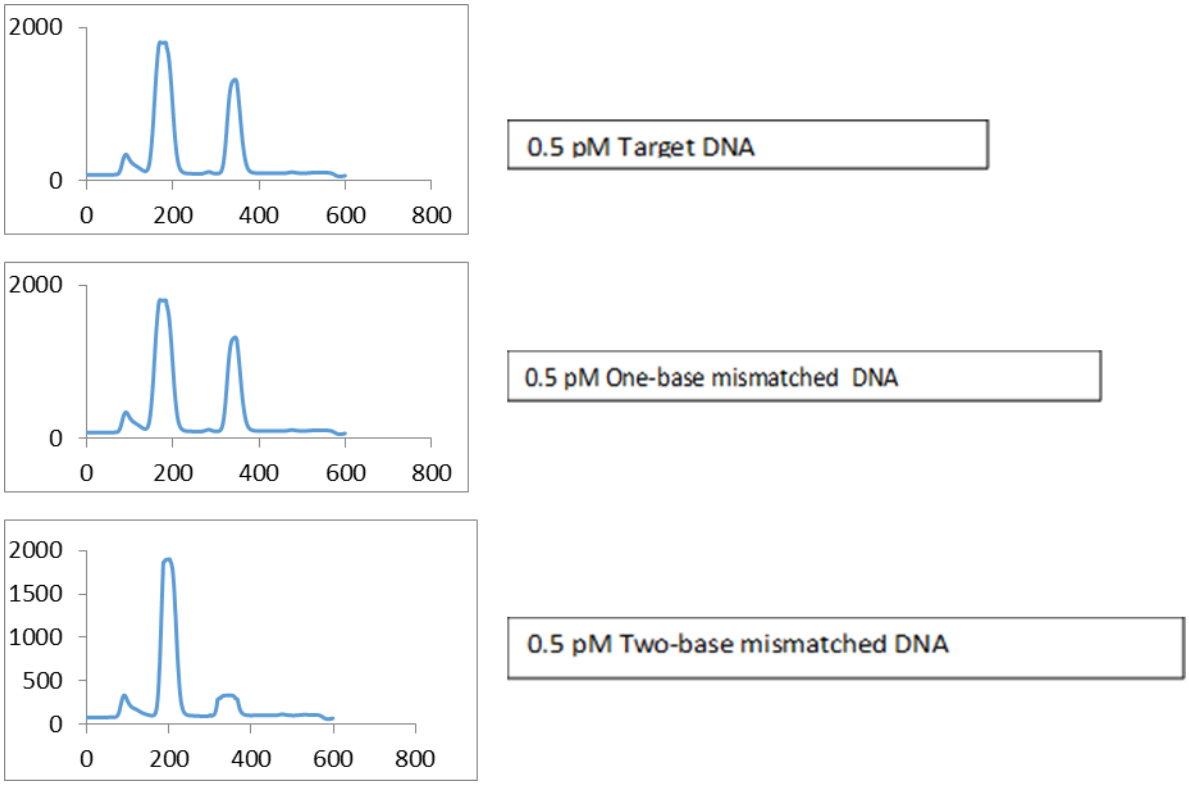

Figure 3.12. The fluorescent responses of the test line and control line of the FCN-based LFNAB in the presence of 0.5pM target DNA, 0.5pM one-base mismatched DNA, 0.5pM two-base mismatched DNA. Left peak: control line; Right peak: test line.

Table 1 shows the detection limits of the reported lateral flow DNA/microRNA assays based on different labels and signal amplification methods. The DL of FCN-based LFNAB in this report is 4 to 6 orders lower than that of GNP-based LFNAB without signal amplification, and is comparable with that of LFNAB with additional signal amplification. Compared with references in table 1, the advantages of the proposed method in this report include: (1) the preparation of FCNs was very convenient; (2) the low detection limit was obtained without complex procedures and additional signal amplification; (3) the cost of FCNs is much lower than that of GNP.

Table 3.1. Comparison of the detection limits of different lateral flow DNA assays

Detection Method	Detection Limit	Reference
Fluorescent DNA Probe based lateral flow assay	10-100 copies plasmid DNA / µL	[102]
Fluorescent dye-doped Nanoparticle based lateral flow assay	0.066 fmols (1 pM)*	[69]
UPT (Upconverting Phosphor Technology) particle based lateral flow assay	0.1 fmol (1 pM)*	[104]
Dye entrapping liposomal nanovesicle based universal biosensor	1 nM	[71]
Copper dependent DNA-cleaving DNAzyme and Gold nanoparticle based lateral flow assay	10 nM	[54]
Blue dye doped latex bead based lateral flow strip	3.75 fmol (28.85 pM)*	[115]
DNA-Gold nanoparticle based lateral flow biosensor	60 pM	[84]
Molecular beacon functionalized Gold nanoparticle based lateral flow assay	50 pM	[67]
DNA-Carbon nanotube based lateral flow biosensor	40 pM	[91]
Gold nanoparticle- Horseradish Peroxidase dual label based lateral flow biosensor	1.25 fM	[66]
ISDPR (Isothermal Strand Displacement Polymerase Reaction) and Gold nanoparticle based lateral flow assay	0.01 fM	[98]
Fluorescent Carbon nanoparticle based lateral flow biosensor (No signal amplification)	0.4 fM	Present Work

The anti-interference ability and applicability of testing DNA in real samples of the proposed method were studied by testing target DNA in spiked human plasma samples. The plasma samples were then diluted to 2.5% with running buffer. The results as shown in figure 3.13 indicates the proposed method has excellent anti-interference ability. The recoveries of 98% and 101% were obtained for 1nM and 0.5 pM, respectively, indicating the potential of the developed assay for further clinical applications.

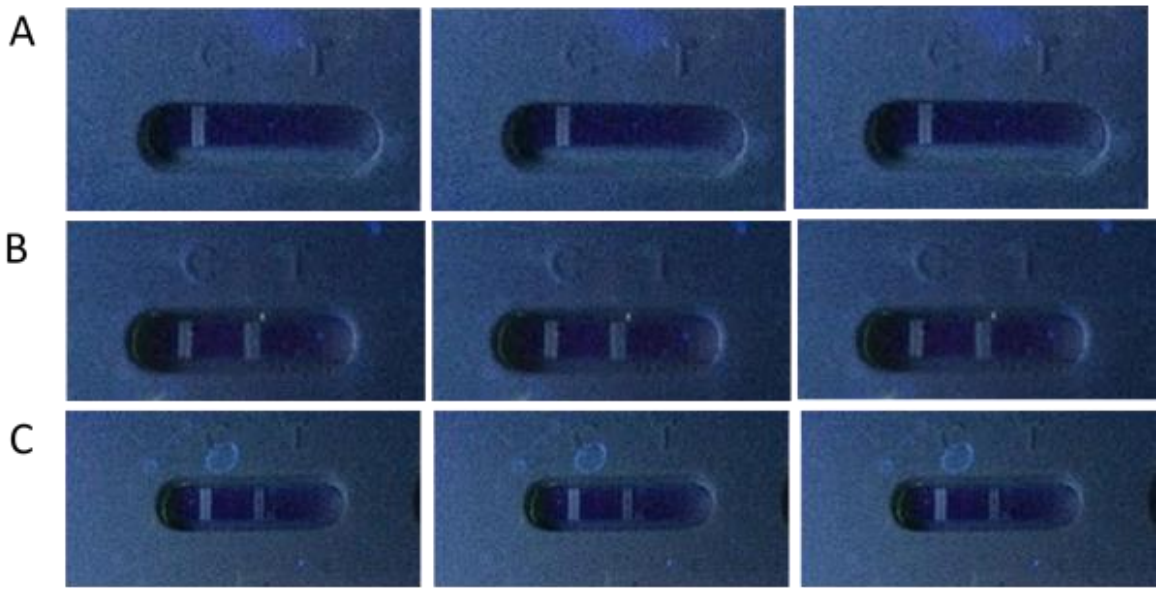

Figure 3.13. Typical photo images of FCN-based LFNAB after applying plasma samples. (A) Only 2.5% plasma (B) 2.5% plasma spiked 1 nM target DNA (C) 2.5% plasma spiked with 0.5pM target DNA concentration. Left band: control line; Right band: test line.

3.4. Conclusion

Fluorescent carbon nanoparticle was first used as a tag to develop a lateral flow nucleic acid biosensor for ultrasensitive and quantitative detection of nucleic acid samples. Under optimal conditions, the FCN-based LFNAB was capable of detecting minimum 0.4 fM target DNA without complex operations and additional signal amplification. The FCN-based LFNAB was used to

detect target DNA in spiked human plasma samples with satisfied recoveries. Further work will study the multiplex capability of the fluorescence carbon nanoparticle tag on the lateral flow nucleic acid biosensor and detect microRNAs in biological samples, which are the biomarkers of cancers. The FCN-based LFNAB in this report shows great promise for in-field and point-of-care diagnosis of genetic diseases and detection of infectious agents or warning against biowarfare agents.

4. CARBON NANOTUBE-ENZYME BASED LATERAL FLOW BIOSENSOR FOR THE DETECTION OF miRNA-210, A PANCREATIC CANCER BIOMARKER

4.1. Introduction

Development of accurate biomarker assays is the need of the hour for early detection of pancreatic cancer (PC) to reduce high mortality rates associated. Pancreatic Cancer remains as one of the most aggressive malignancies in United States.[116] It is the third leading cause of death among all the cancers and is soon expected to the second leading cause of cancer-related deaths by 2020 surpassing colorectal cancer.[117] The high mortality rates could be associated to lack of early detection methods and current available diagnostic strategies available for PC. Current procedures for diagnosis such as endoscopic ultrasound-guided fine needle aspiration are not very suitable or preferred for early detection or screening of the pancreatic cancer due to the invasiveness and cost associated with it.[118-120] Therefore there exists a need for the development of biomarker based point of care assays which are inexpensive, sensitive and convenient for the patients thus facilitating early detection of PC.

miRNAs have recently gained significant attention in the recent years because of their roles in the progression of cancers including pancreatic cancer. The miRNAs are naturally occurring, non-coding small 19-22 nucleotide RNAs which are highly specific indicators of developmental stages and conserved across different species.[121-123] Many reports have suggested that the varying miRNA expression levels in normal, benign and malignant PC patient samples correlating with disease progression offer a new potentially sensitive method for improved detection and diagnosis of the disease.[124-125] miRNA-210 have been recently identified as a potential biomarker for PC among various other miRNA biomarkers and was found to be elevated significantly in the plasma from PC patients compared to normal adults and pancreatitis.[126-127]

The current well-established techniques for the detection of miRNA include microarray, northern blotting and reverse transcription quantitative real-time PCR (RT-qPCR) with the most common ones being PCR.[128-129] But all these techniques have enormous issues of false-positives even with a tiny amount of contamination thus demanding a very clean environment, sophisticated and expensive instruments requiring long assay times making it inconvenient for rapid on site testing.[130] To meet the needs of an ideal detection method, which would detect the target quantitatively with high sensitivity and specificity with the use of inexpensive reagents or equipment, lateral flow biosensors are widely used.

Various groups have proposed colorimetric nucleic acid lateral flow biosensors using various labels, with the most common one being gold nanoparticle (GNP).[131-132] But due to the sensitivity constraint, focus has shifted to using carbon nanotube for the detection due to its large surface area and ease of separation.[133-135] CNTs have been used as a carrier for the detection probe in CNT based lateral flow biosensor.[136] To further improve the sensitivity required for miRNA detection and its application in the detection of real samples such as plasma, blood and also for the detection of cell extracts from various pancreatic cancer cell lines, we propose a carbon nanotube-enzyme-DNA based nucleic acid lateral flow biosensor for ultra-sensitive detection of miRNA-210.

Amine modified DNA detection probe and alkaline phosphatase (ALP) enzyme was coated on the carbon nanotubes to prepare the CNT-DNA-ALP label. Sandwich type reactions were carried out on lateral flow biosensor leading to the capture of the target miRNA between the detection probe of the label and capture probe at the test zone, producing distinct characteristic black bands after the addition of the substrate enabling the visual detection of very low target

concentrations. The elaborate details of the CNT-DNA-ALP based LFB are reported in the following sections.

4.2. Materials and Methods

4.2.1. Apparatus

The Biojet BJQ 3000 dispenser, Clamshell laminator and the Guillotine cutting module CM 4000 were from Biodot Ltd (Irvine, CA). Kinbio portable strip reader was purchased from Shanghai Gold bio Tech. Co.; Ltd. (Shanghai, China). PowerPac^{TM} basic power supply and mini-sub cell GT cell were purchased from Bio-Rad (Hercules, CA).

4.2.2. Reagents

Carboxylated multi-walled carbon nanotubes, Streptavidin, Tween-20, Triton X-100, N-(3- Dimethyl amino propyl)-N'-ethylcarbodiimide hydrochloride (EDC), N-hydroxy sulfo succinimide (Sulfo-NHS), 2-(4-Morpholino) ethane sulfonic acid (MES), Sucrose, Tween-20, phosphate buffer saline (0.01M PBS, pH 7.4), BCIP/NBT-blue liquid substrate, sodium chloride-sodium citrate (SSC) buffer 20X concentrate (pH 7.0), Ethidium bromide and orange-X dye were purchased from Sigma Aldrich (St. Louis, MO). Agarose and TAE buffer from Promega, Alkaline phosphatase (ALP) was bought from Calbiochem and 500-50bp ladder from Norgen. Cellulose fiber sample pads (CFSP001700), glass fibers (GFCP000800), laminated cards (HF000MC100) and nitrocellulose membranes (HFB18004 and HFB24004) were purchased from Millipore (Billerica, MA).

Ultrapure (> 18 MΩ) water from Milli-Q water purification system (Billerica, MA) was used to prepare solutions. All the DNA oligonucleotides were purchased from Integrated DNA technologies, Inc. (Coralville, IA). The sequence information is listed below

Target miRNA: 5' - rCrUrG rUrGrC rGrUrG rUrGrA rCrArG rCrGrG rCrUrG rA – 3'

Amine-modified Detection probe: 5'- /5AmMC6/ TCA GCC GCT GT- 3'

Biotinylated capture DNA probe: 5' – CAC ACG CAC AG/3 Bio/ -3'

Biotinylated control DNA probe: 5' – ACA GCG GCT GA/3 Bio/- 3'

One base mismatch target: 5'- rCrUrG rUrGrC rGrUrG rUrGrA rCrArG rCrGr**C** rCrUrG rA – 3'

Two base mismatch target: 5'- rCrUrG rUrGrC rGrUrG rUrGrA rCr**U**rG rCrGr**C** rCrUrG rA – 3'

4.2.3. Preparation of CNT-DNA-ALP Conjugates

Carbon nanotubes were shortened under ultra-sonication with sulfuric acid: nitric acid (3:1) mixture for three hours and washed with water till the acid is washed off. Following the washes, the carboxylic groups on the CNT's were activated using the standard EDC/NHS procedure for 15 min at room temperature. The activated CNT's were suspended in PBS followed by the addition of appropriate optimized amounts of DNA and enzyme. The mixture was then incubated overnight at 4^{o}c before the final washes to remove excess DNA and Enzyme. The resulting conjugate was finally suspended in eluent buffer (20mM Na_3PO_4, 5% BSA, 10% Sucrose, 0.25% Tween-20) before use.

An agarose gel electrophoresis was run to confirm the formation of carbon nanotube-DNA conjugates. This was done by evaluating the mobility of the single stranded detection probe, the conjugate (carbon nanotube conjugated with detection probe) and the carbon nanotube. All were incubated with complimentary control probe leading to the formation of duplex DNA which facilitated ethidium bromide intercalation aiding the visualization of DNA bands.

The samples were placed in the following lanes: lane 1 contained the DNA ladder, lane 2 was the carbon nanotubes, lane-3 was the duplex DNA and lane-4 was the conjugate (CNT conjugated with the detection probe).

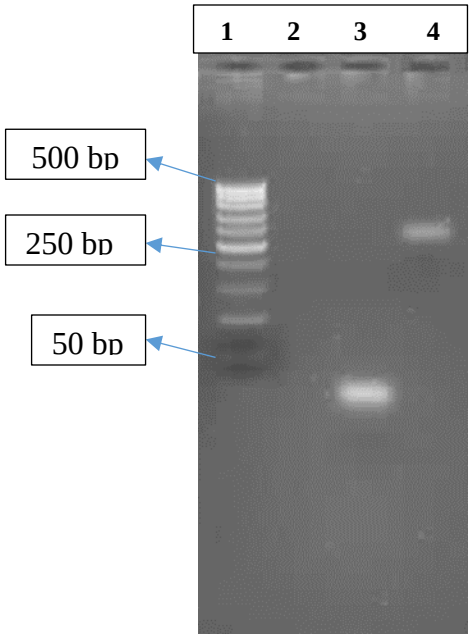

Figure 4.1. Agarose gel electrophoresis. (A) Lane-1: Ladder (500-50 bp); Lane-2: Carbon nanotubes + control DNA probe; Lane-3: Detection probe + control probe; Lane-4: CNT-DNA conjugate + control probe; gel contained 1% w/v Agarose and 0.5ug/ml ethidium bromide.

The formation of the conjugate was confirmed by comparing the mobility of the samples as listed in the figure 4.1. The duplex DNA in the lane-3 with no label had greater mobility than when the detection probe is conjugated on to the CNT as seen in lane-4. Upon the detection probe conjugation, the mass of the particle becomes larger, thus making it more difficult to travel the length of the agarose gel. To ensure that the signal from lane-4 was from the detection probe CNT conjugate, not from the CNT itself, only CNT sample was run in lane-2. As seen in the gel image (figure 4.1.), there is no signal in lane four, contributing to the assurance that the detection probe had indeed conjugated onto the CNT surface in lane-4. From, this data, it is apparent that the method used to make the conjugates was successful.

4.2.4. Preparation of Streptavidin-Biotin Conjugates

Streptavidin (250µl, 2.5mg/ml) was incubated with biotinylated capture probe (100 nano moles) at room temperature with continuous shaking for one hour. Following the incubation, the

complex was washed with a centrifugal filter for 20 min, 6000rpm, 4ºC multiple times to ensure the successful preparation of the unbound DNA and streptavidin. The filtrate on the filter was re-suspended in PBS to a final volume of 600µl before use. Similar procedure was followed to prepare conjugates using biotinylated control probe.

4.2.5. Preparation of Nucleic Acid Biosensors

The nucleic acid biosensor typically consists of four components: sample application pad, conjugate pad, nitrocellulose membrane and absorption pad. The sample application pad was pre-treated with the sample pad solution (0.25% Triton X-100, 0.05M Tris-HCl, 0.15 M NaCl and 5% Tween) before use. Pre-treatment of the sample pad included soaking the pad in the buffer for one hr. at room temperature followed by drying of the sample pad in the oven and their storage in desiccators at RT. The capture probe and control probe were dispensed (dispensing was done using a Biojet BJQ 3000 dispenser) at different positions on the nitrocellulose membrane as the test zone and control zone respectively. To facilitate the immobilization of the DNA probes on the nitrocellulose membrane, the biotinylated DNA probes were incubated with streptavidin to form the streptavidin-biotin DNA conjugates. The nitrocellulose membrane was then dried at 37ºC for an hour before storing them at 4ºC for further use. Lastly, all the four components were assembled on a plastic backing layer using the clamshell laminator. It was ensured that all the parts overlapped at least 2 mm to facilitate the smooth migration of the sample during the assay. After the assembly, the Guillotin cutting module CM 4000 was used to cut the biosensors with a uniform 3mm width. A desired volume of the CNT-ALP-DNA conjugates was then dropped on the conjugate pad of the biosensor with a micro-pipette and was air-dried before the assay.

4.2.6. Sample Assay Procedure

The ALP-CNT-DNA based NALFB was prepared following the procedure by our group. All the optimizations are carried out systematically and after the attainment of the best suitable conditions, the assay was run following the procedure developed by our group. Hundred microliter of the sample solution containing desired concentration of the target prepared in ¼ dilution of SSC buffer with 2% BSA was applied to the sample pad. After 15 min, additional 100ul buffer was added to facilitate the washing step. After 20 min, when two black bands are seen at the test zone and control zone respectively, 20ul of the BCIP/NBT- Blue Liquid Substrate was added to the strip. The formation of an insoluble colored precipitate at the test zone and control zone demonstrate the formation of enzyme-substrate complex resulting in the amplification of the color thus giving a measurable signal. This signal intensities were later recorded using the kinbio strip reader. The total assay time including the enzyme-substrate reaction was 30 min.

4.3. Results and Discussion

4.3.1. Principle of Detection Using ALP-CNT-DNA NALFB

4.3.1.1. Preparation of CNT-DNA-ALP Labels

This current study takes advantage of using the carbon nanotube as a label and carrier of numerous enzyme and DNA molecules simultaneously thus resulting in the enormous amplification of the colorimetric signal. Due to the poor insolubility of the CNTs hampering the movement on the lateral flow strip, pre-treatment of the CNTs was absolutely necessary before the conjugation procedure. Therefore, the CNTs were shortened under ultra-sonication using a mixture of concentrated acids (HNO_3: H_2SO_4 = 1:3). The carboxyl groups on the shortened CNT were then activated using the standard EDC/NHS activation prior to the conjugation with amine groups on

the detection probe and enzyme. The conjugates were subjected to successive washes after overnight incubation to remove the excess of DNA and enzyme.

4.3.1.2. Working Principle of the Lateral Flow Biosensor

CNT-DNA-ALP dual label based LFNAB combines the advantage of CNT as a colored label and the catalytic amplification of an enzyme tracer for a very sensitive detection of miRNA on a lateral flow biosensor. The previous LFNAB based on the carbon nanotube label suffered from a poor detection limit which hampers the detection of miRNA. To enable the detection of miRNA and to develop an ultrasensitive test, an additional signal amplification step in the form of an enzyme label was introduced on to the CNT enabling the preparation of CNT-ALP dual label for the LFNAB. Followed by the activation of carboxylic groups on CNT surface, DNA and ALP were added simultaneously. The whole assay of the detection of miRNA is based on a sandwich reaction between the target miRNA and the detection probe with the label and capture probe, followed by the addition of substrate.

So, the principle of lateral flow assay combined the sandwich DNA hybridization and enzyme catalytic amplification as shown in figure 4.1. The CNT-DNA-ALP conjugate (Detection DNA complimentary to a part of target miRNA) was dispensed on the conjugate pad, biotinylated capture probe (complimentary to a part of target miRNA) and control probes (completely complimentary to the detection probe on the CNT) were incubated with streptavidin before dispensing on the nitrocellulose membrane to form the test and control zones respectively.

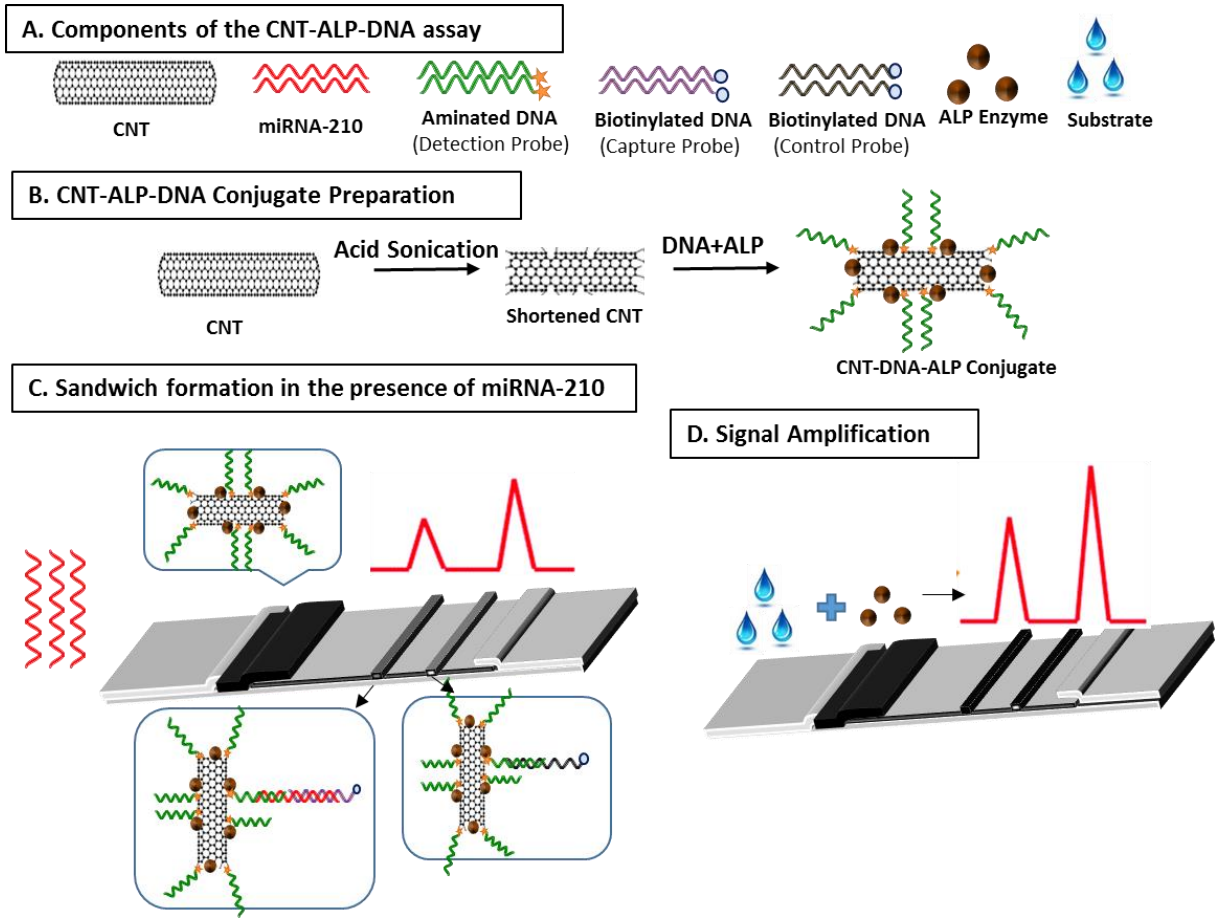

Figure 4.2. Schematic of CNT-ALP-DNA based LFNAB (A) Components of the CNT-ALP-DNA lateral flow assay (B) Shortening of CNTs and preparation of CNT-DNA-ALP conjugates (C) Lateral flow assay in the presence of target miRNA (D) Signal amplification step in which substrate is applied to react with the captured conjugates.

When the sample solution containing desired concentration of target miRNA is applied onto the sample pad, it moves along the strip by the capillary action. Upon reaching the conjugate pad, the target miRNA forms a complex with the detection probe on CNT and this complex as it continues to migrate along the strip gets captured by the capture probe on the test line. This results in the formation of a sandwich and accumulation of CNT-DNA-ALP conjugates which was visualized by a characteristic black line. The excess of the conjugate formed a control line as a result of the control probe on the control zone. In the next step, NBT-blue substrate solution was added which resulted in the formation of insoluble blue colored chromogen product due to the

enzymatic reaction on the test line and control line. In the absence of the target miRNA, no labels were captured on the test line resulting in the formation of only control line.

4.3.1.3. Optimization of Experimental Parameters

To attain ultra-sensitive detection limits, various experimental parameters had to be optimized. The optimizations with respect to the conjugate included volume of ALP-DNA-CNT conjugate on the conjugate pad and the concentration of detection probe on the label, number of dispensing times of the test line on the nitrocellulose membrane and composition of running buffer. The amount of detection probe has a significant impact on the hybridization efficiency and sandwich formation on the test line thus altering the whole performance of the sensor. Therefore, the concentration of detection probe which is to be coated on the CNTs was optimized. As shown in figure 4.2.(A), the S/N was found to be the highest at 0.1 O.D where the signal was found to saturate and decreasing thereafter. The increasing DNA on the CNT might be the possible reason attributing for the decrease in the S/N ratio, reason being the steric hindrance.

The amount of CNT-DNA-ALP conjugates dispensed on the conjugate pad also has a huge impact on the intensity of the test-line. To obtain the best S/N ratio, assays were run with different volumes of the conjugate loaded on the conjugate pad. Figure 4.2.(B),presents the histogram showing the influence of the conjugate volume on the S/N ratio of the LFSB. The S/N ratio increased with the increase in the volume of conjugate up to 5 µl and a decrease in the signal was noticed with further increase. Thus, 5 µl of the conjugate volume was used as an optimum volume for all the assays.

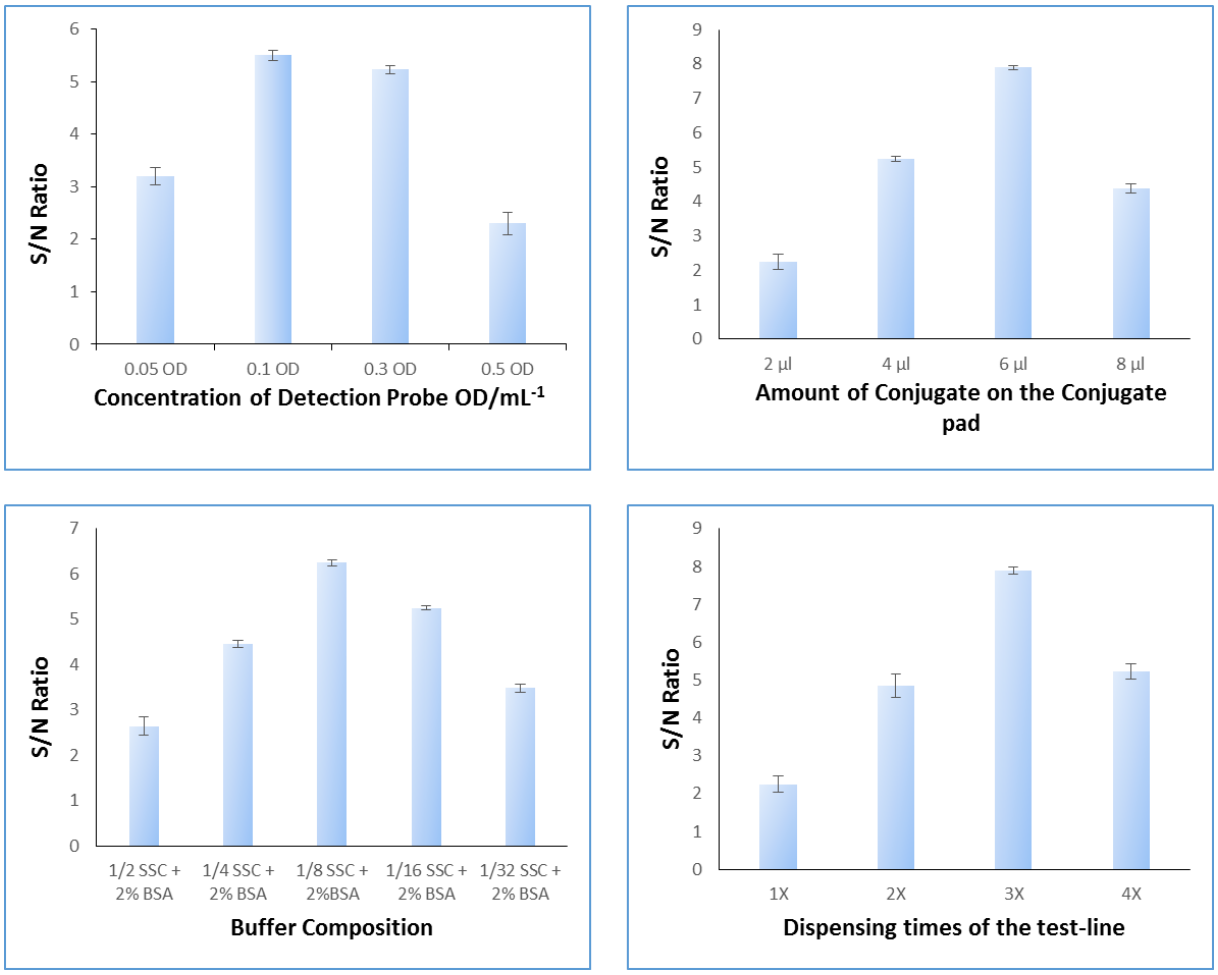

Figure 4.3. Optimization of the assay conditions (A) The concentration of detection probe used for the preparation of the conjugate (B) The volume of the conjugate dropped on the conjugate pad (C) The amount of SSC added into the buffer (D) The number of times the capture probe was dispensed on the test zone.

The effect of running buffer on the S/N ratio of the LFSB was analyzed by varying the amounts of SSC and BSA in the running buffer. After successive optimizations as shown in the histogram 4.2 (C), the best condition was 1/8 SSC + 2% BSA which was used for further experiments and to optimize other conditions.

The amount of capture probes dispensed on the nitrocellulose membrane also has a huge impact on the S/N ratio of the sensor. The amount of capture DNA probes dispensed on the membrane was optimized by controlling the number of dispensing times which would result in

different concentrations of streptavidin-biotinylated DNA complex at the test zone. Figure 4.2.(D), shows that the highest S/N ratio was obtained by 3 times dispensing and the decreased S/N with more dispensing times resulted from increased background signal.

The enzyme substrate reaction time is also an important factor that needs to be taken into consideration to obtain best possible results. Once the enzyme gets captured on the test and control zones respectively, washes were done to remove the excess. Substrate was then applied and the reaction time was measured. The S/N ratio increased till 5 min after which the signal was saturated as shown in Figure 4.3 (A).

Amount of enzyme added during conjugation was also a very important factor contributing to the overall performance of the biosensor. Various volumes ranging from 1-4 µl of the enzyme was added to prepare conjugates during the optimization. There was not much difference between the signals when 1 µl or 2 µl of the enzyme was added after which the signal reduced (Figure 4.3 (B)). So, 1 µl (35 units of the enzyme) was used as the best condition for the preparation of the conjugate. The volume of the substrate added to react with the appropriate amount of the enzyme was also optimized. Different volumes of the substrate solution was applied onto the sensor ranging from 5 – 25 µl and the highest S/N ratio was obtained when 10 µl of the substrate solution was used as shown in 4.3(C).

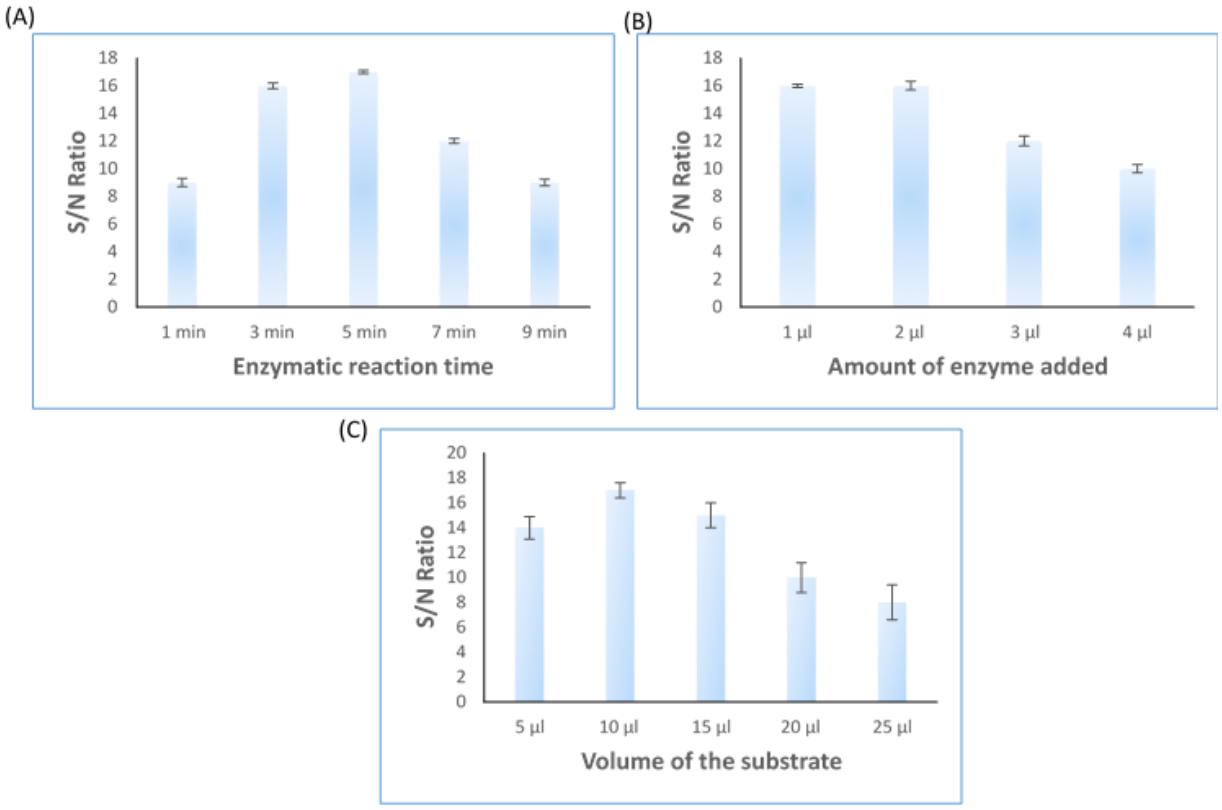

Figure 4.4.Optimization of assay conditions with respect to signal amplification (A) The reaction time required for the captured enzyme to react with the substrate (B) Volume of the enzyme added during the preparation of the conjugate (1 µl corresponds to 35 units of the enzyme) (C) Volume of the substrate added during step-4 of the assay.

4.3.2. Analytical Performance

Various concentrations of target miRNA were tested to evaluate the performance of the sensor under optimized experimental conditions. The average value of three replicates at each concentration was used to plot the calibration curve. Fig 4.4(A) represents the typical photo images of the strips after the assay.

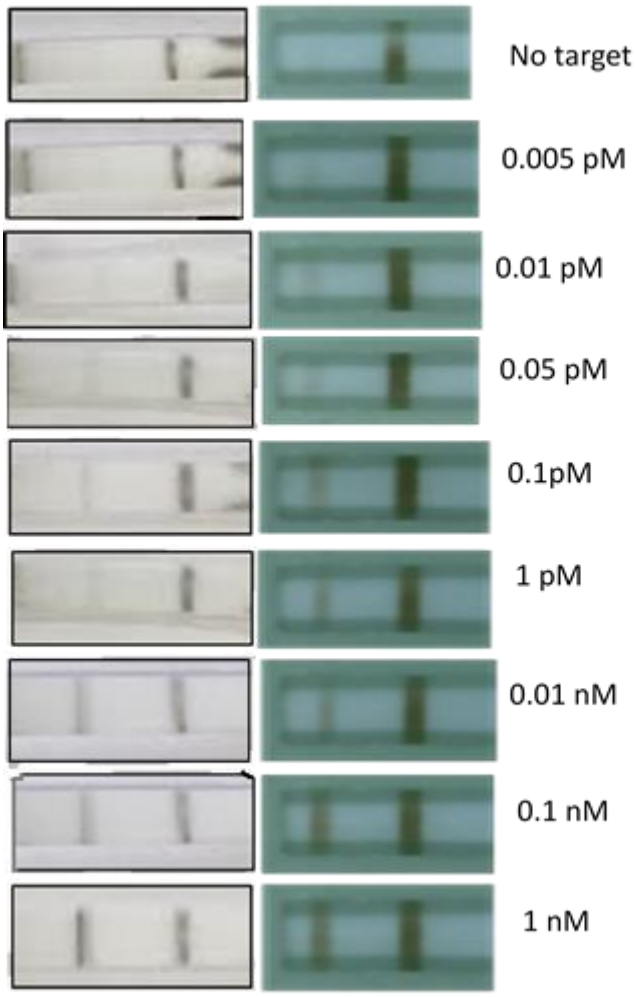

Figure 4.5. Typical photo images of the strips after the assay was run with various concentrations of target miRNA

There was no color at the test zone in the test without target even after the addition of the substrate indicating negligible non-specific adsorption under optimized conditions. In this sandwich type of lateral flow assay, the intensity of the test line was found to increase evidently with increasing target concentration up to 10nM after which it was saturated. A faint line was observed even after the addition of very low concentrations of target around 5fM by the addition of substrate. The calibration curve was plotted with various concentrations versus S/N ratio (figure 4.5) and the detection limit was calculated to be 2.4fM.

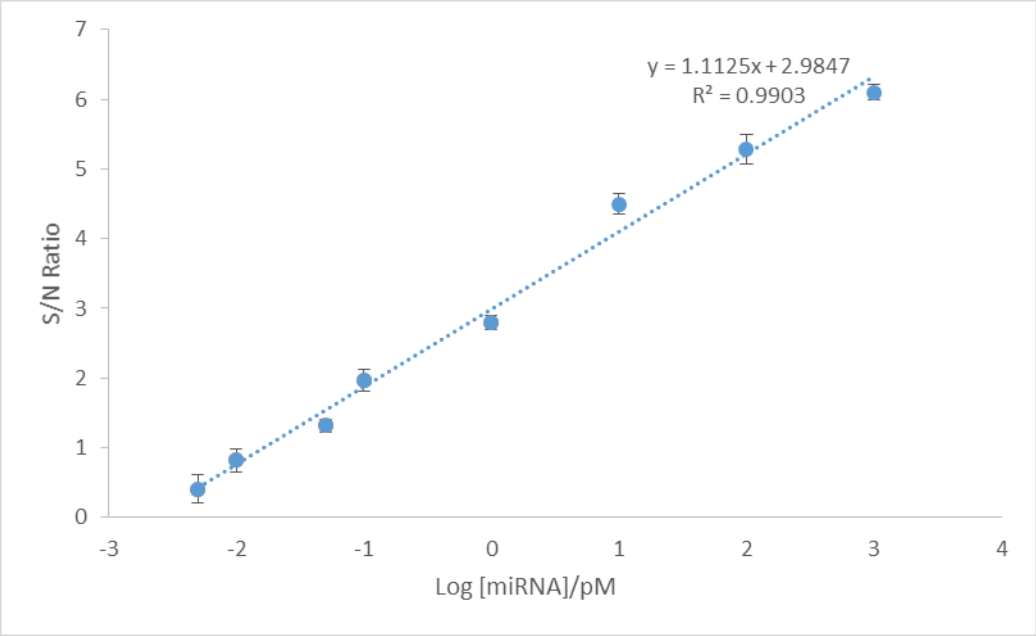

Figure 4.6. Calibration curve plotted against various concentrations of miRNA versus the corresponding S/N ratio

4.3.3. Specificity and Reproducibility of the Assay

To confirm the specificity of the CNT-ALP-DNA based lateral flow biosensor, the signal between the target miRNA and a mixture of target and non-complementary miRNA was compared. The high concentration of the non-complementary miRNA in the mixture did not affect the signal from the target miRNA as there was very negligible difference between the signal intensities (figure 4.6). The reproducibility of the sensor was also tested in the absence and presence of 10fM and 0.1pM target miRNA. The same test with the same concentrations was repeated 6 times and there was negligible difference the intensities with relative standard deviation being 6.0%, 3.8%, 2.7% for control, 10fM and 0.1pM respectively indicating good reproducibility. The biosensor was also tested for stability with the conjugates stored at 4^{o}C for a month. There was negligible difference in the intensities when 0.1pM concentration was tested.

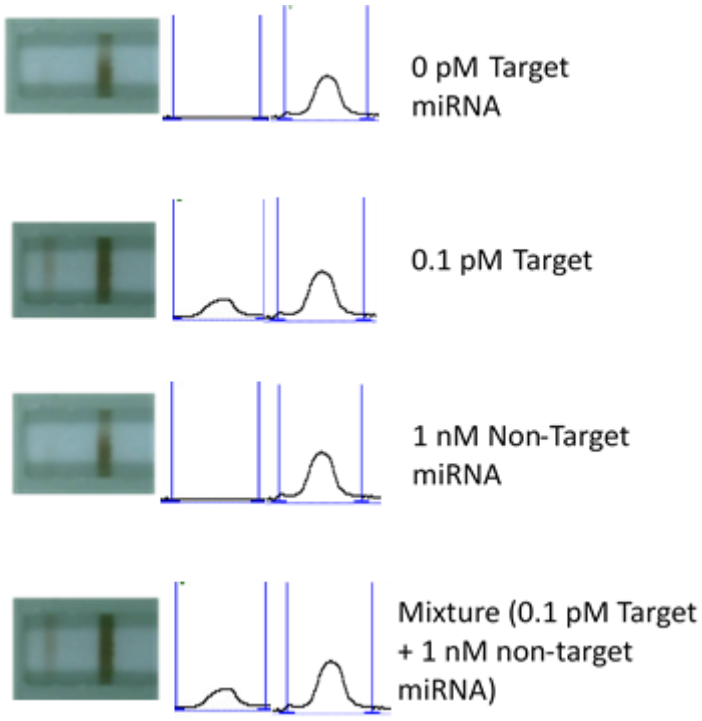

Figure 4.7. Typical photo images of the sensor in the presence of 0pM miRNA (Control), 0.1pM target miRNA, 1nM non-complementary miRNA and mixture of 0.1pM target and 1nM non-complementary miRNA.

4.4. Real Sample Detection

All the above results prove the inherent characteristics of the CNT-ALP-DNA lateral flow biosensor in terms of stability, reproducibility, specificity and sensitivity in detecting very low concentrations of target-miRNA 210. To further evaluate the credibility of this sensor for the detection of miRNA 210, this was applied to test the real sample detection.

4.4.1. Application of NABLFB for the Detection of miRNA-210 in Blood Samples

Healthy plasma samples were purchased from Golden West Biologicals, Inc. These plasma samples were spiked with 10pM and 10fM of the target concentrations respectively and were tested with the CNT-DNA-ALP based lateral flow biosensor (Table 2).The percent recoveries for both the concentrations were within the range of 85-105% indicating a very negligible effect of other components of plasma on the signal intensity.

Table 4.1. Percent recoveries of the plasma samples spiked with 10pM and 10fM target concentrations respectively

Sample	10pM	10fM
1	96%	92%
2	92%	85%
3	99%	102%
4	94%	91%
5	101%	96%

Followed by these preliminary tests, actual pancreatic cancer patient sample was supplied by Sanford clinic in Fargo, ND. The patient sample was centrifuged and plasma was collected. Total miRNA was extracted from 200µl of each human plasma samples using a Qiagen miRNeasy Plasma/Serum kit according to manufacturer's instructions. The total RNA was tested using the CNT-DNA-ALP lateral flow biosensor and was compared to the miRNA extract from healthy sample. There was an obvious difference between PC patient samples versus non-cancer sample (figure 4.7) suggesting that this sensor is capable of differentiating the patient sample by the miRNA content.

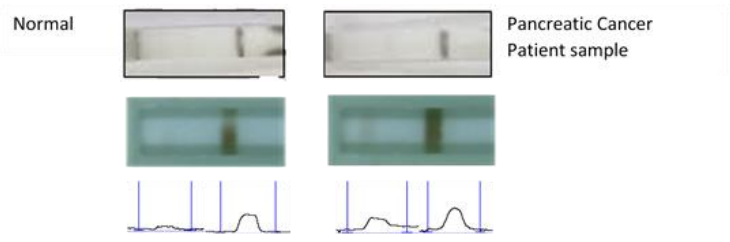

Figure 4.8. Total RNA extract from normal and pancreatic cancer patient blood sample was tested using the reported CNT-ALP-DNA biosensor.

4.4.2. Application of NABLFB for the Detection of miRNA-210 in Tissue Samples

Tissue samples were also tested for the presence of miRNA 210. Tissue samples from the tumor and non-tumor regions were collected from two PC patients. 20mg of each tissue samples were suspended in lysis buffer followed by the homogenization with a tissue disruptor. Tissue homogenate was subjected to total RNA extraction using the All prep DNA/RNA/Plasma miRNeasy-96 kit from Qiagen. The total miRNA extract from the tissues was tested for the presence of miRNA-210 using NABLFB. As shown in the figure 4.8, there was an obvious difference between the signals thus differentiating a tumor tissue samples from a non-tumor tissue sample.

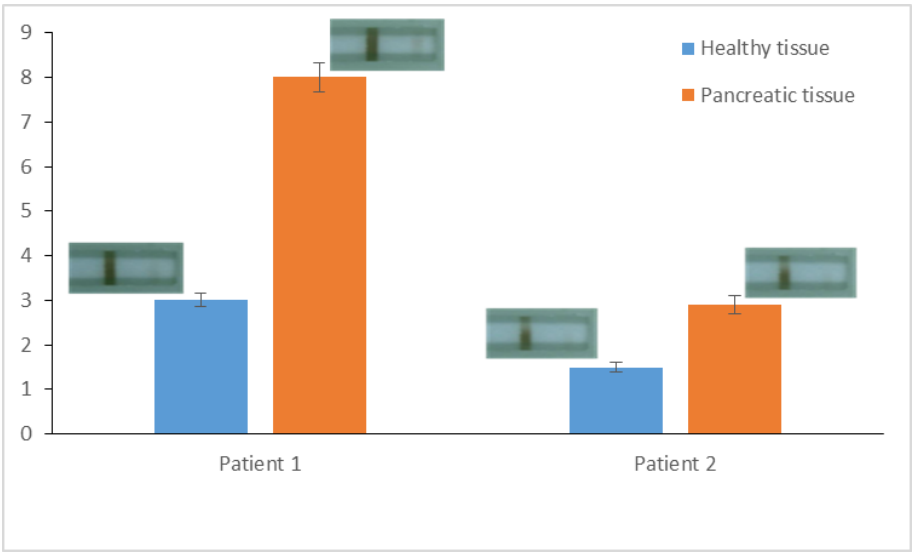

Figure 4.9. Responses from tissue and non-tissue samples from two pancreatic cancer patient samples. Above are the strip images of the respective samples after the assay.

4.4.3. Application of NABLFB for the Detection of miRNA-210 in Various Cell Lines

Adherent cell lines were washed with PBS to remove residual culture media. The cells were treated with trypsin to detach them from culture plates. All collected cells were washed with PBS. Total RNA was extracted from different cell lines using Qiagen All prep DNA/RNA/Protein

Kit according to manufacturer's instructions. The RNA corresponding to the extract from 1 million cells was run on the strip for the detection of miRNA. As seen in the figure 4.9., the cell lines showed different concentrations of miRNA 210 in them.

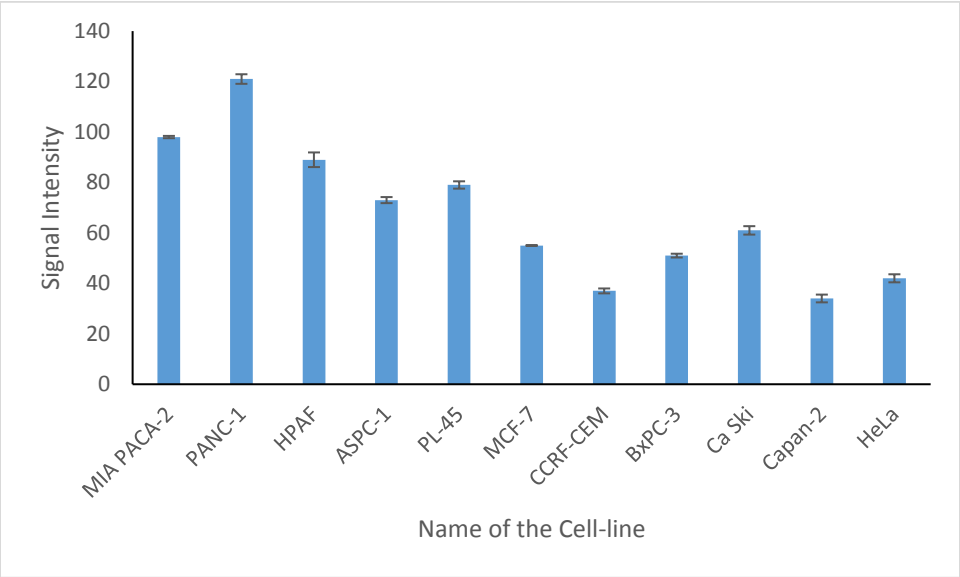

Figure 4.10. Responses from various cell line after the miRNA extract from each cell line was applied on the LFSB.

4.4.4. Validation of the Real Samples Using qRT-PCR

4.4.4.1. cDNA Synthesis

The total RNA extracts from Plasma, tissue and cell line samples were quantified using Nano drop and stored at -80^{o}C until further use. Reverse transcription was performed using SuperScript™ III Reverse Transcriptase system (Thermofisher). Each RT reaction had 50ng total miRNA, 2pmol stem loop primer, 0.5mM dNTP mix, 5mM DTT, 40 units RNaseOUT recombinant ribonuclease inhibitor, 1 Unit SuperScript RT enzyme and 4µL first strand buffer. The total reaction volume was 20µL. RT-PCR reaction was carried out at 55^{o}C for 60 minutes followed by 15 min at 72^{o}C to deactivate the SuperScript RT enzyme.

4.4.4.2. qPCR Reaction

qPCR was performed on an Applied Biosystems Real Time PCR machine using Fast SYBR^{TM} Green master mix. Each sample well contained 4µl cDNA template (RT PCR product), 0.05 µM each forward and reverse primers and 10 µl of 2X fast SYBR^{TM} Green master mix. Reaction volume was topped up to 20 µl with nuclease free water. qPCR cycling conditions were as follows: Initial denaturation at 95 ºC for 5 minutes followed by 45 cycles at 95 ºC for 5 seconds and 60 ºC for 30 seconds.

4.4.4.3. Results

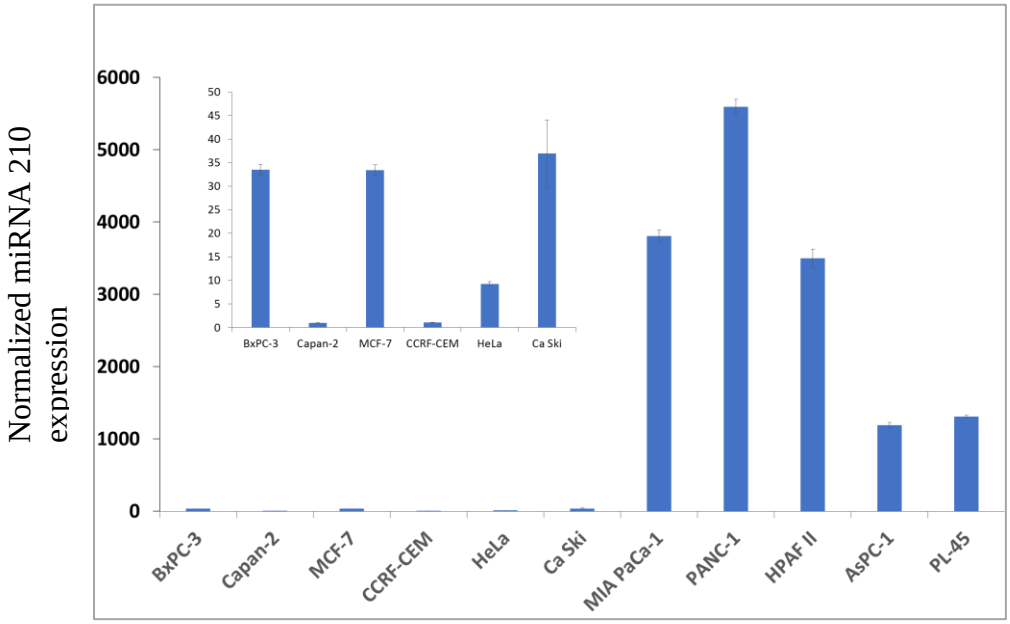

Figure 4.11. Responses from various cell lines after the qPCR reaction.

Note: Capan-2 had the lowest expression. All other cell line miRNA 210 expression was normalized to data from Capan-2.

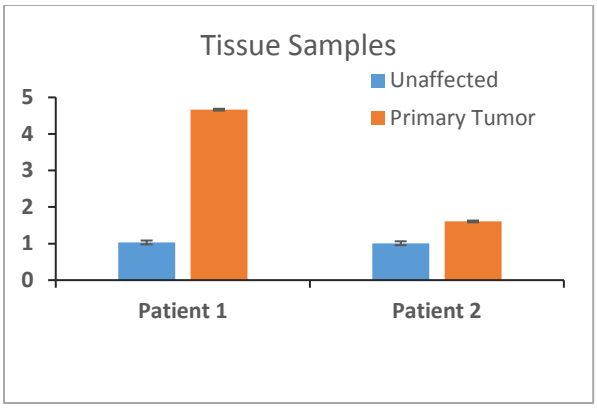

Figure 4.12. Responses from tissues of unaffected and affected patient samples after the qPCR reaction. The responses from two patients were recorded.

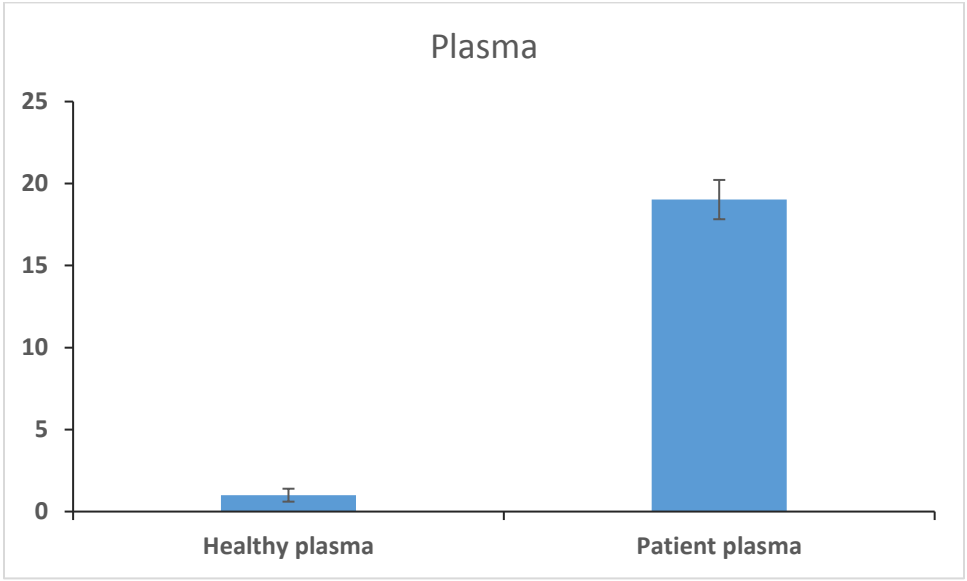

Figure 4.13. Responses from plasma of unaffected and affected PC patient samples after qPCR reaction

4.5. Conclusion

A lateral flow biosensor was successfully developed by using CNT-ALP label for the first time for ultrasensitive detection of miRNA-210. Under optimal conditions, the LFB was capable of detecting low fM ranges without the need for expensive instrumentation and complex chemical reaction. The excellent analytical performance characterized by the enzyme amplification was

further explored by the detection of target miRNA in real pancreatic cancer patient samples including plasma, tissue and various cell lines were also screened. The results were validated using qPCR thus provides a proof that this method of detection is efficient for the application in clinical diagnosis. The CNT-ALP based LFB thus shows a great promise for the early detection of various diseases and further work will aim to study the multiplexing capability of this sensor to detect various protein and nucleic acid biomarkers simultaneously thus increasing the specificity and selectivity of the detection.

5. VISUAL AND MULTIPLEX PLATFORM FOR THE QUANTITATION OF miRNA PANEL (miRNA 16, miRNA 21 and miRNA 196a) COUPLED WITH CNT-ENZYME LABEL FOR THE ULTRA-SENSITIVE DETECTION OF PANCREATIC CANCER

5.1. Introduction

With the achievements and advancements in nanotechnology, various nucleic acid lateral flow biosensors have been reported in literature as described in previous chapters. Attributing to the advantages of using the lateral flow biosensors for nucleic acid detection is the signal amplification characteristic thus contributing significantly to the selectivity and specificity properties of the detection. Several nucleic acid biosensors for the detection of various targets such as protein, [52] biological agents [22, 43, 44] and chemical contaminants [53, 54, 57] have already been reported by various groups including our group. [51, 55, 56] Nevertheless, despite the advantages associated by the multiplex detection, there are very few reports on multiplex nucleic acid detection on lateral flow biosensor.[136-138]

Lateral flow biosensor, the current context of point-of-care assays is a well-known platform for early and accurate diagnosis of a specific disease. But for some major targets, where a rapid and precise confirmation of results is vital for further treatment at the patient site,[139] clinical evidence based on a single biomarker won't be an adequate piece of information for appropriate diagnosis of a disease. Multiplexing capacity is of vital importance in enhancing the detection precision for various targets and plays a key role in increasing the specificity of the target detection. The multiplex technology of detecting a specific target has been devised to detect multiple targets simultaneously in one assay without the need for additional instrumentation. Additionally, it is highly desirable to screen various analytes simultaneously, enabling a rapid, low-cost and reliable quantification. [140-142]

In 2016, close to 60,000 new cases of pancreatic cancer were reported among men and women and 50,000 patients died of the disease.[143] Pancreatic cancer has one of the highest case to mortality rates due to the lack of symptoms for early stages of the disease.[144] Reports have suggested that there are no detectable symptoms in the early stages of the disease and the symptoms that are specific to pancreatic cancer begin to develop after the disease progresses to the advanced stages and has often metastasized to other parts of the body.[145] These reasons attribute significantly to the less than 20% five year survival rate of pancreatic cancer patients.[143] Thus there is a need for developing a simple, convenient, reliable and ultra-sensitive detection platform provocating people to perform routine examinations to keep an eye on the spread of the disease.

CNT-enzyme based nucleic acid lateral flow biosensor has been developed for the detection of miRNA-210 as mentioned in the last chapter. But the recent reports have suggested that the miRNA-210 cannot be considered as an ideal biomarker for pancreatic cancer as the increasing levels of the miRNA were also associated with other cancers like the breast cancer [146] and renal cell carcinoma.[147] Thus only the detection of miRNA-210 as a biomarker for PC may not act as a reliable source for the early detection. In light of this, taking the advantage of the sensitive label and optimized conditions, we propose a lateral flow biosensor for the multiplex detection of a miRNA panel (miRNA-16, miRNA-21, miRNA-196a) on a single platform in a single assay. [148-150] There are several specific miRNAs that can be useful as prognostic biomarkers for predicting survival, monitoring surgical outcome and selecting therapy based on drug sensitivity such as the panel described above. Testing these serum/plasma miRNAs is non-invasive, thus providing a convenient approach for management of pancreatic cancer therapy. The detection of the miRNA panel on the lateral flow biosensor eliminates the issues of reliability thus increasing the overall efficiency, sensitivity and specificity of the detection.

Amine modified DNA detection probes specific for each target miRNA and alkaline phosphatase (ALP) enzyme was coated on the carbon nanotubes to prepare the CNT-DNA-ALP labels separately for the three miRNA targets. Sandwich type reactions were carried out on lateral flow biosensor leading to the capture of the target miRNA between the detection probe of the label and capture probe at the test zone specific for each target, producing distinct characteristic black bands after the addition of the substrate enabling the visual detection of very low target concentrations. The elaborate details of the CNT-DNA-ALP based LFB are reported in the following sections.

5.2. Materials and Methods

5.2.1. Apparatus

The Biojet BJQ 3000 dispenser, Clamshell laminator and the Guillotine cutting module CM 4000 were from Biodot Ltd (Irvine, CA). Kinbio portable strip reader was purchased from Shanghai Gold bio Tech. Co. Ltd. (Shanghai, China).

5.2.2. Reagents

Carboxylated multi-walled carbon nanotubes, Streptavidin, Tween-20, Triton X-100, N-(3- Dimethyl amino propyl)-N'-ethylcarbodiimide hydrochloride (EDC), N-hydroxy sulfo succinimide (Sulfo-NHS), 2-(4-Morpholino) ethane sulfonic acid (MES), Sucrose, Tween-20, phosphate buffer saline (0.01M PBS, pH 7.4), BCIP/NBT-blue liquid substrate and sodium chloride-sodium citrate (SSC) buffer 20X concentrate (pH 7.0) were purchased from Sigma Aldrich (St. Louis, MO). Alkaline phosphatase (ALP) was bought from Calbiochem. Cellulose fiber sample pads (CFSP001700), glass fibers (GFCP000800), laminated cards (HF000MC100) and nitrocellulose membranes (HFB18004 and HFB24004) were purchased from Millipore (Billerica, MA).

Ultrapure (> 18 MΩ) water from Milli-Q water purification system (Billerica, MA) was used to prepare solutions. All the DNA oligonucleotides were purchased from Integrated DNA technologies, Inc. (Coralville, IA). The sequence information is listed below

Table 5.1. Sequence information of the three miRNA sequences

Target-1 (miRNA 16)	5'- rUrArG rCrArG rCrArC rGrUrA rArArU rArUrU rGrGrC rG – 3'
Amine-modified Detection probe	5'- /5AmMC6/ CGC CAA TAT TT- 3'
Biotinylated capture DNA probe	5' – ACG TGC TGC TA/3 Bio/ - 3'
Target-2 (miRNA 21)	5' – rUrArG rCrUrU rArUrC rArGrA rCrUrG rArUrG rUrUrG rA- 3'
Amine-modified Detection probe	5'- /5AmMC6/ TCA ACA TCA GT- 3'
Biotinylated capture DNA probe	5' – CTG ATA AGC TA/3 Bio/ - 3'
Target-3 (miRNA-196a)	5'- rUrArG rGrUrA rGrUrU rUrCrA rArArU rArUrU rGrGrC rG – 3'
Amine-modified Detection probe	5'- /5AmMC6/ CCC AAC ACA AT- 3'
Biotinylated capture DNA probe	5' – GAA ACT ACC TA/3 Bio/ - 3'

5.2.3. Preparation of Conjugates

5.2.3.1. Preparation of CNT-DNA-ALP Conjugates

Three different conjugates were prepared according to the following procedure. The whole process used for the preparation was similar for all three but the DNA which was added in the final step was different for different targets. Firstly, carbon nanotubes were shortened under ultra-sonication with Sulfuric acid: Nitric acid (3:1) mixture for three hours and washed with water till the acid is washed off. Following the washes, the carboxylic groups on the CNT's were activated using the standard EDC/NHS procedure for 15 min at room temperature. The activated CNT's were suspended in PBS followed by the addition of appropriate optimized amounts of DNA and enzyme. The mixture was then incubated overnight at 4^{o}c before the final washes to remove excess

DNA and enzyme. The resulting conjugate was finally suspended in eluent buffer (20mM Na_3PO_4, 5% BSA, 10% Sucrose, 0.25% Tween-20) before use.

5.2.3.2. Preparation of Streptavidin-Biotin Conjugates

Three different streptavidin-biotin conjugates were prepared to be dispensed at different positions on the nitrocellulose membrane thus forming three test zones (one for each target). Similar procedure was followed for the three miRNA targets. Streptavidin (250µl, 2.5mg/ml) was incubated with biotinylated capture probe (100 nano moles) at room temperature with continuous shaking for one hour. Following the incubation, the complex was washed with a centrifugal filter for 20 min, 6000rpm, 4^{o}C multiple times to ensure successful separation of the unbound DNA and Streptavidin. The filtrate on the filter was re-suspended in PBS to a final volume of 600µl before use.

5.2.4. Preparation of Nucleic Acid Biosensors

The Nucleic acid biosensor typically consists of four components: Sample application pad, conjugate pad, nitrocellulose membrane and absorption pad. The sample application pad was pre-treated with the sample pad solution (0.25% Triton X-100, 0.05M Tris-HCl, 0.15 M NaCl and 5% Tween) before use. Pre-treatment of the sample pad included soaking the pad in the buffer for one hr. at room temperature followed by drying of the sample pad in the oven and their storage in desiccators at RT. The biotin-streptavidin conjugates prepared for three test zones were dispensed at three different positions on the nitrocellulose membrane forming test zones for each miRNA target respectively. To facilitate the immobilization of the DNA probes on the nitrocellulose membrane, the biotinylated DNA probes were incubated with streptavidin to form the streptavidin-biotin DNA conjugates. The nitrocellulose membrane was then dried at 37^{o}C for an hour before storing them at 4^{o}C for further use. Lastly, all the four components were assembled on a plastic

backing layer using the clamshell laminator. It was ensured that all the parts overlapped at least 2 mm to facilitate the smooth migration of the sample during the assay. After the assembly, the Guillotin cutting module CM 4000 was used to cut the biosensors with a uniform 3mm width. A desired volume of the mixture of CNT-ALP-DNA conjugates for miRNA 16, miRNA 21 and miRNA 196a was then dropped on the conjugate pad of the biosensor with a micro-pipette and was air-dried before the assay.

5.2.5. Sample Assay Procedure

The ALP-CNT-DNA based NALFB was prepared following the procedure prepared by our group. All the optimizations are carried out systematically and after the attainment of the best suitable conditions, the assay was run following the procedure developed by our group. Hundred microliter of the sample solution containing desired concentration of three targets was prepared in ¼ dilution of SSC buffer with 2% BSA was applied to the sample pad. After 15 min, additional 100ul buffer was added to facilitate the washing step. After 20 min, when two black bands are seen at the test zone and control zone respectively, 20ul of the BCIP/NBT- Blue Liquid Substrate was added to the strip. The formation of an insoluble colored precipitate at the test zone and control zone demonstrate the formation of enzyme-substrate complex resulting in the amplification of the color thus giving a measurable signal. This signal intensities were later recorded using the kinbio strip reader. The total assay time including the enzyme-substrate reaction was 30 min.

5.3. Results and Discussion

5.3.1. Principle of Detection Using ALP-CNT-DNA NALFB

5.3.1.1. Preparation of CNT-DNA-ALP Labels

This current study takes advantage using the carbon nanotube as a label and carrier of numerous enzyme and DNA molecules simultaneously thus resulting in the enormous

amplification of the colorimetric signal. Due to the poor insolubility of the CNTs hampering the movement on the lateral flow strip, pre-treatment of the CNTs was absolutely necessary before the conjugation procedure. Therefore, the CNTs were shortened under ultra-sonication using a mixture of concentrated acids (HNO_3: H_2SO_4 = 1:3). The carboxyl groups on the shortened CNT were then activated using the standard EDC/NHS activation prior to the conjugation with amine groups on the detection probe and enzyme. Three different conjugates were prepared using the detection probe specific for each target. The conjugates were subjected to successive washes after overnight incubation to remove the excess of DNA and enzyme.

5.3.1.2. Working Principle of the Lateral Flow Biosensor

The lateral flow biosensor was developed following the same procedure used for the detection of miRNA 210 (chapter-4). Briefly, CNT is used as a colored label and as a carrier for DNA detection probes and enzyme molecules. The catalytic amplification of an enzyme tracer enables the ultrasensitive detection of target miRNAs. The whole assay of the detection of miRNA is based on a sandwich reaction between the target miRNA and the detection probe with the label and capture probe, followed by the addition of substrate.

So, the principle of lateral flow assay combined the sandwich DNA hybridization and enzyme catalytic amplification as shown in figure-5.1. Three different conjugates were prepared. Conjugate-1: CNT-DNA-ALP conjugate (Detection DNA complimentary to a part of target miRNA 16). Conjugate-2: CNT-DNA-ALP conjugate (Detection DNA complimentary to a part of target miRNA 21). Conjuagte-3: CNT-DNA-ALP conjugate (Detection DNA complimentary to a part of target miRNA 196a). The conjugates were mixed in equal ratios before dispensing them on the conjugate pad, three different biotinylated capture probes (complimentary to a part of specific target miRNA) were incubated with streptavidin before dispensing at three different positions on

nitrocellulose membrane. When the sample solution containing desired concentration of desired or a mixture of all the three target miRNAs is applied onto the sample pad, it moves along the strip by the capillary action. Upon reaching the conjugate pad, the target miRNA forms a complex with the detection probe on CNT and this complex as it continues to migrate along the strip gets captured by the capture probe on the test line. This results in the formation of a sandwich and accumulation of CNT-DNA-ALP conjugates which was visualized by a characteristic black line (Figure 5.1. (C)).

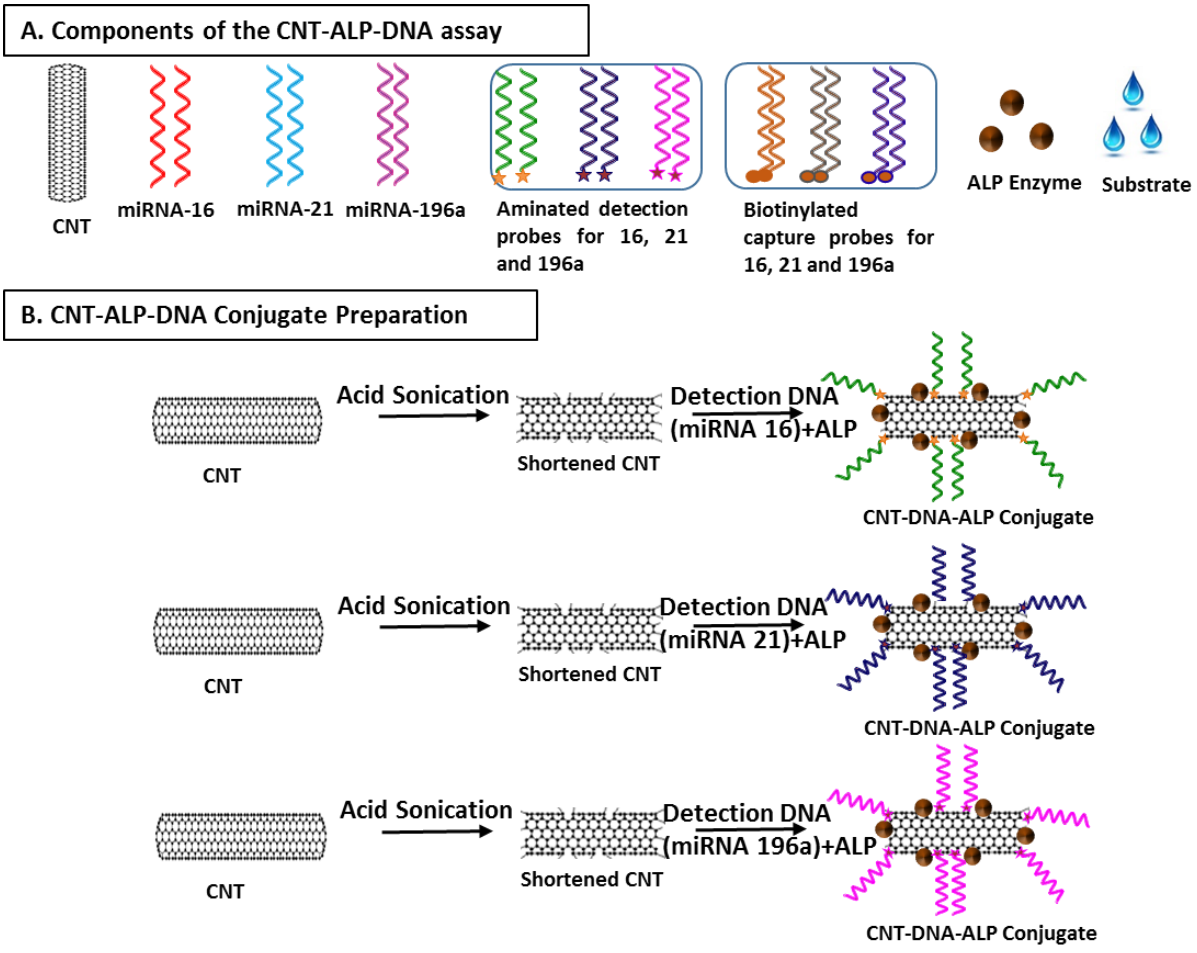

Figure 5.1. (A) Components of the multiplex CNT-ALP-DNA lateral flow assay (B) Shortening of CNTs and preparation of three different CNT-DNA-ALP conjugates with target specific detection DNA probes. (C) Lateral flow assay in the presence of mixture of three target miRNAs (D) Signal amplification step in which substrate is applied to react with the captured conjugates.

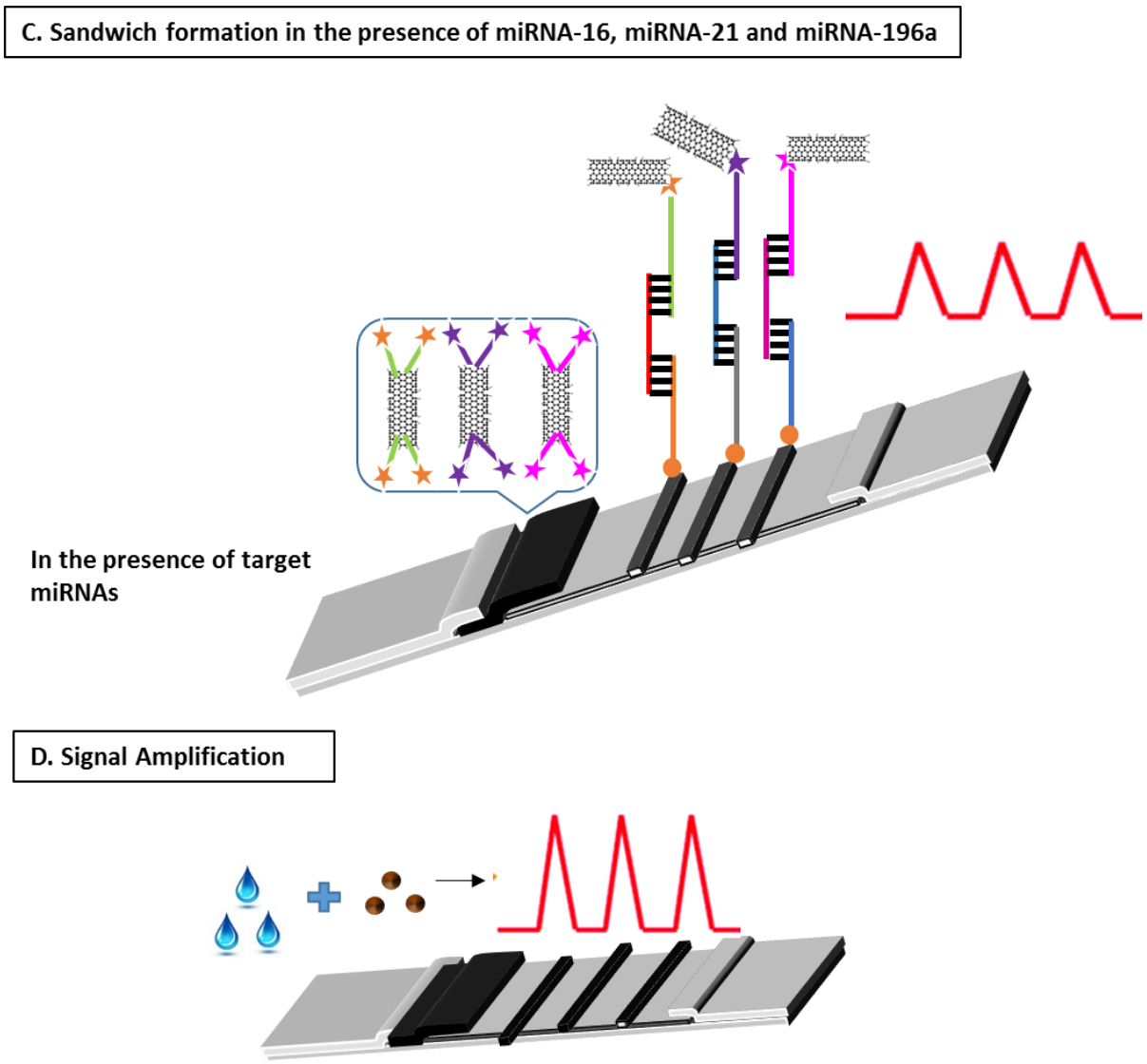

Figure 5.1. (A) Components of the multiplex CNT-ALP-DNA lateral flow assay (B) Shortening of CNTs and preparation of three different CNT-DNA-ALP conjugates with target specific detection DNA probes. (C) Lateral flow assay in the presence of mixture of three target miRNAs (D) Signal amplification step in which substrate is applied to react with the captured conjugates. (Continued)

In the next step, NBT-blue substrate solution was added which resulted in the formation of insoluble blue colored chromogen product due to the enzymatic reaction on the test line and control line (Figure 5.1. (D)).

5.3.1.3. Optimization of Experimental Conditions

The best conditions from the previous chapter were used as the optimal conditions for the detection of these three target miRNAs. As the principle of detection is the same as explained previously, the same conditions such as the buffer, conjugate amounts, number of dispensing times and various other factors were kept unchanged.

Three conjugates were prepared with 0.1 O.D detection probe specific for each target, 5µl of the mixture of three conjugates was dropped on the conjugate pad, 1/8 SSC + 2% BSA and three times dispensing of the test line were used as the best conditions for the assay. 1 µl of the enzyme ALP was added to each conjugate and 10 µl of the substrate was added for signal amplification reaction and 5 minutes of reaction time was considered to be an optimum time for the enzyme substrate reaction after systematic optimizations.

5.3.1.4. Analytical Performance

Various concentrations of target miRNA were tested to evaluate the performance of the sensor under optimized experimental conditions. The average value of three replicates at each concentration was used to plot the calibration curve. Fig 5.2 presents the typical photo images of the strips after assay. The tests were run in the following order. First test was only in the presence of miRNA target 196a, second test was in the presence of miRNA target 196a and miRNA 21, third test was in the presence of miRNA target 196a and miRNA 16 and the last test was in the presence of all the three target miRNAs. There was color observed in the test zones only when specific miRNA target solution was added indicating negligible non-specific adsorption under optimized conditions. This assay can detect the three miRNA targets simultaneously on one lateral flow strip biosensor.

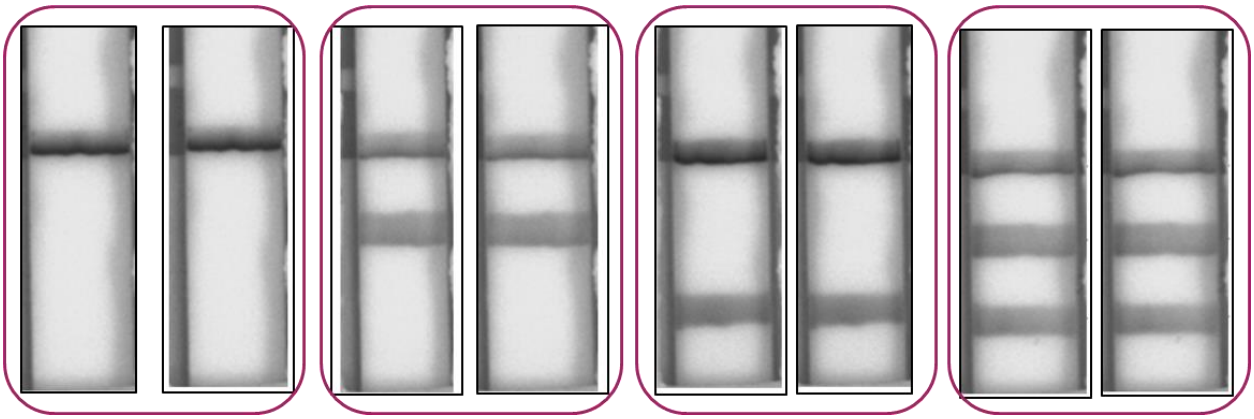

Figure 5.2. Typical photo images of the strips after the assay was run with various combinations of target miRNA.

The calibration curve was plotted with various concentrations versus S/N ratio for all the three targets. The lateral flow biosensor was tested for the presence of various concentrations of target miRNA 196a, miRNA 21 and miRNA 16 and the calculated detection limits were found to be 1.9fM, 3.2fM and 4.9fM respectively. [Figures 5.3. (A) (B) (C)]

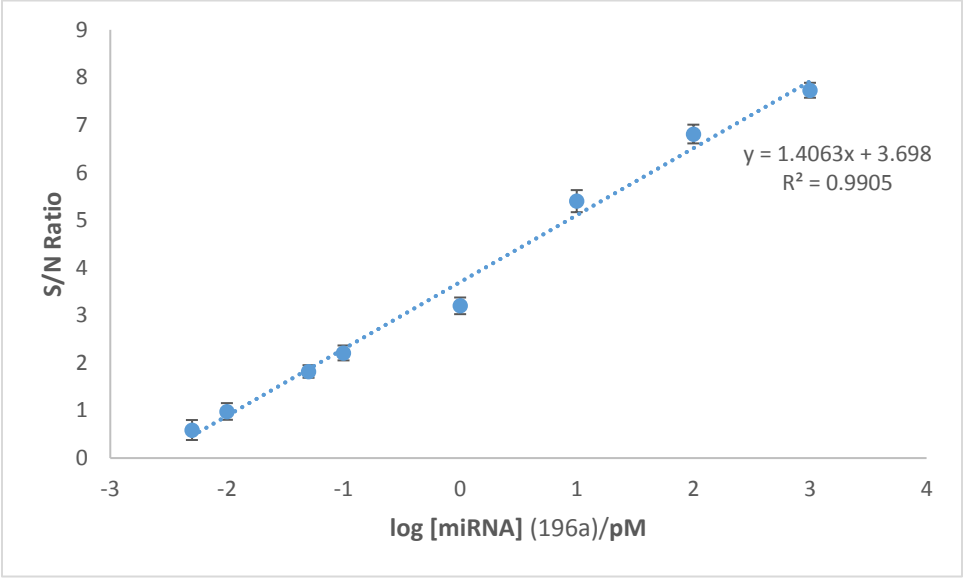

Figure 5.3. Calibration curve plotted against various concentrations of miRNA 196a versus the corresponding S/N ratio.

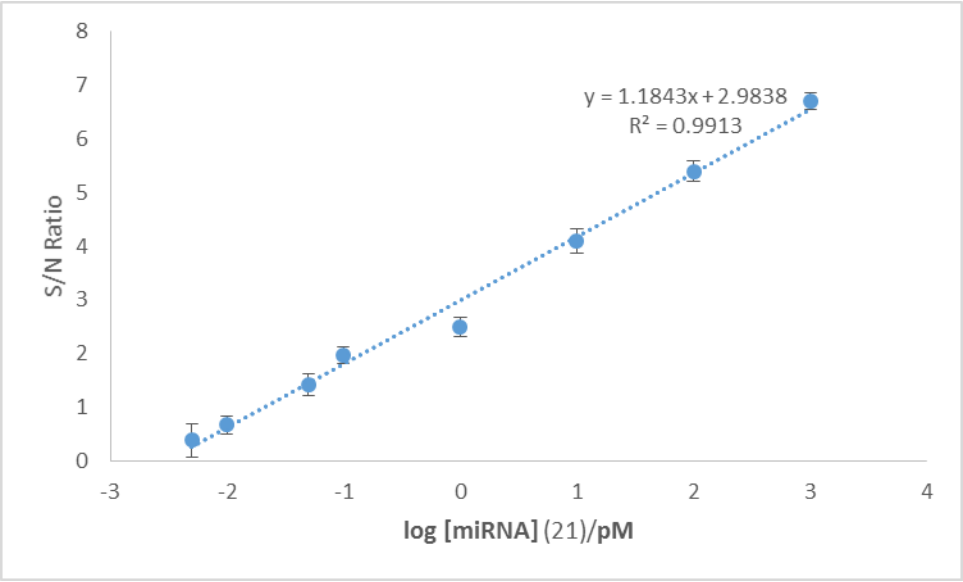

Figure 5.4. Calibration curve plotted against various concentrations of miRNA 21 versus the corresponding S/N ratio.

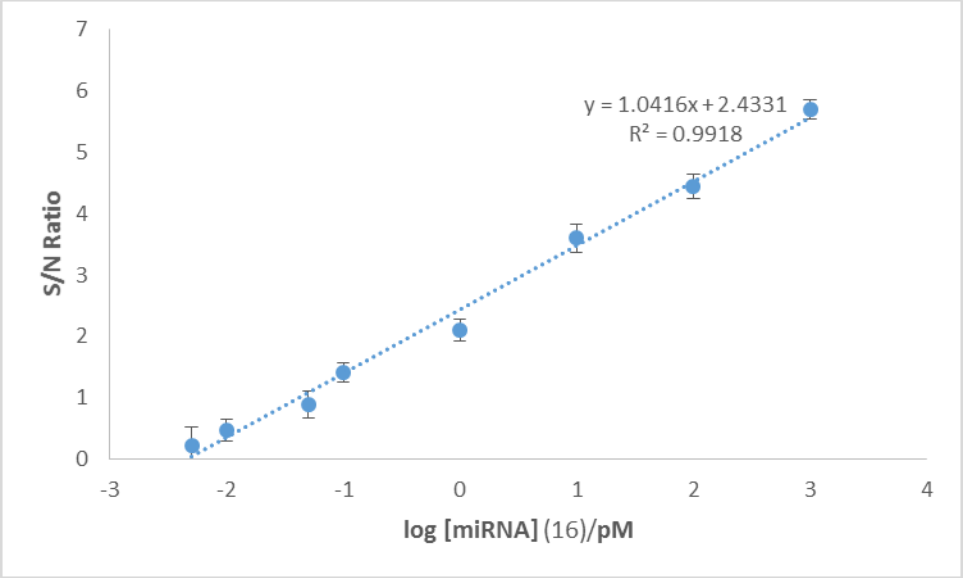

Figure 5.5. Calibration curve plotted against various concentrations of miRNA 16 versus the corresponding S/N ratio.

5.4. Real Sample Detection

All the above results prove the inherent characteristics of the CNT-ALP-DNA lateral flow biosensor in terms of stability, reproducibility and sensitivity in detecting very low

concentrations of target miRNAs 16, 21 and 196a. To further evaluate the credibility of this sensor for the detection of miRNA panel, this was applied to real sample detection.

5.4.1. Application of NABLFB for the Detection of Target miRNAs in Blood Samples

Pancreatic cancer patient sample was obtained from Sanford clinic in Fargo, ND. The patient sample was centrifuged and plasma was collected. Total miRNA was extracted from 200µl of each human plasma samples using a Qiagen miRNeasy Plasma/Serum kit according to manufacturer's instructions. The total RNA was tested using the CNT-DNA-ALP lateral flow biosensor and was compared to the miRNA extract from healthy sample. There was an obvious difference between PC patient samples versus non-cancer sample (figure 5.4) suggesting that this sensor is capable of differentiating the patient sample by the miRNA content.

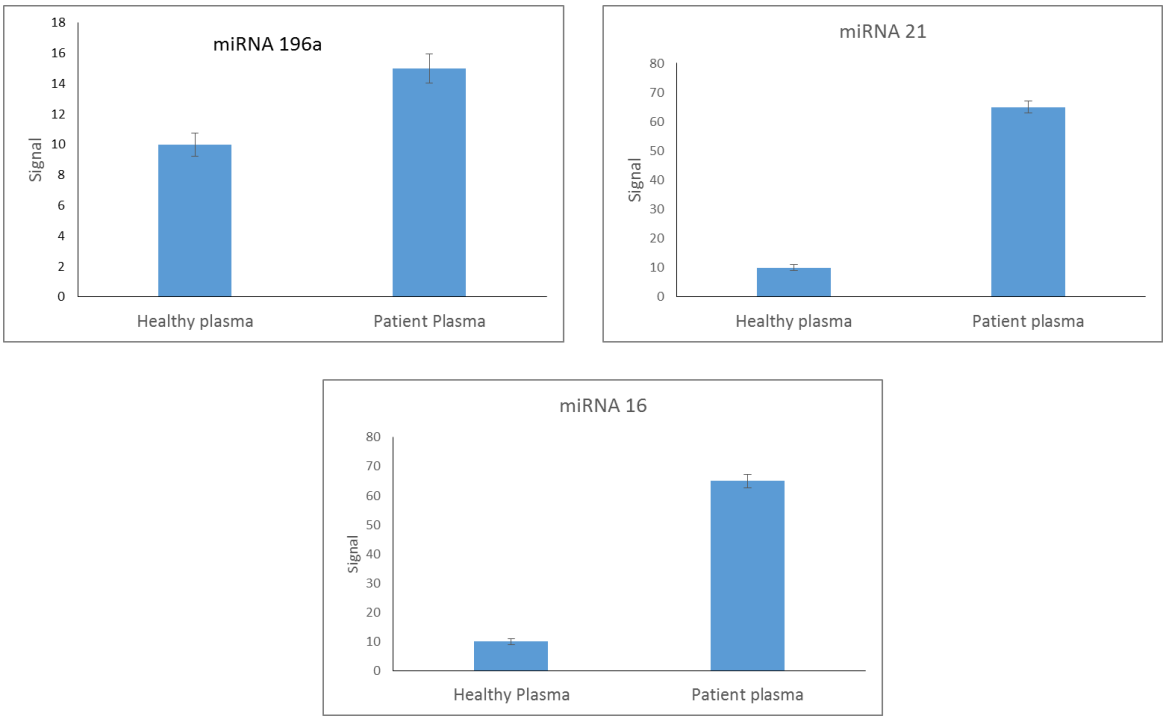

Figure 5.6. Total RNA extract from normal and pancreatic cancer patient blood sample was tested using the reported lateral flow biosensor

5.4.2. Application of NABLFB for the Detection of miRNA Panel in Tissue Samples

Tissue samples were also tested for the presence of miRNA biomarker panel miRNA 196a, miRNA 21 and miRNA 16. Tissue samples from the tumor and non-tumor regions were collected from two PC patients. 20mg of each tissue samples were suspended in lysis buffer followed by the homogenization with a tissue disruptor. Tissue homogenate was subjected to total RNA extraction using the All prep DNA/RNA/Plasma miRNeasy-96 kit from Qiagen. The total miRNA extract from the tissues was tested for the presence of target miRNAs using NABLFB. As shown in the figure 5.5, there was an obvious difference between the signals thus differentiating a tumor tissue samples from a non-tumor tissue sample.

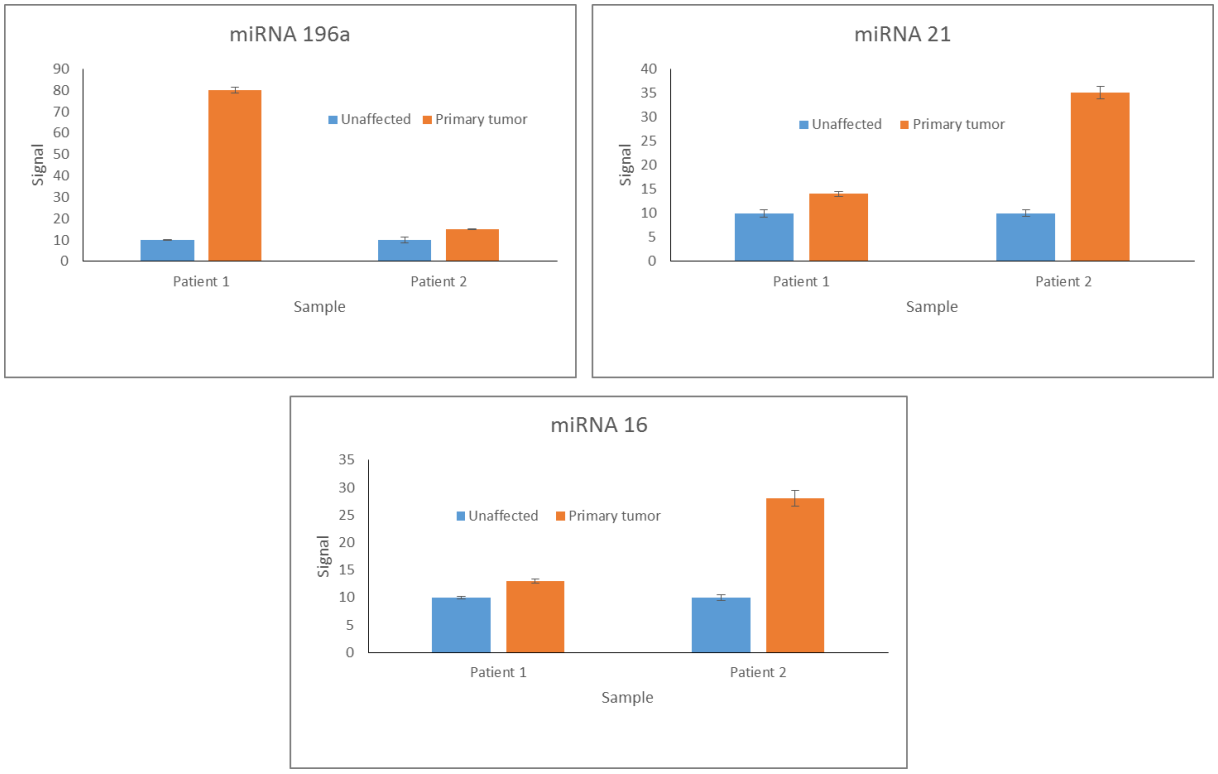

Figure 5.7. Responses from unaffected and primary tumor samples from two pancreatic cancer patient samples

5.4.3. Application of NABLFB for the Detection of miRNA Panel in Various Cell Lines

Adherent cell lines were washed with PBS to remove residual culture media. The cells were treated with trypsin to detach them from culture plates. All collected cells were washed with PBS. Total RNA was extracted from different cell lines using Qiagen All prep DNA/RNA/Protein Kit according to manufacturer's instructions. The RNA corresponding to the extract from 1 million cells was run on the strip for the detection of miRNA targets. As seen in the figure 5.6., the cell lines showed different concentrations of each target.

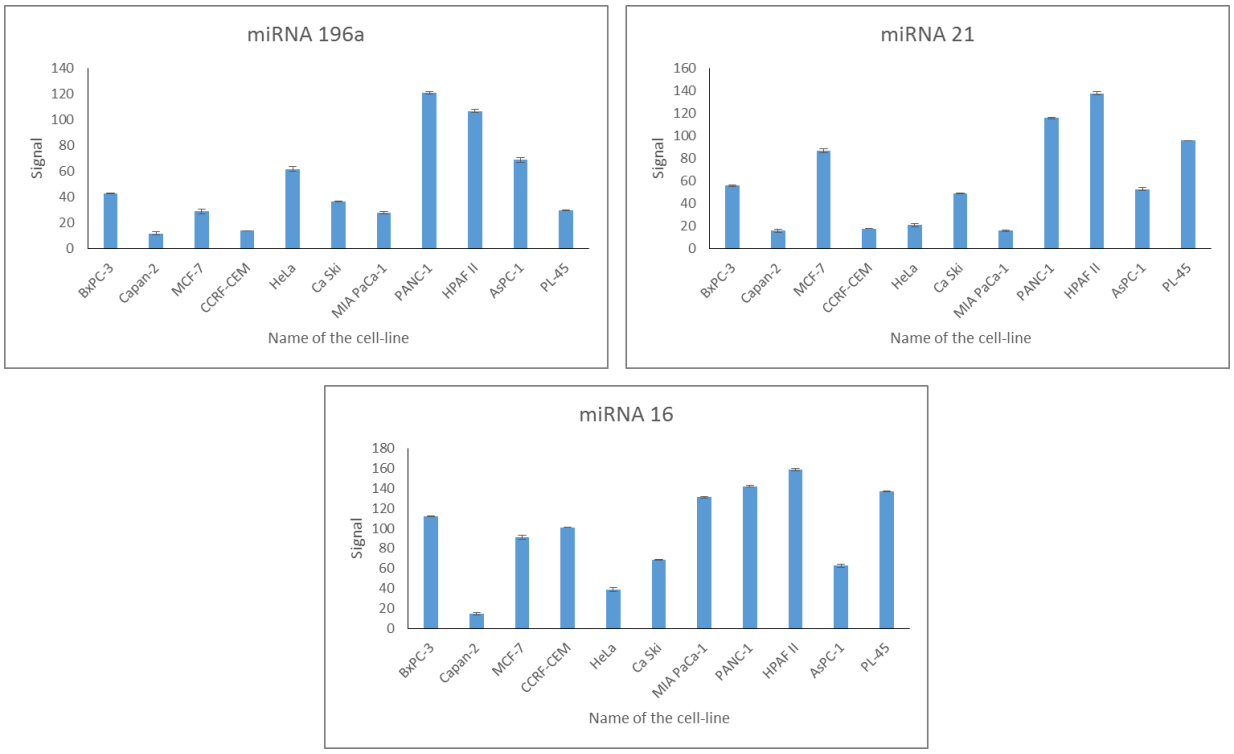

Figure 5.8. Responses from various cell lines after the miRNA extract from each cell line was applied on the strip

5.4.4. Validation of the Real Samples Using qRT-PCR

5.4.4.1. cDNA Synthesis

The total RNA extracts from plasma, tissue and cell line samples were quantified using nano drop and stored at -80^{o}C until further use. Reverse transcription was performed using

SuperScript™ III Reverse Transcriptase system (Thermofisher). Each RT reaction had 50ng total miRNA, 2pmol stem loop primer, 0.5mM dNTP mix, 5mM DTT, 40 units RNaseOUT recombinant ribonuclease inhibitor, 1 Unit SuperScript RT enzyme and 4µL first strand buffer. The total reaction volume was 20µL. RT-PCR reaction was carried out at 55°C for 60 minutes followed by 15 min at 72°C to deactivate the SuperScript RT enzyme.

5.4.4.2. qPCR Reaction

qPCR was performed on an Applied Biosystems Real Time PCR machine using Fast SYBR™ Green master mix. Each sample well contained 4µl cDNA template (RT PCR product), 0.05 µM each forward and reverse primers and 10 µl of 2X fast SYBR™ Green master mix. Reaction volume was topped up to 20 µl with nuclease free water. qPCR cycling conditions were as follows: Initial denaturation at 95 °C for 5 minutes followed by 45 cycles at 95 °C for 5 seconds and 60 °C for 30 seconds.

5.4.4.3. Results

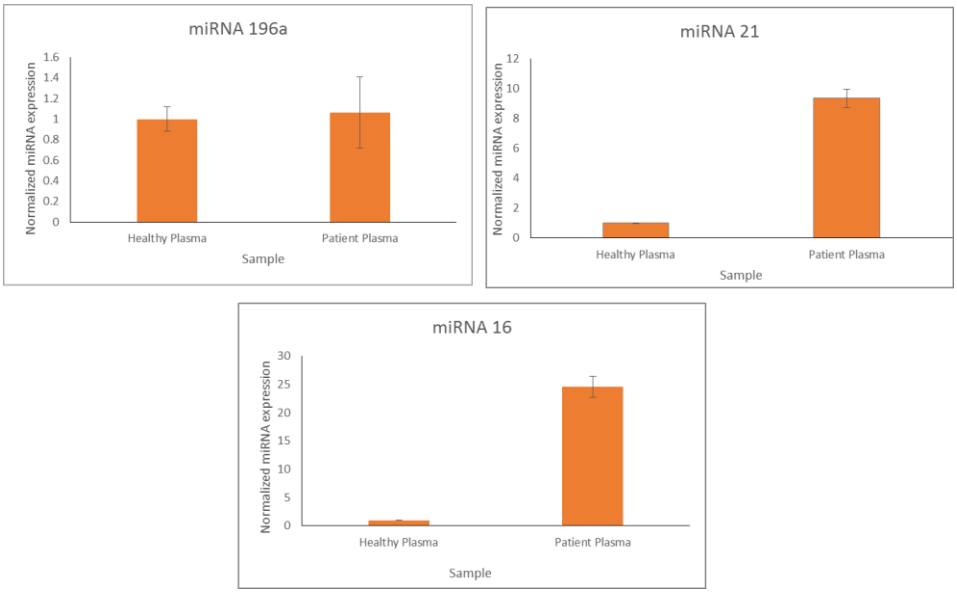

Figure 5.9. Responses from plasma of healthy and affected PC patient samples for the miRNA targets after qPCR reaction

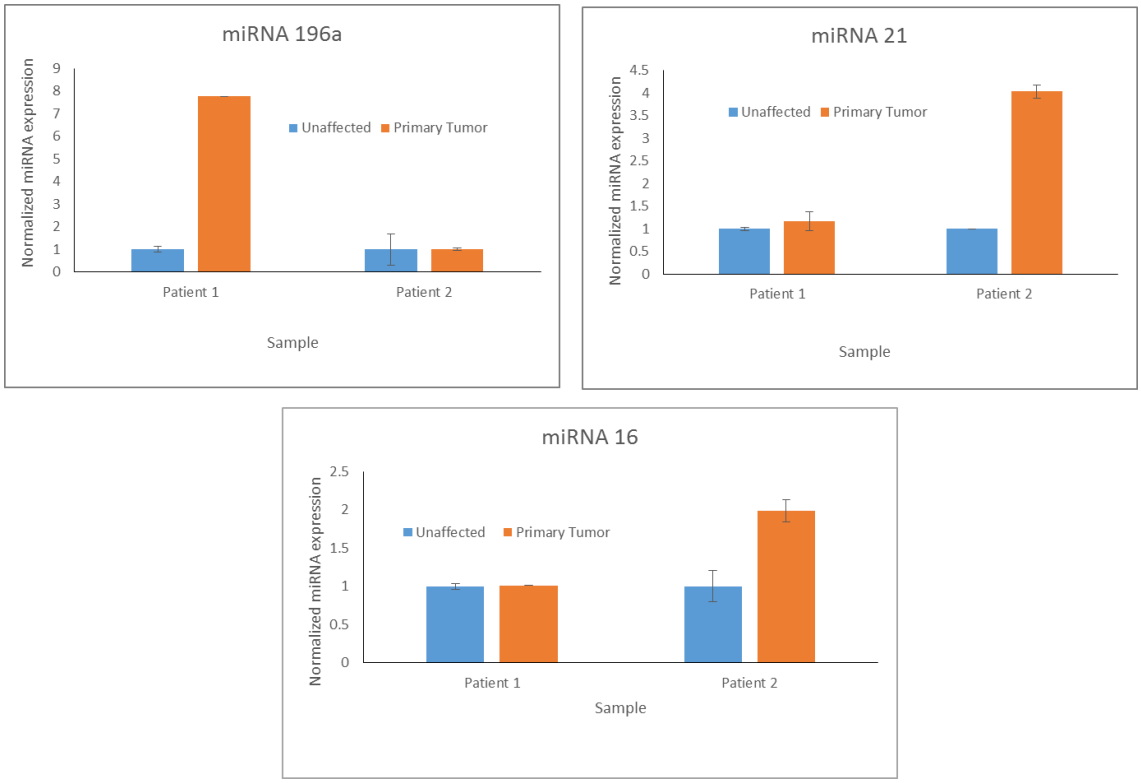

Figure 5.10. Responses from tissues of unaffected and primary tumor patient samples for the miRNA targets after the qPCR reaction. The responses from two patients were recorded

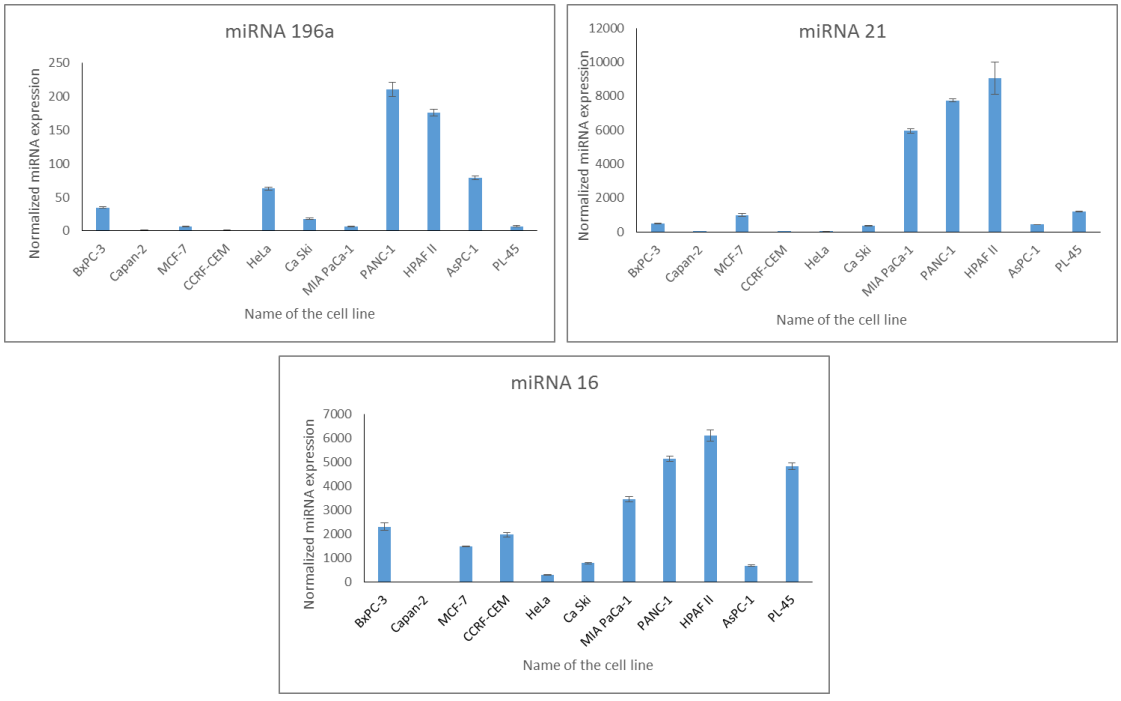

Figure 5.11. Responses from various cell lines for the three miRNA targets after qPCR reaction

Note: Capan-2 had the lowest expression. All other cell lines miRNA target expression was normalized to data from Capan-2.

5.5. Conclusion

A lateral flow biosensor for the multiplex detection of the biomarker panel miRNA 196a, miRNA 16 and miRNA 21 was successfully developed for early detection of PC. This assay was made ultrasensitive by using the CNT-ALP label for the first time. Under optimal conditions, the LFB was capable of detecting low fM ranges without the need for expensive instrumentation and complex chemical reaction. The excellent analytical performance characterized by the enzyme amplification was further explored by the detection of target miRNA's in real pancreatic cancer patient samples including plasma, tissue and various cell lines were also screened. The results were validated using qPCR thus providing a proof that this method of detection is efficient for the application in clinical diagnosis. The multiplex detection greatly enhances the specificity of the detection of target miRNA's thus showing a great promise as a tool for early detection in the field of molecular diagnosis.

6. CONCLUSION

This dissertation aims on developing ultra-sensitive nucleic acid based lateral flow biosensors for the detection of various nucleic acid biomarkers. Improved sensitivity was demonstrated in the detections on the lateral flow biosensor were observed in combination with novel nanomaterials, enzymes and advanced detection strategies. We aim to use these biosensors in the field of real sample detection of nucleic acids which is not possible with the conventional lateral flow biosensors. The nucleic acid biosensors when present in the body are in trace levels making the whole detection process very tedious, but these novel lateral flow biosensors are expected to simplify the whole procedure and stand out as an ideal point of care device for the detection of nucleic acid biomarkers. This improvement in the sensitivity should broaden the application of the biosensors in the field of molecular diagnostics and aid in the early detection of various diseases like Cancer and many other infectious diseases where nucleic acids (DNA, miRNA) act as effective biomarkers.

The lateral flow biosensors reported with improved sensitivities are listed below.

1. Gold nanoparticle-decorated silica nanorods (AuNP-SiNRs) were synthesized and used as the labels for the fabrication of lateral flow nucleic acid biosensors. Owing to its biocompatibility and convenience in surface modification, silica nanorods proved to be efficient carriers in loading numerous AuNPs. Sandwich type reactions were performed on the lateral flow strips, and the accumulation of AuNP-SiNRs on the test zone produced intense colored characteristic colored bands, enabling visual detection of target nucleic acids without instrumentation. The visual detection limit of miRNA on the lateral flow nucleic acid biosensors was enhanced dramatically. The quantitative detection of target miRNA was done by reading the intensities of the colored

bands with a portable strip reader and the calculated detection limit with the AuNP-SiNR was six times lower than that of the AuNP-based lateral flow nucleic acid biosensors.

2. An improved Fluorescent lateral flow nucleic acid biosensor was developed for ultra-sensitive detection of nucleic acid biomarker using fluorescent carbon nanoparticles as a tag and signal-trigger. The FCN-based LFNAB in this research is by far the most sensitive method reported for the rapid detection of DNA sequence on a lateral flow device without additional signal amplification and the use of conventional fluorophores and QDs. To the best of our knowledge, this is the first report on FCN based lateral flow biosensor which took the advantage of using relatively cheaper and easy synthesizable carbon nano dots as a fluorescent tag thus replacing the widely used expensive quantum dots. We demonstrated that the biosensor was able to detect a minimum concentration of 0.4fM DNA. The resulting fluorescent lateral flow assay presents a rapid, low-cost and a very sensitive DNA detection method without the need for target amplification or any expensive instrumentation.

3. A colorimetric enzyme based lateral flow assay for the detection of miRNA-210 was developed. Improved detection sensitivity was obtained by using Carbon nanotubes as carriers to load a large amount of enzymes. The more enzymes on the test zone resulted in color enhancement because of the colored insoluble precipitate formed after the enzyme-substrate reaction. The resulting colorimetric lateral flow biosensor presents a rapid, low cost ultra-sensitive method of detecting very low concentrations of miRNA 210 as low as 2.4fM. The fabricated sensor was applied in screening of various pancreatic cancer cell lines and was used to detect miRNA in real patient samples including pancreatic cancer tissue and blood samples.

4. To develop a more reliable lateral flow biosensor against the detection of pancreatic cancer, a multiplex detection assay was developed for the detection of miRNA 16, miRNA 21, miRNA 196a

as this is the reported miRNA panel for the detection of pancreatic cancer. The resulting colorimetric lateral flow biosensor was capable of detecting one target or two targets or three targets simultaneously on a single biosensor. There was no interference between the targets and they could be detected simultaneously. Detection limits of 1.9fM, 3.2fM and 4.9fM for miRNA 196a, miRNA 21 and miRNA 16 respectively was achieved with a good linear detection range. With the simultaneous detection of the biomarker panel, we believe that this platform would aid in the early detection of pancreatic cancer thus decreasing the high mortality rates associated with the disease.

With the highly enhanced sensitivities, the nucleic acid based lateral flow biosensors should be an excellent platform for point-of-care diagnosis or on-field application. We were able to demonstrate that this method is feasible for the detection of not only the commercial products but also the real clinical patient samples thus providing a huge scope in the early detection of deadly diseases like cancer. Moreover, excellent specificity in validation of miRNA biomarkers for cancer development and progression has been achieved by the accurate detection of multiple biomarkers on a single platform thus eradicating the problems of low specificity caused when using a single biomarker. More work in the future would aim in developing multiple such assays which would be able to detect or validate multiple biomarkers in a single assay thus increasing the specificity of the whole detection.

7. REFERENCES

1. Strimbu, K.; Tavel, J. A. What are Biomarkers? *Curr Opin HIV Aids*. **2010**, *5* (6), 463-466.

2. Schwarzenbach, H. Circulating nucleic acids as biomarkers in breast cancer. *Breast Cancer Res.* **2013**, *15* (5), 211.

3. Jahr, S.; Hentze, H.; Englisch, S.; Hardt, D.; Fackelmayer, F. O.; Hesch, R. D.; Knippers, R. DNA fragments in the blood plasma of cancer patients: quantitations and evidence for their origin from apoptotic and necrotic cells. *Cancer Res*. **2001,** *61*, 1659-1665.

4. American Cancer Society. *Cancer Facts & Figures* 2013. Atlanta: American Cancer Society; **2013**.

5. Wu, S. L.; Amato, H.; Biringer, R.; Choudhary, G.; Shieh, P.; Hancock, W. S. Targeted proteomics of low-level proteins in human plasma by LC/MSn: using human growth hormone as a model system. *J. Proteome. Res.* **2002**, *1* (5), 459-465.

6. Barnidge, D. R.; Goodmanson, M. K.; Klee, G. G.; Muddiman, D. C. Absolute quantification of the model marker prostate-specific antigen in serum by LC/MS using protein cleavage and isotope dilution mass spectrometry. *J. Proteome. Res*. **2004**, *3* (3), 644-652.

7. Anderson, L.; Hunter, C. L. Quantitative mass spectrometric multiple reaction monitoring assays for major plasma proteins. *Mol. Cell. Proteomics*. **2006**, *5*(4), 573-588.

8. Johnson, I. R.; Parkinson-Lawrence, E. J.; Butler, L. M.; Brooks, D. A. Prostate cell lines as models for biomarker discovery: performance of current markers and the search of new biomarkers. *Prostate*. **2014**, *74* (5), 547-560.

9. Pockley, A. G.; Fairburn, B.; Mirza, S.; Slack, L. K.; Hopkinson, K.; Muthana, M. A non-receptor mediated mechanism for internalization of molecular chaperones. *Methods.* **2007**, *43* (3), 238-244.

10. Hellman, L. M.; Fried, M. G. Electrophoretic mobility shift assay (EMSA) for detecting protein-nucleic acid interactions. *Nat. Protoc*. **2007**, *2* (8), 1849-1861.

11. Grandjean, M.; Dieu, M.; Raes, M.; Feron, O. A new method combining sequential immunoaffinity depletion and differential in gel electrophoresis to identify autoantibodies as cancer biomarkers. *J. Immunol. Methods*. **2013**, *396*, 23-32.

12. Wayner, E. A.; Quek, S. I.; Ahmad, R.; Ho, M. E.; Loprieno, M. A.; Zhou, Y.; Ellis, W. J.; True, L. D.; Liu, A. Y. Development of an ELISA to detect the secreted prostate cancer biomarker AGR2 in voided urine. *Prostate*. **2012**, *72* (9), 1023-1034.

13. Zong, C.; Wu, J.; Wang, C.; Ju, H.; Yan, F. Chemiluminiscence imaging immunoassay of multiple tumor markers for cancer screening. *Anal. Chem*. **2012**, *84*(5), 2410-2415.

14. Wilson, M. S.; Nie, W. Multiplex measurement of seven tumor markers using an electrochemical protein chip. *Anal. Chem*. **2006**, *78* (18), 6476-6483.

15. Wu, M. S.; Shi, H. W.; He, L. J.; Xu, J. J.; Chen, H. Y. Microchip device with 64-site electrode array for multiplexed immunoassay of cell surface antigens based on electro chemiluminiscence resonance energy transfer. *Anal. Chem*. **2012**, *84* (9), 4207-4213.

16. Lee, H.; Sun, E.; Ham, D.; Weissleder, R. Chip-NMR biosensor for detection and molecular analysis of cells. *Nat. Med*. **2008**, *14*(8), 869-874.

17. Shao, H.; Min, C.; Issadore, D.; Liong, M.; Yoon, T. J.; Weissleder, R.; Lee, H. Magnetic nanoparticles and microNMR for diagnostic applications. *Theranostics*. **2012**, *2* (1), 55-65.

18. Knoll, J. H. M.; Lichter, P.; Bakdounes, K.; Eltoum, I. A. In situ hybridization and detection using nonisotopic probes. *Curr. Protoc. Mol. Biol*. **2007**, *79*, 1-17.

19. Olatunbosun, O.; Deneer, H.; Pierson, R. Human papillomavirus DNA detection in sperm using polymerase chain reaction. *Obstet Gynecol*. **2001**, *97* (3), 357-60.

20. John, A. St. The evidence to support Point-of-Care testing. *Clin Biochem Rev*. **2010**, *31* (3), 111-119.

21. He, Y.; Zhang, S.; Zhang, X.; Baloda, M.; Gurung, A. S.; Xu, H.; Zhang, X.; Liu, G. Ultrasensitive nucleic acid biosensor based on enzyme-gold nanoparticle dual label and lateral flow strip biosensor. *Biosens. Bioelectron*. **2011**, *26*, 2018-2024.

22. Bruno, J. G. Application of DNA aptamers and quantum dots to lateral flow test strips for detection of foodborne pathogens with improved sensitivity versus colloidal gold. *Pathogens*. **2014**, *3* (2), 341-355.

23. Gubala, V.; Harris, L. F.; Ricco, A. J.; Tan, M. X.; Williams, D. E. Point of care diagnostics: status and future. *Anal. Chem*. **2012**, *84*(2), 487-515.

24. Farrell, B. O. Evolution in lateral flow-based immunoassay systems. *In Lateral Flow Immunoassay*, Wong, R. C.; Tse, H. Y. Humana Press: New York**, 2009**, 1-4.

25. Patel, S.; Nanda, R.; Sahoo, S.; Mohapatra, E. Biosensors in health care: the milestones achieved in their development towards lab-on-chip analysis. *Biochem. Res. Int*. **2016**, ID *3130469*, 12 pages.

26. Posthuma-Trumpie, G. A.; Korf, J.; Amerongen, A. Lateral flow (immuno) assay: its strengths, weaknesses, oppurtunities and threats. A literature survey. *Anal. Bioanal. Chem*. **2009**, *393* (2), 569-582.

27. Sajid, M.; Kawde, A.; Daud, M. Designs, formats and applications of lateral flow assay: A literature review. *J. Saudi Chem. Soc*. **2015**, *19* (6), 689-705.

28. Nimjee, S. M.; Rusconi, C. P.; Sullenger, B. A. Aptamers: An emerging class of therapeutics. *Annu. Rev. Med*. **2005**, *56*, 555-583.

29. Lee, J. H.; Kim, H.; Ko, J.; Lee, Y. Interaction of C5 protein with RNA aptamers selected by SELEX. *Nucleic Acids Res*. **2002**, *30* (24), 5360-5368.

30. Mosing, R. K.; Mendonsa, S. D.; Bowser, M. T. Capillary electrophoresis- SELEX selection of aptamers with affinity for HIV-1 reverse transcriptase. *Anal. Chem*. **2005**, *77* (19), 6107-6112.

31.Gu, G.; Wang, T.; Yang, Y.; Xu, X.; Wang, J. An Improved SELEX-Seq Strategy for Characterizing DNA-Binding Specificity of Transcription Factor: NF-kB as an Example. *PLoS ONE*. **2013**, *8* (10): e76109.

32. Wang, Q.; Liu, W.; Xing, Y.; Yang, X.; Wang, K.; Jiang, R.; Wang, P.; Zhao, Q. Screening of DNA aptamers against myoglobin using a positive and negative selection units integrated microfluidic chip and its biosensing application. *Anal. Chem*. **2014**, *86* (13), 6572-6579.

33. Tang, Z.; Shangguan, D.; Wang, K.; Shi, H.; Sefah, K.; Mallikratchy, P.; Chen, H. W.; Li, Y.; Tan. W. Selection of aptamers for molecular recognition and characterization of cancer cells. *Anal. Chem*. **2007**, *79* (13), 4900-4907.

34. Jimenez, E.; Sefah, K.; Lopez-colon, D.; Van Simaeys, D.; Chen, H. W.; Tockman, M. S.; Tan, W. Generation of lung adenocarcinoma DNA aptamers for cancer studies. *PLoS ONE*. **2012**, *7* (10): e46222.

35. Hamula, C. L. A.; Zhang, H.; Guan, L. L.; Li, X.; Le, X. C. Selection of aptamers against live bacterial cells. *Anal. Chem*. **2008**, *80* (20), 7812-7819.

36. Kim, Y. S.; Song, M. Y.; Jurng, J.; Kim, B. C. Isolation and characterization of DNA aptamers against *Escherichia coli* using a bacterial cell-SELEX. *Anal. Biochem*. **2013**, *436* (1), 22-28.

37. Rajendran, M.; Ellington, A. D. Selection of fluorescent aptamer beacons that light up in the presence of zinc. *Anal. Biochem*. **2008**, *390* (4), 1067-1075.

38. Wu, Y.; Zhan, S.; Wang, L.; Zhou, P. Selection of a DNA aptamer for cadmium detection based on cationic polymer mediated aggregation of gold nanoparticles. *Analyst*. **2014**, *139* (6), 1550-1561.

39. Saran, D.; Frank, J.; Burke, D. H. The tyranny of adenosine recognition among RNA aptamers to coenzyme A. *BMC. Evol. Biol*. **2003**, *3*:26.

40. Tang, J.; Yu, T.; Guo, L.; Xie, J.; Shao, N.; He, Z. In vitro selection of DNA aptamer against abrin toxin and aptamer based abrin direct detection. *Biosens. Bioelectron*. **2007**, *22* (11), 2456-2463.

41. Atkins, S. D.; Clark, I. M. Fungal molecular diagnostics: a mini review. *J. Appl. Genet*. **2004,** *45* (1), 3-15.

42. Lopez, M. M.; Bertolini, E.; Olmos, A.; Caruso, P.; Gorris, M. T.; Llop, P.; Penyalve, R.; Cambra, M. Innovative tools for detection of plant pathogenic viruses and bacteria. *Int. Microbiol*. **2003**, *6* (4), 233-243.

43. Suzuki, T.; Tanaka, M.; Otani, S.; Matsuura, S.; Sakaguchi, Y.; Nishimura, T.; Ishizaka, A.; Hasegawa, N. New rapid detection test with a combination of polymerase chain reaction and immunochromatographic assay for Mycobacterium tuberculosis complex. *Diagn. Microbiol. Infect. Dis*. **2006**, *56* (3), 275-280.

44. Corstjens, P. L. A. M.; Zuiderwijk, M.; Nilsson, M.; Feindt, H.; Niedbala, R. S.; Tanke, H. J. Lateral-flow and up-converting phosphor reporters to detect single-stranded nucleic acids in a sandwich-hybridization assay. *Anal. Biochem*. **2003**, *312* (2), 191-200.

45. Aveyard, J.; Mehrabi, M.; Cossins, A.; Braven, H.; Wilson, R. One step visual detection of PCR products with gold nanoparticles and a nucleic acid lateral flow (NALF) device. *Chem. Commun*. **2007**, *41*, 4251-4253.

46. Chua, A.; Yean, C. Y.; Ravichandran, M.; Lim, B.; Lalitha, P. A rapid DNA biosensor for the molecular diagnosis of infectious disease. *Biosens. Bioelectron*. **2011**, *26* (9), 3825-3831.

47. kiatpathomchai, W.; Jaroenram, W.; Arunrut, N.; Jitrapakdee, S.; Flegel, T. W. Shrimp Taura syndrome virus detection by reverse transcription loop-mediated isothermal amplification combined with a lateral flow dipstick. *J. Virol. Met*. **2008**, *153* (2), 214-217.

48. Chen, Y.; Cheng, N.; Xu, Y.; Huang, K.; Luo, Y.; Xu, W. Point-of-care and visual detection of *P. aeruginosa* and its toxin genes by multiple LAMP and lateral flow nucleic acid biosensor. *Biosens. Bioelectron*. **2016**, *81*, 317-323.

49. He, Y.; Zeng, K.; Gurung, A. S.; Baloda, M.; Xu, H.; Zhang, X.; Liu, G. Visual detection of Single-nucleotide polymorphism with hairpin oligonucleotide-functionalized gold nanoparticles. *Anal. Chem.* **2010**, *82* (17), 7169-7177.

50. Xiao, Z.; Lie, P.; Fang, Z.; Yu, L.; Chen, J.; Liu, J.; Ge, C.; Zhou, X.; Zeng, L. A lateral flow biosensor for detection of single nucleotide polymorphism by circular strand displacement reaction. *Chem. Commun*. **2012**, *48*, 8547-8549.

51. Xu, H.; Mao, X.; Zeng, Q.; Wang, S.; Kawde, A.; Liu, G. Aptamer-functionalized gold nanoparticles as probes in a dry-reagent strip biosensor for protein analysis. *Anal. Chem*. **2009**, *81* (2), 669-675.

52. Chen, J.; Fang, Z.; Lie, P.; Zeng, L. Computational lateral flow biosensor for proteins and small molecules: a new class of strip logic gates. *Anal. Chem*. **2012**, *84* (15), 6321-6325.

53. Mazumdar, D.; Liu, J.; Lu, G.; Zhou, J.; Lu, Y. Easy-to-use dipstick tests for detection of lead in paints using non-cross-linked gold nanoparticle-DNAzyme conjugates. *Chem. Commun*. **2010**, *46* (9), 1416-1418.

54. Fang, Z.; Huang, J.; Lie, P.; Xiao, Z.; Ouyang, C.; Wu, Q.; Wu, Y.; Liu, G.; Zeng, L. Lateral flow nucleic acid biosensor for Cu^{2+} detection in aqueous solution with high sensitivity and selectivity. *Chem. Commun*. **2010**, *46*, 9043-9045.

55. He, Y.; Zhang, X.; Zeng, K.; Zhang, S.; Baloda, M.; Gurung, A. S.; Liu, G. Visual detection of Hg^{2+} in aqueous solution using gold nanoparticles and thymine-rich hairpin DNA probes. *Biosens. Bioelectron*. **2011**, *26* (11), 4464-4470.

56. Mao, X.; Phillips, J. A.; Xu, H.; Tan, W.; Zeng, L.; Liu, G. Aptamer-nanoparticle strip biosensor for rapid and sensitive detection of cancer cells. *Anal. Chem*. **2009**, *81* (24), 10013-10018.

57. Liu, J.; Mazumdar, D.; Lu, Y. A simple and sensitive "Dipstick" test in serum based on lateral flow separation of aptamer-linked nanostructures. *Angew. Chem. Int. Ed.* **2006**, *45* (47), 7955-7959.

58. Fang, Z.; Ge, C.; Zhang, W.; Lie, P.; Zeng, L. A lateral flow biosensor for rapid detection of DNA-binding protein c-jun. *Biosens. Bioelectron*. **2011**, *27* (1), 192-196.

59. Hou, S.; Hsiao, Y.; Lin, M.; Yen, C.; Chang, C. microRNA detection using lateral flow nucleic acid strips with gold nanoparticles. *Talanta*. **2012**, *99*, 375-379.

60. Pohlmann, C.; Dieser, I.; Sprinzl, M. A lateral flow assay for identification of Escherichia coli by ribosomal RNA hybridization. *Analyst*. **2014**, *139* (5), 1063-1071.

61. Rastogi, S. K.; Gibson, C. M.; Branen, J. R.; Aston, D. E.; Branen, A. L.; Hrdlicka, P. J. DNA detection on lateral flow test strips: enhanced signal sensitivity using LNA-conjugated gold nanoparticles. *Chem. Commun*. **2012**, *48* (62), 7714-7716.

62. Rohrman, B. A.; Leautaud, V.; Molyneux, E.; Richards-kortum, R. R. A lateral flow assay for quantitative detection of amplified HIV-1 RNA. *PLoS ONE*. **2012**, *7* (9): e45611.

63. Shyu. R.; Shyu, H.; Liu, H.; Tang, S. Colloidal gold-based immunochromatographic assay for the detection of ricin. *Toxicon.* **2002**, *40* (3), 255-258.

64. Cho, I.; Seo, S.; Paek, E.; Paek, S. Immunogold-silver staining-on-a-chip biosensor based on cross-flow chromatography. *J. Chromatogr. B.* **2010**, *878* (2), 271-277.

65. Shen, G.; Zhang, S.; Hu, X. Signal enhancement in a lateral flow immunoassay based on dual gold nanoparticle conjugates. *Clin. Biochem*. **2013**, *46* (16), 1734-1738.

66. Mao, X.; Ma, Y.; Zhang, A.; Zhang, L.; Zeng, L.; Liu, G. Disposable nucleic acid biosensors based on gold nanoparticle probes and lateral flow strip. *Anal. Chem*. **2009**, *81* (4), 1660-1668.

67. Mao, X.; Xu, H.; Zeng, Q.; Zeng, L.; Liu, G. Molecular beacon functionalized gold nanoparticles as probes in dry-reagent strip biosensor for DNA analysis. *Chem. Commun.* **2009**, *21*, 3065-3067.

68. Wang, J., Wang, X., Li, Y., Yan, S., Zhou, Q., Gao, B., Peng, J., Du, J., Fu, Q., Jia, S., Zhang, J., Zhan, L. A novel, universal and sensitive lateral-flow based method for the detection of multiple bacterial contamination in platelet concentrations. *Anal. Sci.* **2012**, *28* (3), 237-241.

69. Wang, Y.; Nugen, S. R. Development of fluorescent nanoparticle-labeled lateral flow assay for the detection of nucleic acids. *Biomed. Microdev*. **2013**, *15* (5), 751-758.

70. Juntunen, E.; Myyrylainen, T.; Salminen, T.; Soukka, T.; Pettersson, K. Performance of fluorescent europium (III) nanoparticles and colloidal gold reporters in lateral flow bioaffinity assay. *Anal. Biochem*. **2012**, *428* (1), 31-38.

71. Baeumner, A. J.; Pretz, J.; Fang, S. A universal nucleic acid sequence biosensor with nanomolar detection limits. *Anal. Chem*. **2004**, *76* (4), 888-894.

72. Kumanan, V.; Nugen, S. R.; Baeumner, A. J.; Chang, Y. A biosensor assay for the detection of Mycobacterium avium subsp. paratuberculosis in fecal samples. *J. Vet. Sci.* **2009**, *10*, 35-42.

73. Corstjens, P.L.A.M., Zuiderwijk, M., Brink, A., Li, S., Feindt, H., Niedbala R.S., Tanke H.J. Use of up-converting phosphor reporters in lateral flow assays to detect specific nucleic acid sequences: A rapid, sensitive DNA test to identify Human Papillomavirus type 16 infection. *Clin. Chem*. **2001**, *47* (10), 1885-1893.

74. Croce, C. M. Causes and consequences of microRNA dysregulation in cancer. *Nat. Rev. Genetics*. **2009**, *10*, 704-714.

75. Bartel, D. P. MicroRNAs: Genomics, Biogenesis, Mechanism and function. *Cell.* **2004**, *116* (2), 281-297.

76. Plasterk, R. H. A. Micro RNAs in animal development. *Cell*. **2006**, *124* (5), 877-881.

77. Shivdasani. R. A. MicroRNAs: regulators of gene expression and cell differentiation. *Blood*. **2006**, *108*, 3646-3653.

78. He, L.; Hannon, G. J. MicroRNAs: small RNAs with a big role in gene regulation. *Nat. Rev. Genetics.* **2004**, *5*, 522-531.

79. Planell-Saguer, M.; Rodicio, M. C. Analytical aspects of microRNA in diagnostics: A review. *Anal. Chim. Acta*. **2011**, *699* (2), 134-152.

80. Jia, H.; Li, Z.; Liu, C.; Cheng. Y. Ultrasensitive detection of microRNAs by exponential isothermal amplification. *Angew. Chem. Int. Ed.* **2010**, *49* (32), 5498-5501.

81. Li, C.; Li, Z.; Jia, H.; Yan, J. One-step ultrasensitive detection of microRNAs with loop-mediated isothermal amplification. *Chem. Commun*. **2011**, *47* (9), 2595-2597.

82. Dong, H.; Lei, J.; Ding, L.; Wen, Y.; Ju, H.; Zhang, X. MicroRNA: Function, detection and bioanalysis. *Chem. Rev*. **2013**, *113* (8), 6207-6223.

83. Wang, J. Electrochemical biosensors: towards point-of-care cancer diagnostics. *Biosens. Bioelectron*. **2006**, *21* (10), 1887-1892.

84. Gao, X.; Xu, H.; Baloda, M.; Gurung, A. S.; Xu, L.; Wang, T.; Zhang, X.; Liu, G. Visual detection of microRNA with lateral flow nucleic acid biosensor. *Biosens. Bioelectron*. **2014**, *54*, 578-584.

85. Xu, H.; Chen, J.; Birrenkott, J.; Zhao, J. X.; Takalkar, S.; Baryeh, K.; Liu, G. Gold-nanoparticle-decorated silica nanorods for sensitive visual detection of proteins. *Anal. Chem*. **2014,** *86* (15), 7351-7359.

86. Xu, S.; Hartvickson, S.; Zhao, J. X. Engineering of SiO_2-Au-SiO_2 sandwich nanoaggregates using a building block: Single, double and triple cores for enhancement of near infrared fluorescence. *Langmuir*. **2008**, *24* (14), 7492-7499.

87. Shipp, G. Ultrasensitive measurement of protein and nucleic acid biomarkers for earlier disease detection and more effective therapies. *Biotechnol Healthc.* **2006**, *3*(2), 38-40.

88. Weller, M.G. Immunochromatographic techniques-a critical review. *Fresenius J Anal. Chem*. **2000**, *366* (6), 635-645.

89. Sajid, M.; Kawde, A.; Daud, M. Designs, formats and applications of lateral flow assay. A literature review. *J. Saudi Chem. Soc*. **2015**, *19* (6), 689-705.

90. Ge, X.; Asiri, A. M.; Du, D.; Wen, W.; Wang, S.; Lin, Y. Nanomaterial-enhanced paper-based biosensors. *Trends Anal. Chem. TrAC*. **2014**, *58*, 31-39.

91. Qiu, W.; Xu, H.; Takalkar, S.; Gurung, A. S.; Liu, B.; Zheng, Y.; Guo, Z.; Baloda, M.; Baryeh, K.; Liu, G. Carbon nanotube-based lateral flow biosensor for sensitive and rapid detection of DNA sequence. *Biosens. Bioelectron*. **2015**, *64*, 367-372.

92. Mens, P. F.; de Bes, H. M.; Sondo, P.; Laochan, N.; Keereecharoen, L.; Amerongen, JA. V.; Flint, J.; Sak, J. R. S.; Proux, S.; Tinto, H.; Schallig, H. D. F. H. Direct blood PCR in

combination with nucleic acid lateral flow immunoassay for detection of plasmodium species in settings where malaria is endemic. *J. Clin. Microbiol*. **2012**, *50* (11), 3520-3525.

93. Ang, G. Y.; Yu, C. Y.; Yean, C. Y. Ambient temperature detection of PCR amplicons with a novel sequence-specific nucleic acid lateral flow biosensor. *Biosens. Bioelectron*. **2012**, *38* (1), 151-156.

94. Carter, D. J.; Cary, R. B. Lateral flow microarrays: a novel platform for rapid nucleic acid detection based on miniaturized lateral flow chromatography. *Nucleic Acids Res*. **2007**, *35* (10): e74.

95. Jaroenram, W.; Kiatpathomchai, W.; Flegel, T. W. Rapid and sensitive detection of white spot syndrome virus by loop-mediated isothermal amplification combined with a lateral flow dipstick. *Mol. Cell. Probes*. **2009**, *23* (2), 65-70.

96. He, Y.; Zeng, K.; Zhang, X.; Gurung, A. S.; Baloda, M.; Xu, H.; Liu, G. Ultrasensitive electrochemical detection of nucleic acid based on isothermal strand-displacement polymerase reaction and enzyme dual amplification. *Electrochem. Commun*. **2010**, *12* (7), 985-988.

97. Liu, J.; Chen, L.; Lie, P.; Dun, B.; Zeng, L. A universal biosensor for multiplex DNA detection based on hairpin probe assisted cascade signal amplification. *Chem. Commun*. **2013**, *49* (45), 5165-5167.

98. Lie, P.; Liu, J.; Fang, Z.; Dun, B.; Zeng, L. A lateral flow biosensor for the detection of nucleic acids with high sensitivity and selectivity. *Chem. Commun*. **2012**, *48* (2), 236-238.

99. Zheng, D.; Zou, R.; Lou, X. Label-free fluorescent detection of ions, proteins and small molecules using structure-switching aptamers, SYBR gold and exonuclease I. *Anal. Chem*. **2012**, *84* (8), 3554-3560.

100. Kim, S.; Ahn, K.; Park, J.; Kim, K.; Lee, K.; Han, S.; Lee, J. Fluorescent ferritin nanoparticles and application to the aptamer sensor. *Anal. Chem*. **2011**, *83* (15), 5834-5843.

101. Li, Z.; Wang, Y.; Wang, J.; Tang, Z.; Pounds, J. G.; Lin, Y. Rapid and sensitive detection of protein biomarker using a portable fluorescence biosensor based on quantum dots and a lateral flow test strip. *Anal. Chem*. **2010**, *82* (16), 7008-7014.

102. Xu, Y.; Liu, Y.; Wu, Y.; Xia, X.; Liao, Y.; Li, Q. Fluorescent probe-based lateral flow assay for multiplex nucleic acid detection. *Anal. Chem*. **2014**, *86* (12), 5611-5614.

103. Wang, Y.; Nugen, S. R. Development of fluorescent nanoparticle-labeled lateral flow assay for the detection of nucleic acids. *Biomed. Microdev*. **2013**, *15* (5), 751-758.

104. Corstjens, P. L. A. M.; Zuiderwijk, M.; Nilsson, M.; Feindt, H.; Niedbala, R. S.; Tanke, H. J. Lateral-flow and up-converting phosphor reporters to detect single-stranded nucleic acids in a sandwich-hybridization assay. *Anal. Biochem*. **2003**, *312* (2), 191-200.

105. Fang, Y.; Guo, S.; Li, D.; Zhu, C.; Ren, W.; Dong, S.; Wang, E. Easy synthesis and imaging applications of cross-linked green fluorescent hollow carbon nanoparticles. *ACS Nano*. **2012**, *6* (1), 400-409.

106. Cao, L.; Wang, X.; Meziani, M. J.; Lu, F.; Wang, H.; Luo, P. G.; Lin, Y.; Harruff, B. A.; Veca, L. M.; Murray, D.; Xie, S.; Sun, Y. Carbon dots for multiphoton bioimaging. *J. Am. Chem. Soc.* **2007**, *129* (37), 11318-11319.

107. Yang, S.; Cao, L.; Luo, P. G.; Lu, F.; Wang, X.; Wang, H.; Meziani, M. J.; Liu, Y.; Qi, G.; Sun, Y. Carbon dots for optical imaging in Vivo. *J. Am. Chem. Soc*. **2009**, *131* (32), 11308-11309.

108. Li, H.; He, X.; Kang, Z.; Huang, H.; Liu, Y.; Liu, J.; Lian, S.; Tsang, C.A.; Yang, X.; Lee, S. Water-soluble fluorescent carbon quantum dots and photo catalyst design. *Angew. Chem. Int. Ed*. **2010**, *49* (26), 4430-4434.

109. Cao, L.; Sahu, S.; Anilkumar, P.; Bunker, C. E.; Xu, J.; Fernando, K. A.; Wang, P.; Guliants, E. A.; Tackett, K. N.; Sun, Y. Carbon nanoparticles as visible-light photocatalysts for efficient CO_2 Conversion and beyond. *J. Am. Chem. Soc*. **2011**, *133* (13), 4754-4757.

110. Wang, F.; Chen, Y.; Liu, C.; Ma, D. White light-emitting devices based on carbon dots electroluminescence. *Chem. Commun*. **2011**, *47* (12), 3502-3504.

111. Dai, H.; Shi, Y.; Wang, Y.; Sun, Y.; Hu, J.; Ni, P.; Li, Z. A carbon dot based biosensor for melamine detection by fluorescence resonance energy transfer. *Sens. Actuators. B*. **2014**, *202*, 201-208.

112. Wang, Y.; Bao, L.; Liu, Z.; Pang, D. Aptamer biosensor based on fluorescence resonance energy transfer from up converting phosphors to carbon nanoparticles for thrombin detection in human plasma. *Anal. Chem*. **2011**, *83* (21), 8130-8137.

113. Cui, X.; Zhu, L.; Wu, J.; Hou, Y.; Wang, P.; Wang, Z.; Yang, M. A fluorescent biosensor based on carbon dots-labeled oligodeoxyribonucleotide and graphene oxide for mercury (II) detection. *Biosens. Bioelectron*. **2015**, *63*, 506-512.

114. Guo, Y.; Zhang, L.; Zhang, S.; Yang, Y.; Chen, X.; Zhang, M. Fluorescent carbon nanoparticles for the fluorescent detection of metal ions. *Biosens. Bioelectron*. **2015**, *63*, 61-71.

115. Mao, X.; Wang, W.; Du, T. E. Dry-reagent nucleic acid biosensor based on blue dye doped latex beads and lateral flow strip. *Talanta*. **2013**, *114*, 248-253.

116. Maitra, A.; Hruban, R. H. Pancreatic cancer. *Ann. Rev. Pathol*. **2008**, 3, 157-88.

117. Siegel, R. L.; Miller, K. D.; Jemal, A. Cancer Statistics, 2017. *CA Cancer. J. Clin*. **2017**, *67*, 7-30.

118. Vilmann, P.; Saftoiu, A. Endoscopic ultrasound-guided fine needle aspiration biopsy: equipment and technique. *J. Gastroenterol Hepatol*. **2006**, *21*, 1646-1655.

119. Chen, Y.; Zheng, B.; Robbins, D. H.; Lewin, D. N.; Mikhitarian, K.; Graham, A.; Rumpp, L.; Glenn, T.; Gillanders, W. E.; Cole, D. J.; Lu, X.; Hoffman, B. J.; Mitas, M. Accurate discrimination of pancreatic ductal adenocarcinoma and chronic pancreatitis using multimarker expression data and samples obtained by minimally invasive fine needle aspiration. *Int. J. Cancer*. **2007**, *120*, 1511-1517.

120. Eloubeidi, M. A.; Jhala, D.; Chhieng, D. C.; Chen, V. K.; Eltoum, I.; Vickers, S.; Mel wilcox, C.; Jhala, N. Yield of endoscopic ultrasound-guided fine-needle aspiration biopsy in patients with suspected pancreatic carcinoma. *Cancer*. **2003**, *99* (5), 285-92.

121. Friedman, R. C.; Farh, K. K.; Burge, C. B.; Bartel, D. P. Most mammalian mRNAs are conserved targets of microRNAs. *Genome Res*. **2009**, *19*, 92-105.

122. Lewis, B. P.; Burge, C. B.; Bartel, D. P. Conserved seed pairing, often flanked by adenosines, indicates that thousands of human genes are microRNA targets. *Cell*. **2005**, *120*, 15-20.

123. Chang, T. C.; Mendell, J. T. microRNAs in cell proliferation, cell death and tumorigenesis. *Br J Cancer*. **2006**, *94*, 776-80.

124. Li, Y.; Sarkar, F. H. MicroRNA targeted therapeutic approach for pancreatic cancer. *Int. J. Biol. Sci.* **2016**, *12* (3), 326-337.

125. Chin, L. J.; Slack, F. J. A truth serum for cancer - microRNAs have major potential as cancer biomarkers. *Cell. Res*. **2008**, *18* (10), 983-84.

126. Lu, J.; Xie, F.; Geng, L.; Shen, W.; Sui, C.; Yang, J. Potential role of microRNA-210 as biomarker in human cancers detection: A meta-analysis. *Biomed. Res. Int*. **2015**, ID: 303987, 1-9

127. Wang, J.; Chen, J.; Chang, P.; Leblanc, A.; Li, D.; Abbruzzesse, J. L.; Frazier, M. L.; Killary, A. M.; Sen, S. MicroRNAs in plasma of pancreatic ductal adenocarcinoma patients as novel blood-based biomarkers of disease. *Cancer. Prev. Res*. **2009**, *2* (9), 807-813.

128. Bartlett, J. M. S.; Stirling, D. A. Short history of the polymerase chain reaction. PCR protocols. **2003**, *226*, 3-6.

129. Joshi, M.; Deshpande, J. D. Polymerase chain reaction: methods, principles and application. *Int. J. Biomed. Sci.* **2011**, *2* (1), 81-97.

130. Smith, C.; Osborn, M. Advantages and limitations of quantitative PCR (qPCR)-based approaches in microbial ecology. *FEMS Microbial Ecol*. **2009**, *67*(1), 6-20.

131. Hou, S.; Hsiao, Y.; Lin, M.; Yen, C.; Chang, C. miRNA detection using lateral flow nucleic acid strips with gold nanoparticles. *Talanta*. **2012**, *99*, 375-379.

132. Mao, X.; Ma, Y.; Zhang, A.; Zhang, L.; Zeng, L.; Liu, G. Disposable nucleic acid biosensors based on gold nanoparticle probes and lateral flow strip. *Anal. Chem*. **2009**, *81* (4), 1660-1668.

133. Park, S.; Vosguerichian, M.; Bao, Z. A review of fabrication and applications of carbon nanotube film-based flexible electronics. *Nanoscale*. **2013**, *5*, 1727-1752.

134. Hirlekar, R.; Yamagar, M.; Garse, H.; Vij, M.; Kadam, V. Carbon nanotubes and its applications: A review. *Asian J. Pharm. Clin. Res*. **2009**, *2* (4), 17-27.

135. Qu, L.; Dai, L.; Stone, M.; Xia, Z.; Wang, Z. L. Carbon nanotube arrays with strong shear binding-on and easy normal lifting-off. *Science*. **2008**, *322* (5899), 238-242.

136. Wan, Y.; Deng, W.; Su, Y.; Zhu, X.; Peng, C.; Hu, H.; Peng, H.; Song, S.; Fan, C. Carbon nanotube-based ultrasensitive multiplexing electrochemical immunosensor for cancer biomarkers. *Biosens. Bioelectron*. **2011**, *30*, 93-99.

137. Xu, Y.; Liu, Y.; Wu, Y.; Xia, X.; Liao, Y.; Li, Q. Fluorescent probe-based lateral flow assay for multiplex nucleic acid detection. *Anal. Chem.* **2014**, *86*, 5611-5614.

138. Zhao, Y.; Wang, H.; Zhang, P.; Sun, C.; Wang, X.; Wang, X.; Yang, R.; Wang, C.; Zhou, L. Rapid multiplex detection of 10 foodborne pathogens with an up-converting phosphor technology-based 10-channel lateral flow assay. *Sci. Rep*. **2016**, *6*:21342.

139. Jung, W.; Han, J.; Choi, J.; Ahn, C. H. Point-of-care testing (POCT) diagnostic systems using microfluidic lab-on-a-chip technologies. *Microelectron. Eng*. **2015**, *132*, 46-57.

140. Spindel, S.; Sapsford, K. E. Evaluation of optical detection platforms for multiplexed detection of proteins and the need for point-of-care biosensors for clinical use. *Sensors.* **2014**, *14* (12), 22313-22341.

141. Li, J.; Mcdonald, J. Multiplexed lateral flow biosensors: technological advances for radically improving point-of-care diagnosis. *Biosens. Bioelectron*. **2016**, *83*, 177-192.

142. Shadfan, B. H.; Simmons, A. R.; Simmons, G. W.; Ho, A.; Wong, J.; Lu, K. H.; Bast, R. C.; McDevitt, J. T. A multiplexable, microfluidic platform for the rapid quantitation of a biomarker panel for early ovarian cancer detection at the point-of-care. *Cancer. Prev. Res*. **2015**, *8* (1), 37-48.

143. American Cancer Society. *Cancer Facts & Figures 2016*. Atlanta: American Cancer Society; **2013**.

144. Ilic, M.; Ilic, I. Epidemology of Pancreatic Cancer. *World. J. Gastroenterol.* **2016**, *22* (44), 9694-9705.

145. Goggins, M. Markers of Pancreatic Cancer: working toward early detection. *Clin. Cancer Res*. **2011**, *17* (4), 635-639.

146. Hong, L.; Yang, J.; Han, Y.; Lu, Q.; Cao, J.; Syed, L. High expression of miR-210 predicts poor survival in patients with breast cancer: A meta-analysis. *Gene*. **2012**, *507*, 135-138.

147. Zhao, A.; Li, G.; Peoch, M.; Genin, C.; Gigante, M. Serum miR-210 as a novel biomarker for molecular diagnosis of clear cell renal cell carcinoma. *Exp. Mol. Pathol*. **2013**, *94*, 115-120.

148. Li, Y.; Sarkar, F. H. MicroRNA targeted therapeutic approach for pancreatic cancer. *Int J. Biol. Sci*. **2016**, *12*, 326-337.

149. Wang, J.; Chen, J.; Chang, P.; Leblanc, A.; Li, D.; Abbruzzesse, J. L.; Frazier, M. L.; Killary, A. M.; Sen, S. MicroRNAs in plasma of pancreatic ductal adenocarcinoma patients as novel blood-based biomarkers of disease. *Cancer. Prev. Res*. **2009**, *2* (9), 807-813.

150. Huang, J.; Liu, J.; Chen-Xiao, K.; Zhang, X.; Lee, W. N. P.; Go, V. W.; Xiao, G. G. Advance in microRNA as a potential biomarker for early detection of pancreatic cancer. *Biomarker. Res*. **2016**, *4*, 20-25.